# Feedbacks Between Fires and Soil Erosion Processes at the Desert Margins

Sujith Ravi
Trivandrum, Kerala, India

Master of Science (Environmental Sciences), University of Virginia, 2005
Bachelor of Science (Agriculture), Kerala Agricultural University, 2001

A Dissertation presented to the Graduate Faculty
of the University of Virginia in Candidacy for the Degree of
Doctor of Philosophy

Department of Environmental Sciences

University of Virginia
May, 2008

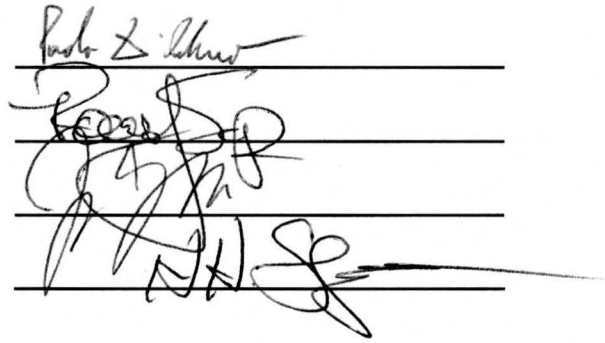

## ABSTRACT

Shrub encroachment at the desert margins, a worldwide phenomenon, results in a heterogeneous landscape characterized by a mosaic of nutrient-depleted barren soil bordered by nutrient-enriched shrubby areas known as “fertile islands”. Even though shrub encroachment is considered as a major contributor to the desertification of several regions around the world, little is known about mechanisms favoring the reversibility of the early stages of this process. In this dissertation, it is shown that fires interact with soil erosion processes to encourage a more homogeneous distribution of soil resources. To this end, I used a combination of replicated field scale techniques for soil erosion monitoring, microtopography measurements, infiltration experiments and isotope tracer studies conducted at a shrub-grass transition zone in the northern Chihuahuan desert (New Mexico, USA). The results indicate that fires tend to counteract the heterogeneity-forming dynamics of land degradation associated with shrub encroachment, thereby enhancing the reversibility of the early stages of this process. The enhancement of post fire redistribution of soil resources is attributed to the enhancement of post fire soil erodibility, in particular, erosion by wind, which dominates in these landscapes. Further, it is hypothesized that the mechanisms causing the enhancement of post-fire soil erodibility are induced by post-fire soil hydrophobicity. These mechanisms (as well as their ecological implications) are a unique finding of this dissertation, in that, to my knowledge, they had never been reported before in the case of wind erosion. The effect of fire induced water repellency on soil susceptibility to wind erosion is demonstrated by wind tunnel experiments using laboratory treated clean sands and natural soils sampled after wild fires and prescribed burns. A theoretical model is developed to explain the

observed effects. The possible impacts of fire-wind erosion interactions on vegetation composition and structure are investigated using a spatially explicit model of vegetation dynamics. The modeling study shows the possible long-term effect of fires on the stability and resilience of fertility island systems. In particular, it is found that the fertility islands are dynamic rather than static features of these landscapes.

## ACKNOWLEDGEMENTS

I would like to express by sincere gratitude to my advisor Dr. Paolo D'Odorico for his excellent guidance and encouragement thoughout my graduate studies. In every sense, this dissertation research would not have been possible without him. I am thankful to my other dissertation committee members: Dr. Gregory Okin, Dr. Hank Shugart, Dr. Robert Swap and Dr. James Smith.

I was very fortunate to have several positive interactions and research collaborations with other scientists and faculty members which helped me to develop a strong interest in dryland ecosystems: Dr. Scott Collins (University of New Mexico, Albuquerque), Dr. Ted Zobeck (USDA-ARS, Lubbock), Dr. Thomas Over (Eastern Illinois University, Charleston), Dr. Stephen Macko (University of Virginia, Charlottesville), Dr. Bruce Herbert (Texas A&M University, College Station), Dr. Carleton White (University of New Mexico, Albuquerque), Mike Friggens and Jennifer Johnson (Sevilleta LTER).

I greatly acknowledge the technical guidance and research/academic support provided by Dean Holder (USDA-ARS, Lubbock, Texas), Don Kearney and John Thornburg (Sevilleta NWR), Lixin Wang, James Kathilankal, Jacquie Hui, Junran Li, Ian McGlynn, Ryan Emanuel and Virginia Seamster (University of Virginia, Charlottesville). I am deeply indebted to the staff at Sevilleta NWR, Sevilleta LTER, Jornada LTER and Cimarron National Grasslands for providing access to field and laboratory facilities.

I am indebted to the following organizations for their financial support during the past three years: NSF-EAR 0409305, USDA (Cooperative Agreement No 2002-35102-

11585), Moore Research Endowment (University of Virginia, Charlottesville) and partially supported by grant NSF - DEB-0620482 and DEB-0217774 to the University of New Mexico for Long-term Ecological Research. I acknowledge the Graduate School of Arts and Sciences, University of Virginia for supporting the final year of my doctoral program by providing the Dissertation Year Fellowship. Last, but not the least, I would like to thank my wife Anjana, for her love and support. I would also like to express my deepest gratitude to my parents and my brother for their love and support through out my life.

# TABLE OF CONTENTS

## LIST OF FIGURES

| NUMBER | TITLE | PAGE NO. |
|---|---|---|

| NUMBER | TITLE | PAGE NO. |
|---|---|---|

| NUMBER | TITLE | PAGE NO. |
|---|---|---|

| NUMBER | TITLE | PAGE NO. |
|---|---|---|

# LIST OF TABLES

# CHAPTER: 1

# INTRODUCTION

Drylands cover about 41% of the earth's surface [*MEA*, 2005] and include all terrestrial regions where production of crops, forage, wood and other ecosystem services are limited by water [*MEA*, 2005]. These regions include hyper-arid, arid, semiarid and dry sub humid areas of the world (Figure 1.1), where the aridity index, defined as the ratio between long-term mean annual precipitation and potential evapotranspiration, is less that 0.65 [*Middleton and Thomas*, 1997]. The world's drylands support a human population of over 2 billion, mostly in the developing world [*MEA*, 2005]. Rangelands (65%) and croplands (25%) account for 90% of all drylands on Earth [*MEA*, 2005]. These regions are of critical concern as 10-20% of them are already degraded [*Oldeman et al*., 1991; *Middleton and Thomas*, 1997], while 70% of these drylands are thought to be affected by degradation of soil and vegetation leading to substantial reduction in ecosystem function and services [*Dregne and Chou*, 1992]. Even though it can be argued that these figures overestimate the reality [*Lepers et al*., 2005], it is well understood that in arid and semiarid environments land degradation is happening at an alarming pace, contributing to the depletion of resources in productive rangelands and cultivated lands [*Dregne*, 1976; *Glantz*, 1977; *Dregne*, 1983; *Reynolds and Stafford-Smith*, 2002]. Climate change, grazing, lack of proper soil management practices and shifts in vegetation composition (e.g. woody plant encroachment and invasion of exotic species) have rendered these landscapes susceptible to degradation with important implications on regional climate change and global desertification [*Glantz*, 1977; *Hare*, 1977; *Dregne*,

1983; *Schlesinger et al*., 1990; *D'Antonio and Vitousek*, 1992; *Nicholson et al*., 2000; *Van Auken*, 2000]. Land degradation may lead to desert-like conditions, a process commonly referred to as "Desertification" [*UNCCD*, 1994].

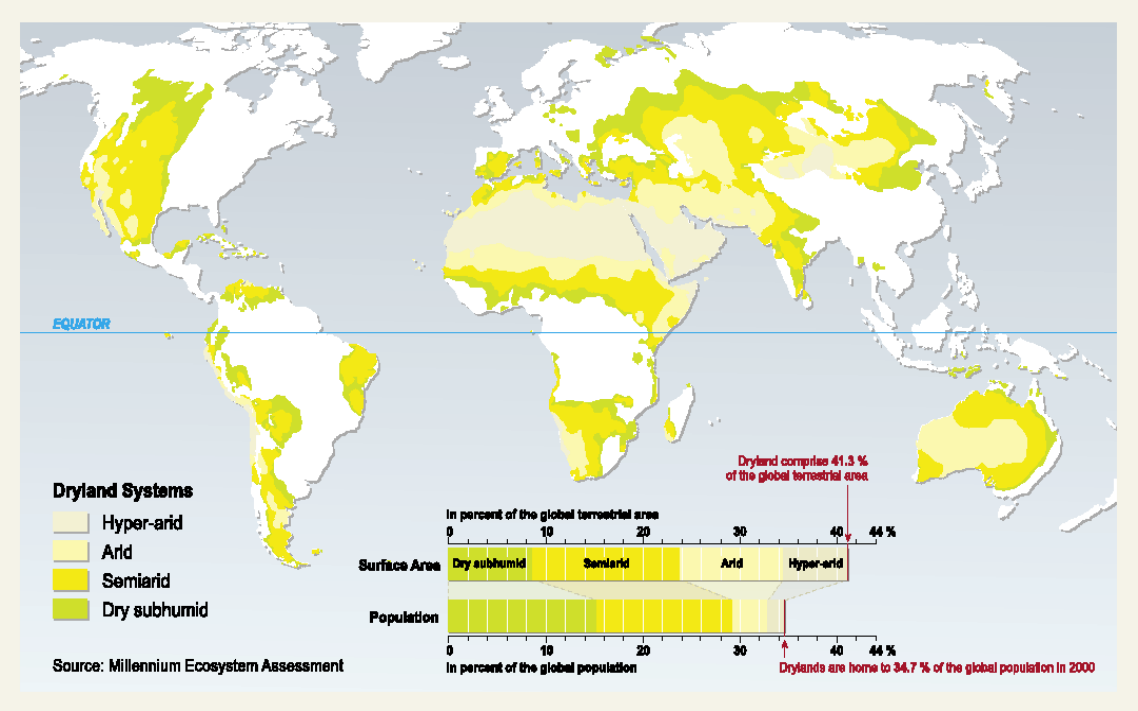


**Figure 1.1** Present day dryland categories [Source: *MEA, 2005*]

## THE PROBLEM OF DRYLAND DEGRADATION

The causes and consequences of dryland degradation, sometimes arguably referred to as "Desertification", remains controversial and poorly understood [*Thomas*, 1997; *Geist and Lambin*, 2004; *Herrmann and Hutchinson*, 2005; *Veron et al*., 2006]. The term "Desertification" was first used by *Aubreville* (1949) to describe transformation of productive tropical rain forest areas into desert as a result of human activity. Some authors even consider desertification as a potential but not necessary outcome of land degradation process. It results in environmental and socio-economic-political implications through a complex interplay of biophysical and anthropogenic factors acting

at different scales [*Geist and Lambin*, 2004]. The United Nations Conference to Combat Desertification [*UNCCD*, 1994] defines desertification as "land degradation in arid, semi arid and dry sub-humid areas resulting from various factors, including climatic variations and human activities" (*first adopted by the United Nations Conference on Environment and Development, Earth Summit, UNCED 1992*).

Recent studies have shown that triggering factors of land degradation like global climate change have resulted in drier conditions in arid and semi arid regions [*Nicholson et al*., 1998]. The increase in aridity results in the dominance of propagation factors (mainly abiotic) of land degradation such as aeolian and hydrological transport processes [*Okin*, 2002]. Wind and water erosion are considered to have contributed to 87% of the degraded land [*Middleton and Thomas*, 1997; *Lal*, 2001]. Further, aeolian processes, the dominant erosion process in these landscapes [*Breshears et al*., 2004, *Ravi et al*., 2007], redistribute soil particles and nutrients and thereby affect the soil surface texture and water holding capacity [*Lyles and Tatarko*, 1986; *Zobeck and Fryrear*, 1986]. These changes affect the productivity and spatial pattern of soil resources and vegetation in these landscapes [*Schlesinger et al*., 1990; *Okin and Gillette*, 2001]. Dust emissions resulting from wind erosion contribute to dust aerosols that are transported to long distances [*Swap et al*., 1996] and deposited over continents and oceans [*Okin et al*., 2004; *Duce and Tindale*, 1991]. The desert dust is a major contributor of tropospheric aerosols, which affect global climate, air quality and hydrological-biogeochemical cycles [*Schlesinger et al*., 1990; *Pope et al*., 1996; *Ramanathan et al*., 2001; *Rosenfield et al*., 2001; *Neff et al*., 2008]. Thus the impacts of dryland degradation can extend beyond the geographic boundaries of arid and semiarid regions.

Human activities have a profound influence on the degradation trends and patterns in drylands [*Reynolds and Stafford-Smith,* 2002; *Asner et al*., 2004; *Neff et al*., 2008]. A typical example of the anthropogenic impacts of dryland degradation is the "Dust Bowl" period (the 1930s) in the Great Plains of the United States, when dramatic soil loss and dust emissions were observed as a result of poor land management practices in conjunction with dry climatic conditions [*Worster,* 1979]. Anthropogenic disturbances of dryland soils after the European colonization have also been reported in the case of the southwestern United States, Australia, Southern Africa, and South America. Large scale commercial grazing in conjunction with management practices such as fire suppression led to an increase in woody plants (shrub encroachment) and to the invasion of desert grasslands by exotic grasses, with negative impacts on ecosystem function and services [*Archer,* 1989; *D'Antonio and Vitousek,* 1992; *Pickup*, 1998; *van Auken,* 2000].

The overexploitation of grazing lands - which comprise around 70% of the world's drylands - due to overgrazing and conversion to croplands, contribute to the pressure of anthropogenic disturbances on these marginal landscapes. In Mongolia and China (Inner Mongolia province) the most important anthropogenic factor contributing to land degradation is animal husbandry, by livestock grazing [*Batjargal,* 1992; *Zhao et al*., 2005]. The carrying capacities of these grazing systems are increasingly exceeded, resulting in the degradation of vegetation and enhanced soil erosion (Figure 1.2). Even in the case of monsoon deserts like the Thar in India, which turns lush green following precipitation events, the overexploitation of fodder and fuel wood has caused the ecological destruction of the desert ecosystem resulting in slow rates of natural regeneration of vegetation following precipitation [*Sinha et al*., 1999; *Chauhan,* 2003].

The increased pressure on drylands is further enhanced by climatic changes, urbanization and management factors, as the degrading landscapes are very dynamic in nature and are very sensitive to climate change and disturbances. A typical example is the Sahel region of Africa [*Nicholson et al*., 1998; *Taylor et al*., 2002], where a feedback between vegetation and climate resulted in alternative stable states of the system, with a stable dry (desertified) and stable moister (vegetated) climate regime [*Charney*, 1975; *Xue and Shukla*, 1993; *Wang and Elthair*, 1999; *Zeng and Neelin*, 1999].

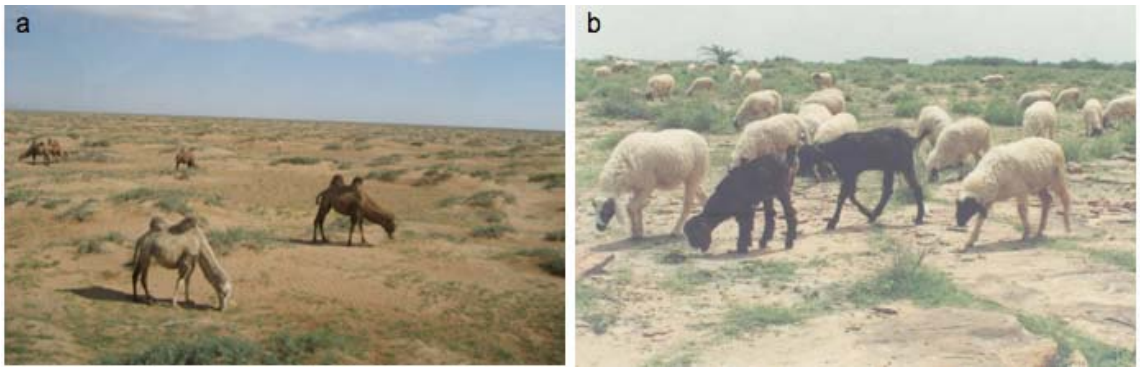


**Figure 1.2** Grazing as a cause of land degradation at desert margins (a) margins of the Badain Jaran Desert, Inner Mongolia, China and (b) margins of the Thar Desert in Rajasthan, India [source: (b) CAZRI, Jodhpur, India].

As desertification is considered to be a cause and a consequence of poverty [*UN Press Release*, 2003], the mitigation of desertification would induce the reduction of poverty in dryland areas [*MEA*, 2005]. In the case of the sub-Saharan Africa, climatic disasters (the series of droughts from the later 1960s) combined with weak economies and unsustainable use of marginal resources increased the stress on the dryland ecosystems [*Glantz*, 1987; *Hutchinson*, 1996], which were unable to sustain the demands of the increasing human population [*Drakoh*, 1998]. These factors caused famines and large-scale human migrations with important socio-economic and political consequences.

[*Glantz*, 1987; *Kassas*, 1977; *Mabbut and Wilson*, 1980; *Nnolli*, 1990; *Drakoh*, 1998]. Even though desertification affects over one-third of the world population; the factors contributing to desertification remain poorly understood [*Reynolds and Stafford Smith*, 2002]. Hence understanding the biophysical processes contributing to land degradation in drylands is motivated by the increasing need to estimate long-term changes in food supply, designing and evaluating soil conservation and land reclamation programs, assessing the rate of entrainment of dust in the atmosphere and its contribution to global climate change, and analyzing the effect of climate change and management scenarios on drylands.

## SHRUB ENCROACHMENT: A MANIFESTATION OF LAND DEGRADATION

The grasslands at the desert margins, which are very sensitive to external drivers like climate change, are areas affected by rapid land degradation processes [*Nicholson et al*., 1998]. The common form of land degradation at desert margins involves the rapid shift from grasses to woody plants, *i.e.*, the encroachment of woody plants into areas historically dominated by grasses, a process that will be here referred to as "shrub encroachment" [*Archer*, 1989; *van Auken*, 2000]. The encroachment of woody plants into grasslands at desert margins (Figure 1.3) can result from the complex interaction among several factors including climate change, increase in $CO_2$ concentration and anthropogenic disturbances [*Archer*, 1989; *Schlesinger et al*., 1990; *van Auken*, 2000]. The shrub encroachment process, thought to be irreversible and sustained by the biophysical feedbacks of desertification, results in the formation of a patchy landscape with nutrient rich shrub patches ("Islands of fertility") scattered among patches of grasses

and nutrient depleted bare interspaces [*Schlesinger et al*., 1990; *Okin and Gillette*, 2001]. These landscapes are characterized by increased erosion processes, mostly aeolian [*Okin and Gillette*, 2001; *Breshears et al*., 2003], which maintain and enhance the local heterogeneities in the system.

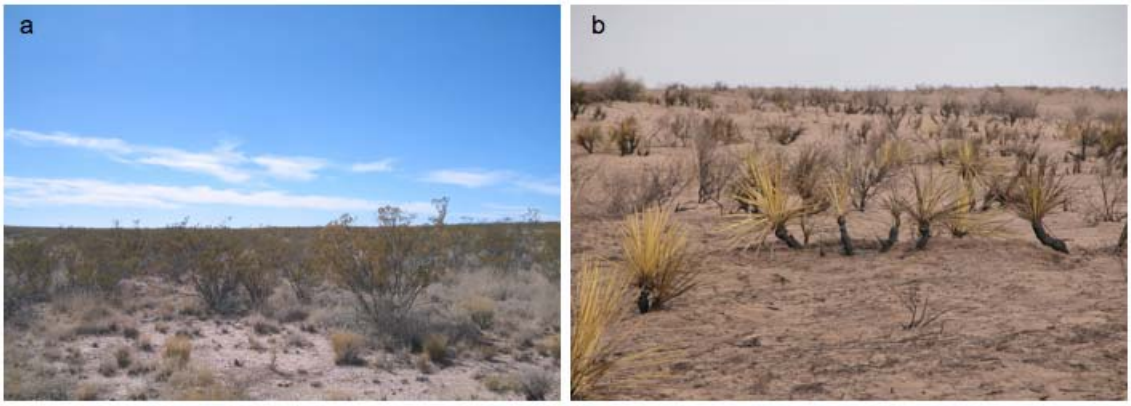


**Figure 1.3** Shrub encroachment into grasslands (a) Creosote bush in a black grama grassland at Sevilleta Wildlife Refuge, New Mexico, USA (b) Yuccas in a burned blue grama grassland at Cimarron National Grasslands in Kansas, USA.

A set of positive feedbacks has been invoked to explain the persistent and catastrophic character of land degradation dynamics as the result of a self-sustaining feedback loop [*Schlesinger et al*., 1990; *Anderies et al*., 2002]. For example, in the case of the southwestern United States, the introduction of cattle after European settlement led to an enhancement of mesquite seed dispersal, the degradation of the grass layer, and a reduction in fire frequency and intensity [*Archer*, 1989; *van Auken*, 2000]. These processes triggered a self-sustained cycle of erosion, depletion of soil resources, and vegetation loss in grass-dominated areas, while the encroachment of shrubs was favored by the deposition of nutrient-rich sediments transported by wind and water, and the consequent formation of fertile shrub patches (Figure 1.4). At the same time, loss in grass

fuel decreased the pressure of fires on shrub vegetation thereby further enhancing woody plant encroachment. Overall, this landscape-scale degradation is manifested as an increase in the heterogeneity in the spatial distribution of soil resources, microtopography and vegetation and by an increase in the extent of nutrient-depleted bare soil areas [*Schlesinger et al*., 1990; *Okin and Gillette*, 2001].

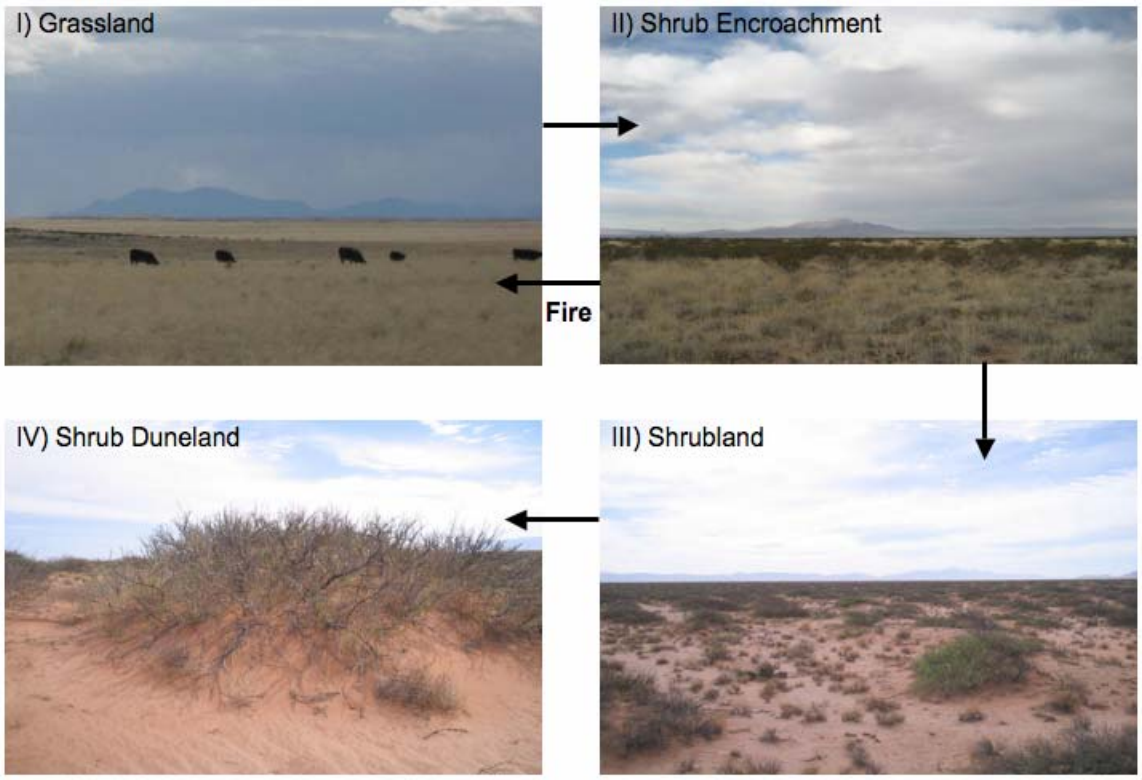


**Figure 1.4** Stages of grassland to shrubland conversion in the Chihuahuan Desert, New Mexico, USA.

Factors like fire suppression and overgrazing have presumably led to the dominance of woody plants. These processes resulted in grass mortality and subsequent loss of fuel load and grass connectivity, which further suppressed or limited fires in the system. Further, as the grass cover decreases, wind and water erosion increase in importance, eventually driving landscapes with sandy soils into a coppice duneland state

(Figure 1.4) [*Ravi et al*., 2007]. Figure 1.5 provides a schematic representation of the four conceptual states characterizing the transition from grassland to shrubland. The research presented in **this dissertation demonstrates the ability of fires to mitigate the early stages of land degradation associated with the shrub-grass transition state.** It will be shown how prescribed fire can counteract the resource hetereogeneity-forming dynamics of shrub encroachment process by enhancement of local scale resource redistribution resulting in post fire alteration in soil erosion rates.

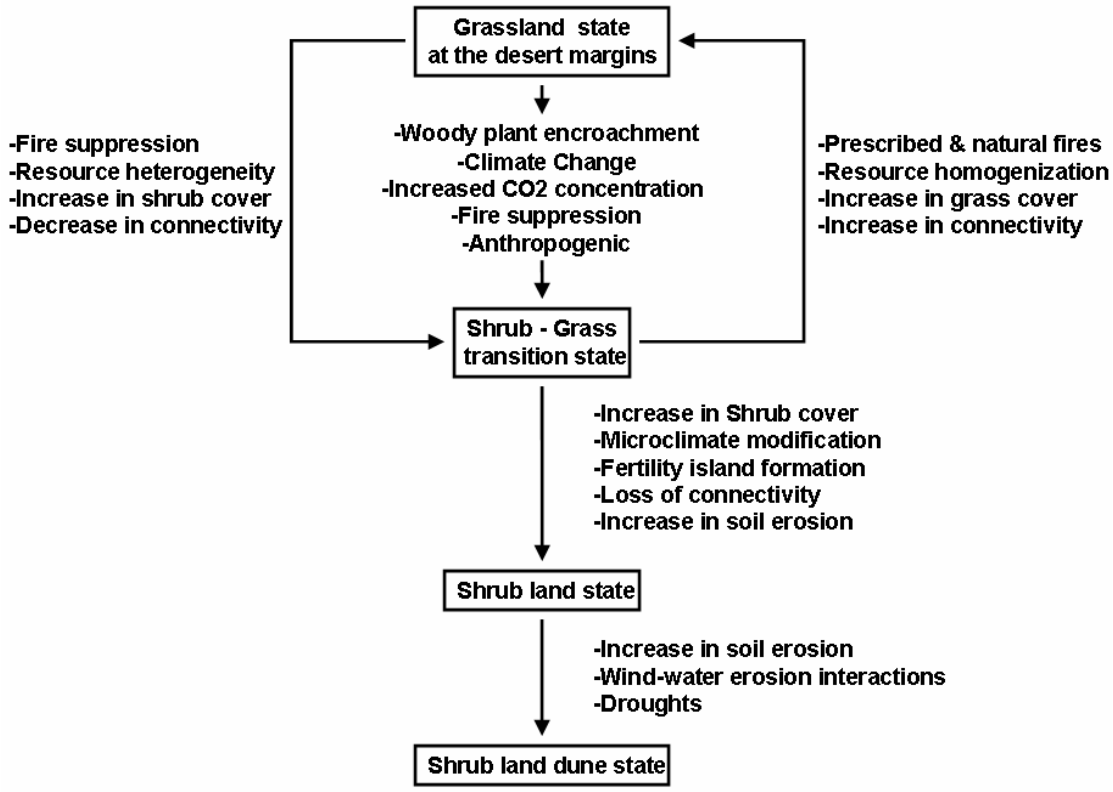


**Figure 1.5** Conceptual diagram of the grassland to shrubland transition.

## INTERACTIONS BETWEEN FIRES AND SOIL EROSION PROCESSES

In arid landscapes, soil erosion is mainly due to aeolian processes - as opposed to water erosion [*Breshears et al.,* 2003] - which maintain local heterogeneities in nutrient and vegetation distribution through the removal of nutrient-rich soil from intercanopy areas and subsequent deposition onto vegetation patches [*Schlesinger et al.,* 1990; *Okin and Gillette,* 2001]. Dryland systems are also prone to disturbances like fires and grazing which can render soils more susceptible to erosion processes. Fires affect the abundance and distribution of shrubs and grasses in arid ecosystems [*van Langevelde et al.,* 2003; *Sankaran et al.,* 2004]. Vegetation cover, in turn, affects the fire regime, in that both fire intensity and frequency depend on the relative abundance of shrubs and grasses [*Anderies et al.,* 2002]. Further, fires are known for having a major impact on infiltration, runoff and water erosion [e.g., *DeBano,* 2000; *Doerr et al*., 2000]. The post-fire increase in runoff and soil erosion is caused by the decrease in infiltration capacity resulting from fire-induced water repellency [*DeBano,* 2000; *Doerr et al*., 2000]. Hence, erosion processes can interact with disturbances such as fires to affect the rates of soil erosion and redistribution in these systems. This fact is especially important in the case of land degradation caused by encroachment of shrubs in the grasslands at the desert margins. At the early stages of the encroachment of desert grasslands by shrubs, there exists enough grass cover to carry the fires from one shrub patch to the neighboring patch. Thus fire-erosion feedbacks can be major factors in the redistribution of soil resources and the formation of spatial pattern in dryland vegetation. **While the effect of post-fire water repellency on runoff and water erosion is relatively well-understood, its impact on wind erosion, which is the dominant erosion process in these dryland landscapes,**

**has never been assessed before.** In this dissertation I will show that fire-induced soil hydrophobicity results in the enhancement of soil erosion in and around the shrub patches, which therefore become more erodible after the fire. By affecting the strength of interparticle wet-bonding forces, fire-induced water repellency enhances soil erodibility, causing a drop in wind erosion threshold velocity (the minimum velocity for erosion to occur). Thus, **I hypothesize that the mechanisms causing the enhancement of post-fire soil erodibility are induced by post-fire soil hydrophobicity.** These effects will be demonstrated by field experiments, and wind tunnel tests using both laboratory treated sands, and natural soils from areas affected by wildfires and prescribed burn experiments. A theoretical framework will be developed to explain the observed effects. Further, **I hypothesize that the enhancement of soil erosion after fires can lead to a decrease in the spatial heterogeneity of resources and alter the patchy structure of vegetation.**

Until recently the process of fertility island formation in the grassland to shrubland conversion was thought to be highly irreversible. However this study shows that there exists a very dynamic state of shrub-grass transition, in which fire may play a major role in determining the recovery of grasses. Hence the “fertility islands” are not necessarily static features of the landscape, but they can be dynamic. **This dissertation is particularly concerned with the fertility island dynamics resulting from the interaction between wind and fire. This study shows that fire-wind erosion feedbacks are major factors controlling spatial patterns of vegetation and soil resources in heterogeneous arid landscapes. The post fire enhancement of resource redistribution counteracts the heterogeneity-forming processes contributing to the emergence of fertility islands and the encroachment of shrub vegetation. Thus, the**

**interaction between fires and aeolian processes is thought to have a possible negative feedback on the encroachment of shrubs into desert grasslands.** Thus findings of this dissertation research also highlight the role of fire as a management tool in the early states of land degradation due to shrub encroachment.

## GOALS AND ORGANIZATION OF THIS DISSERTATION

**Major goals of this dissertation are:**

**1. TO DEMONSTRATE THE ROLE OF HYDROLOGIC AND AEOLIAN PROCESSES IN DETERMINING THE VEGETATION PATTERNS AND SOIL HYDROLOGIC PROCESSES IN ARID LANDSCAPES.**

- **(i)** Hydrologic and aeolian controls on vegetation patterns in arid landscapes: Coppice dune formation. **[Chapter 2]**
- **(ii)** Form and function of grass ring patterns in arid landscapes: the role of abiotic controls. Grass ring patterns. **[Chapter 3]**

**2. TO INVESTIGATE HOW, BY ALTERING THE SOIL EROSION RATES, FIRE-WIND EROSION INTERACTIONS MODIFY THE LANDSCAPE HETEROGENEITIES IN SHRUB ENCROACHED LANDSCAPES.** To this end plot-scale manipulative field experiments have been conducted in a shrub-grass transition zone in the Northern Chihuahuan desert. **[Chapter 4]**

## 3. TO DEMONSTRATE THE ROLE OF FIRE INDUCED WATER REPELLENCY IN THE POST FIRE ENHANCEMENT OF WIND EROSION

**(i)** **To investigate the effect of fire-induced water repellency on soil susceptibility to wind erosion using laboratory treated sands.** In this case wind tunnel measurements have been carried out on soils that have not been burned, but treated with chemical compounds to "artificially" induce water repellency. In case these soils exhibit higher erodibility we can conclude that repellency is capable of weakening interparticle bonding forces. **[Chapter 5]**

**(ii)** **To develop a theoretical framework to investigate and model the effect of water repellency on interparticle bonding forces and on the threshold velocity for erosion.** This framework mechanistically explains the dependence of soil erodibility on the water-soil contact angle for uniform spherical sand grains. **[Chapter 5]**

**(iii)** **To demonstrate the effect of fire induced water repellency on wind erosion in natural soils.** For this part of the study I have collected soil samples from areas affected by major burns (Cimarron National grasslands, KS) and tested them in a wind tunnel to show that fires indeed decrease the threshold shear velocity. To assess whether the increase in erodibility in the burned areas is due to fire-induced water repellency, a number of laboratory tests have been carried out to measure soil water repellency in the burned soils and in the controls. **[Chapter 6]**

**(iv)** **To modify the theoretical framework for the case of natural soils.** Natural soils are not necessarily composed of well-rounded grains as in the

assumption made in the laboratory study. Hence the theoretical framework has been modified for a more general soil geometry. **[Chapter 6]**

**(v) To investigate the importance of vegetation types on fire-erosion interactions**: The effects of fires on wind erosion thresholds in different ecosystems have been assessed (and compared) for different vegetation types: A grassland and a shrubland at the Cimarron National grasslands (Kansas) and a heterogeneous patchy landscape with shrubs, grasses and bare interspaces at the Sevilleta Wildlife Refuge (New Mexico)**. [Chapter 7]**

**4. EFFECT OF WIND AND FIRES AT THE FIELD TO LANDSCAPE SCALE: FERTILITY ISLAND DYNAMICS**

**(i) To model the possible impact of fire-wind erosion interactions on vegetation dynamics and the effect of vegetation composition/structure on soil erodibility**. The effects of fire-wind erosion interactions on the stability and resilience of fertility island systems have been investigated using a spatially explicit cellular automata model. **[Chapter 8]**

# CHAPTER: 2

# HYDROLOGICAL AND AEOLIAN CONTROLS ON VEGETATION PATTERNS IN ARID LANDSCAPES

(This paper is published in *Geophysical Research Letters*)


## Abstract

Hydrological and aeolian processes redistribute sediments and nutrients within arid landscapes with important effects on the composition and structure of vegetation. Despite the relevance of wind and water erosion to the dynamics of arid and semiarid ecosystems, the interactions between these two processes remain poorly understood. In this chapter we present the results of an intensive set of infiltration experiments from the Chihuahuan Desert, showing that in this system the infiltration capacity under the shrub canopy is lower than that at the outer edges of the vegetated patches. Hence, runoff is more likely to occur from the middle of these shrub-dominated areas to the edges. These experimental results show that the differential rates of soil deposition and removal by aeolian processes result in differential rates of hydrological processes such as infiltration and runoff with important implications for the formation and expansion of mesquite dunes in arid landscapes.

## 1. Introduction

Hydrological and aeolian processes redistribute sediments and nutrients within arid landscapes with important implications on the composition and structure of vegetation. The interactions between these processes are thought to play a major role in the conversion of disturbed desert grasslands into shrublands, with possible impacts on regional climate and desertification [*Schlesinger et al.*, 1990]. Aeolian processes, which are presumably the dominant mechanism of soil detachment and transport in many arid environments [*Breshears et al*., 2003], are largely responsible for the removal of nutrient-rich soil particles from the intercanopy areas and the deposition onto shrub patches [*Li et al*., 2007]. This sediment redistribution leads to the accumulation of nutrients under the shrub canopies, a process known as "fertility island formation" [*Schlesinger et al.*, 1990]. Thus, the landscape exhibits a mosaic of sources and sinks, with bare soil interspaces acting as sources and vegetated patches as sinks of nutrients and sediments [*Virginia and Jarrell*, 1983; *Puigdefabregas*, 2005]. Through their impact on the soil moisture regime, hydrological processes such as infiltration and runoff determine the conditions favorable for the establishment and survival of different vegetation functional types, with a consequent impact on the structure and function of water-limited ecosystems [*Thurow et al.*, 1986; *Bhark and Small*, 2003]. Thus, wind erosion maintains and enhances the local heterogeneities in nutrient and vegetation distribution existing in arid landscapes, while hydrological processes, such as infiltration and runoff, control soil water availability with important effects on the successful establishment and growth of dryland vegetation.

The heterogeneity in vegetation and resource distribution determines the heterogeneity in the spatial distribution of soil infiltration capacity, runoff and erosion rates [*Puigdefabregas*, 2005], which, in turn, result in the formation of areas of hydrologically enhanced plant productivity [*Rango et al.*, 2006]. The biological response to water availability is also heterogeneous, due to the differences in plant and soil characteristics typically existing within a patchy landscape [*Rango et al*, 2006; *Wang et al*., 2007]. Positive feedbacks between vegetation and surface soil moisture [*Breman and Kessler*, 1995] may further enhance heterogeneities in vegetation and soil distribution, contributing to the emergence of alternative stable states in dryland vegetation [*Walker et al*., 1981, *Rietkerk and van de Koppel*, 1997] and vegetation pattern formation [e.g., *Lefever and Lejeune*, 1997; *van de Koppel et al*., 2002; *D'Odorico et al*., 2006]. In fact, the wetter surface soils existing under the canopy may facilitate vegetation establishment, while the drier soil in the interspaces may prevent vegetation growth.

Even though, the role of hydrological [*Reid et al*., 1999; *Neave and Abrahams*, 2002; *Bhark and Small*, 2003] and aeolian processes [*Okin and Gillette*, 2001; *Ravi et al*., 2004; *Li et al*., 2007] in the dynamics of dryland ecosystems has been well documented, very few studies have addressed how the interactions between these processes affect fertility island dynamics. Until recently, the common understanding of sediment redistribution and transport processes in desert shrublands was based on the notion that runoff originating from bare soil interspaces converges towards the "vegetated islands", thereby leading to the deposition and accumulation of nutrient-rich sediments beneath the canopy. Previous studies on infiltration rates in these landscapes have rarely considered the variations in infiltration rates within the shrub-dominated resource islands. Here, we

show, through a an extensive series of infitrometer measurements and laboratory analyses, that the infiltration rates inside the fertility islands may be lower than the outer edges, indicating that runoff occurs also from the center of these islands to the outer edges. This investigation shows that the differential rates of soil deposition and removal by aeolian processes, which results in differential rates of hydrological processes such as infiltration and runoff, may be responsible for the formation and expansion of mesquite dunes in arid landscapes.

## 2. Materials and methods

The study site was a honey mesquite (*Prosopis glandulosa*) dominated shrubland at the USDA ARS Jornada Experimental Range (+32.5 N, -106.8W), located in the northern Chihuahuan Desert, near Las Cruces, NM. The infiltration experiments and soil sampling were conducted during the dry period of the year (April - May 2006). The mesquite mounds in the study sites were unevenly distributed with bare interspaces of 3-5 m separating the mounds. Infiltration rates were measured using a mini disk infiltrometer (Decagon Devices, Pullman, Washington) using a suction of 2 cm. The mini disk infiltrometer is ideal of this kind of situations as it requires small amounts of water for its operation (135ml), and is small enough to measure infiltration at several points within the vertical projection of shrub canopies. Infiltration was measured upwind, in the middle and downwind from each mesquite and also in the bare interspaces, where the upwind and downwind positions were determined using long-term wind data of Helm and Breed [*Helm and Breed*, 1999]. More than hundred infiltration tests were performed around 30 mesquite mounds (total) and bare interspaces in two selected areas (more than

100m apart). The mesquite mounds selected for the study were further classified based on the height of the mound (height of the center of the mound with respect to the bare interspaces) into small mounds (ht < 15cm) and large mounds (ht > 15cm). The dimensions of mesquite shrubs (length, width, height) and mound (height of the mound) were also measured. The height of the mounds varied from 5cm to 30 cm and the shrubs on the mounds were 0.5m - 1 m tall and 1m to 3 m wide. Soil samples (top 5 cm) were collected from upwind, center and downwind of the shrubs.

Soil texture was determined using the standard hydrometer method [*ASTM D422*, 1981]. A soil hydrometer (Fisher brand Specific Gravity Scale Soil Hydrometer) was calibrated to measure the specific gravity of the soil suspension; the size fractions (wet method) were calculated based on the settling time of the suspended particles (Table 2.1). The particle size fractions (dry method) at the center of shrub islands and bare interspaces were compared using Ro-Tap Test sieve shakers (W.S. Tyler) which provides accurate and consistent particle size analysis in five particle size classes (45, 125, 250, 355, 500 microns). Total soil carbon and nitrogen were determined using the standard combustion method [*Gavlak et al.*, 1994]. To investigate how differences in infiltration rates and nutrient content change with the development of the dunes/mounds, the results of all these measurements are reported separately for small (i.e., <15 cm ht) and large (i.e., >15 cm ht) dunes. Statistical tests (single factor ANOVA) were carried out to show that the differences in particle size distribution and nutrient contents were significantly different upwind, in the center and downwind of the mesquite mounds.

## 3. Results

The infiltrometer measurements show that the infiltration rates are lower in the center of the shrub mounds compared to upwind and downwind areas (Figure 2.1.a). The downwind areas of the shrub mounds had lower infiltration rates compared to the upwind areas.

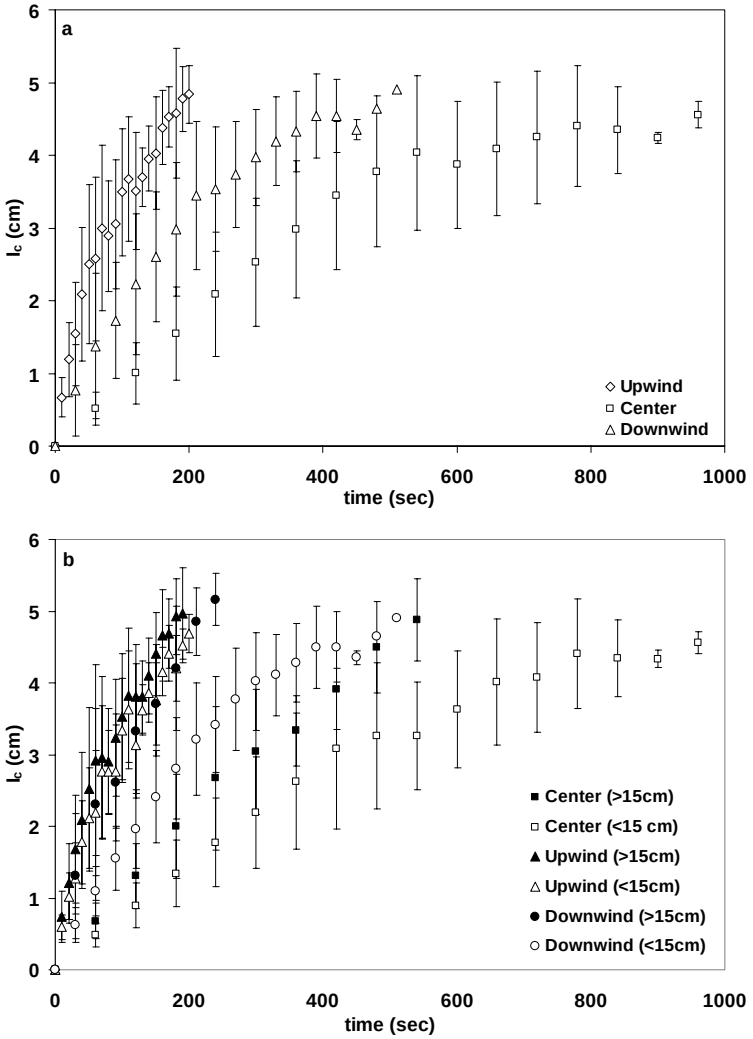


**Figure 2.1** (a) Average infiltration rates at the upwind, central and downwind locations for all the shrubs mounds considered in the study. (b) Comparison of average infiltration rates at upwind, central and downwind locations in big and small mounds

This heterogeneity of infiltration rates are more noticeable in the case of small mounds (<15 cm) when compared to large shrub mounds (> 15cm), clearly indicating the dependence of infiltration rates on mound height and development stage (Figure 2.1.b).The infiltration rates in the bare interspaces were generally found be lower than the upwind areas of the shrub mounds. However the interspace infiltration rates were very inconsistent depending on the soil surface crust characteristics. The results from the Ro-Tap Test sieve shakers show that there is more accumulation of finer particles (clay, silt, very fine sand, and fine sand) in the center of the mesquite mounds compared to the bare interspaces (Figure 2.2).

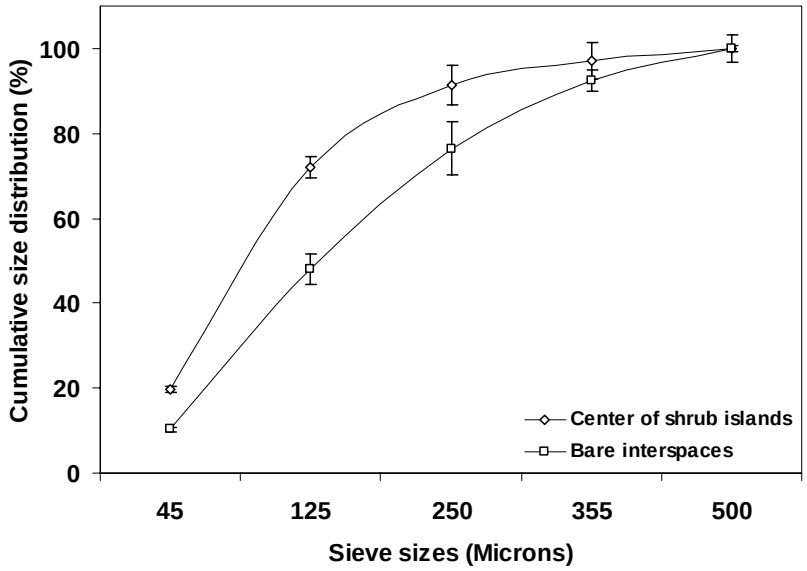


**Figure 2.2** Accumulation of finer particles at the center of the shrub mounds compared to the bare interspaces (Using Ro-Tap Test sieve shakers)

The soil particle size distribution using the hydrometer method shows that there was a significant variation (based on a single factor ANOVA, *P-value* < 0.0002 for both sand and fines (silt and clay)) in particle size distribution between the upwind, center and downwind areas of the shrub mounds. The average sand content in the center of the shrub

mounds was 88 % (considering all shrubs studied), while fine particles (silt and clay) were 13%. In contrast, the upwind areas of the dunes had on average 94% sand content and 7% content of fine particles. The downwind side showed an intermediate particle size distribution with 91% average sand content and 10% of fine particles.

**Table 2.1** Textural and nutrient status of the soils used in this study (standard deviation values in brackets)

| | | Particle size (%) | | | Nutrient status (%) | |
|---|---|---|---|---|---|---|
| | | Sand | Silt | Clay | Total N | Total C |
| Shrubs with small mounds ( < 15 cm) | Upwind | 92.2 (1.4) | 2.7 (1.2) | 5.3 (1.6) | 0.039 (0.008) | 0.324 (0.038) |
| | Center | 84.8 (4.4) | 7.4 (4.0) | 7.8 (3.0) | 0.110 (0.023) | 1.006 (0.221) |
| | Downwind | 89.4 (2.6) | 4.4 (2.6) | 6.1 (1.6) | 0.040 (0.006) | 0.352 (0.048) |
| Shrubs with large mounds ( > 15 cm) | Upwind | 94.4 (1.4) | 1.6 (1.0) | 4.0 (1.6) | 0.033 (0.011) | 0.199 (0.056) |
| | Center | 91.0 (1.2) | 4.0 (2.0) | 5.0 (1.8) | 0.064 (0.008) | 0.477 (0.101) |
| | Downwind | 91.6 (2.7) | 3.6 (2.7) | 4.8 (1.6) | 0.038 (0.013) | 0.266 (0.067) |
| Bare interspaces | | 95.01 (1.05) | 1.07 (0.78) | 3.93 (1.26) | 0.019 (.007) | 0.173 (0.075) |

The corresponding values of saturated hydraulic conductivity (k) were calculated using the method proposed by Zhang (1997), for dry soils. The value of k at the center bare patches ($8 \times 10^{-5}$ cm/sec) were significantly smaller than those at microsites located in upwind ($1.9 \times 10^{-3}$ cm/sec) and downwind areas ($4.4 \times 10^{-4}$ cm/sec). The middle of the mounds had higher concentration of fine particles (silt and clay) and lower sand content compared to upwind and down wind areas of the mounds.

Even though this significant variation in particle size distribution between the upwind, center and downwind areas of the shrub mounds was noticed in both small mounds (*P-value* < 0.001 for both sand and fines) and large mounds (*P-value* < 0.009 for both sand and fines), the variation in particle size distribution was more noticeable in the case of small mounds compared to large mounds (Table 2.1). The total soil carbon and nitrogen contents were higher in the center of the shrub mounds compared to upwind and downwind areas (and bare interspaces), consistent with the notion of "fertility islands" formation (Table 2.1). The statistical test (single factor ANOVA) confirmed that the total nitrogen (*P-value* < 0.0004) and total carbon (*P-value* < 0.001) are significantly different for the center, upwind and downwind of the shrubs.

**4. Discussion**

The infiltration experiments show that, even though infiltration rates in the fertility island are greater than in bare interspaces consistently with previous studies [*Bhark and Small*, 2003; *Rango et al.*, 2006], a wide variation exists within these vegetated islands, with the infiltration rates being significantly lower in the center than in the upwind and down wind locations. This is explained by the higher clay and silt content

in the center of the shrub mounds compared to the edges (Table 2.1) and by the ability of vegetation to enhance soil infiltration capacity (e.g., due to the presence of roots, macropores, organic matter). The average sand content in the center of the shrub mounds (considering all shrubs studied), were lower than the upwind areas of the mounds, while fine particles (silt and clay) showed the reverse trend. The downwind side showed an intermediate particle size distribution, probably due to the settling of fine particles in the wake of the wind stream. The variation in particle size distribution and the associated variations in infiltration rates between these areas within the shrub mounds are more prominent in the case of small mounds (height < 15 cm) compared to large mounds (height >15 cm). The results from this study suggest that water redistribution occurs down slope from the center of the dunes to the edges (upwind and down wind areas) where infiltration occurs at a higher rate. Mesquite roots extend to the upwind, downwind areas and also to the bare interspaces, so the shrubs can still exploit water infiltrating outside of the vertical projection of their canopy. Further, the higher run off from the nutrient rich center of the dunes to the edges also results in the transport of nutrients to the outer edges. The nutrient data (Table 2.1) indicates that the centers of the shrub mounds have a higher nutrient content than the upwind and downwind areas.

Our data suggest that fine sediments are redistributed by aeolian processes from the interspaces onto the vegetated islands (mesquite dunes), where they remain sheltered by the shrub vegetation. This process leads to the formation of an area of fine textured soils with higher concentration of wind borne fines (hence with lower infiltration rate) inside the shrub patch (Figure 2.2). The differential redistribution of soil particles on to the vegetation by aeolian and hydrological processes can create textural changes in and

around the vegetation which can alter the infiltration and runoff processes, as surface soil texture (top few centimeters) is thought to be a major factor determining the rate of water infiltration in to the soil [*Wood et al*., 1987, *Bestelmeyer et al*., 2006]. Due to slower infiltration within these patches, runoff likely occurs from the middle of mesquite mounds toward the edges where it likely infiltrates at the outer edges of the mound. Thus the outside of mesquite mounds are ideal sites for the uptake of water by the existing plants or growth and establishment of new plants, especially in the case of nitrogen-fixing shrubs like the mesquites, which are less sensitive to nitrogen limitations (Figure 2.3). As the mound grows, however, runoff-driven redistribution of sediments from the middle to the edges of the dune appears to cause a decrease in the differences in soil texture, soil hydraulic properties, and nitrogen content between the center and the edges of the dunes. While these differences decrease with the dune age, gravity-driven redistribution of water as overland flow remains within the bigger mounds, with the dune edges becoming preferential sites for water uptake and plant growth. These interactions between windborne sediment patterns and water infiltration and redistribution results in the outward growth of vegetation, both in the upwind and downwind directions. This outward growth pattern creates bare open spaces within the shrubs. Similar growth pattern of dune vegetation was observed in previous studies [e.g. *Shen*, 1988; *Fearnehough et al.*, 1998] in the stabilized desert dunes of Northern China, where the deposition of finer soils resulted in considerable changes in soil texture. The retention of moisture at the surface by the finer soils existing at the center of the mounds combined with the formation of physical and biological soil crusts [*Danin et al.*, 1989] resulted in the decline of planted shrubs [*Shen*, 1988]. As this barren area in the middle of a shrub

patch increases in size, its ability to retain fine particles decreases. This fact contributes to the explanation of why, compared to small mounds, big mounds exhibited smaller differences in particle size distribution and hence in infiltration rates among upwind, central and downwind areas.

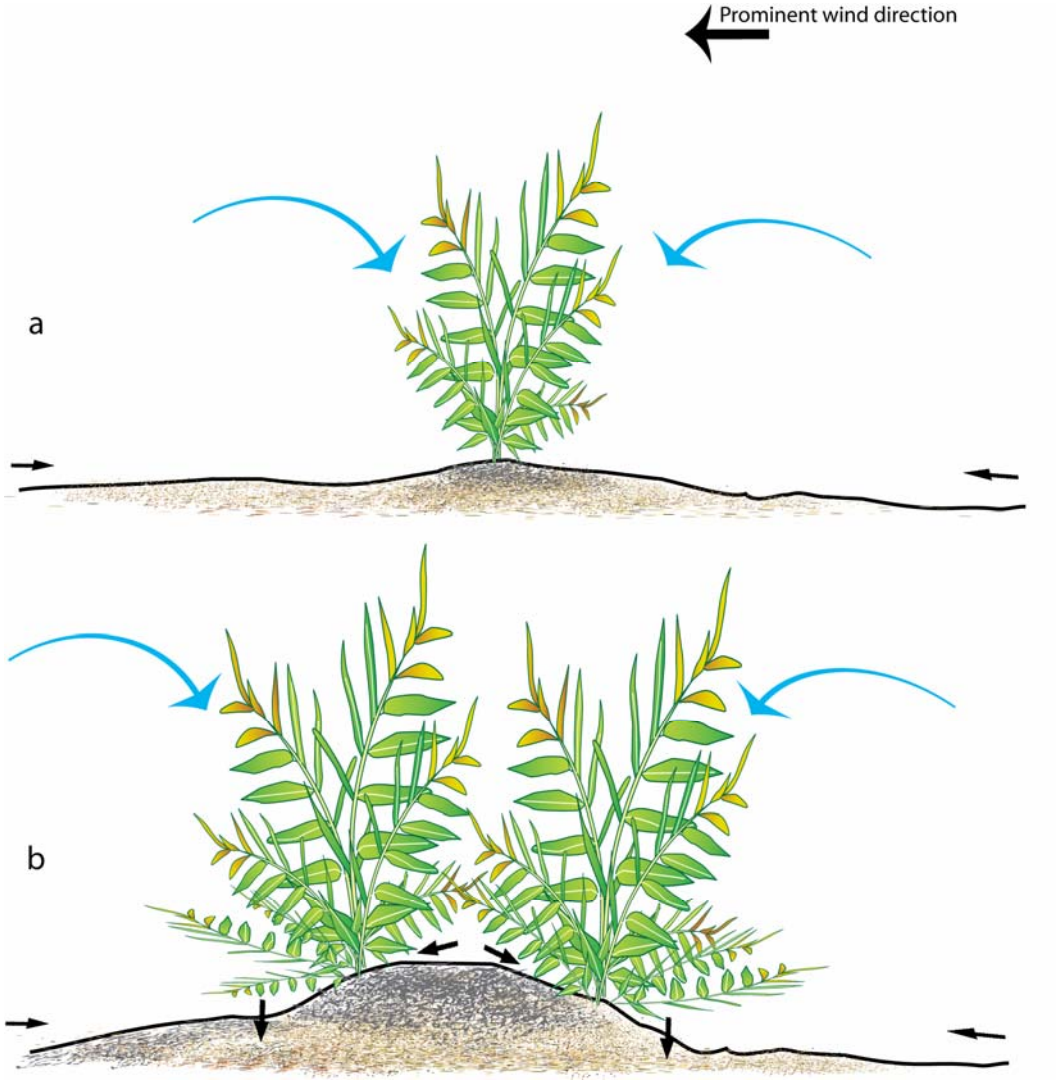


**Figure 2.3** Conceptual diagram showing the interaction of hydrological and aeolian processes (straight black arrows indicates hydrological processes and curved grey arrows indicate aeolian processes). (a) Diagram showing the formation of islands of fertility around the shrub by the deposition of wind borne fines. (b) Diagram showing the changes in hydrologic processes (infiltration and runoff) which results in changes in the growth patterns of the shrubs.

## 5. Conclusions

In the case of the system investigated in this study, runoff generation does not tend to augment the size of coppice dunes. These patterns are best explained by the deposition/accumulation of wind-borne (finer) sediments onto mesquite dunes. Runoff contributes to the redistribution of water and nutrient-rich sediments from the middle to the edges of the dune, and to the consequent preferential establishment/growth of mesquite shrubs at the edges. Thus the formation and development of coppice dunes, and of associated vegetation patterns results from the interaction between hydrologic and aeolian processes. Mesquite shrubs contribute to coppice dune formation and augmentation by the differential trapping of fine wind-borne sediments among areas located at the center, upwind and downwind of the shrub. Even though the center of shrub mounds is richer in nutrients due to the aeolian deposition of fine sediments, the observed patterns of vegetation growth at the mound edges indicate that shrub establishment and growth is controlled by hydrologic processes. Due to the lower water infiltration and elevated runoff, the center of the mounds is not a preferred site for this vegetation, when compared with the mound edges, where soils exhibit higher infiltration capacity and elevated run-on rates. Thus, the interaction of aeolian processes with a sparse shrub cover leads to heterogeneity in soil texture and soil hydrological processes (infiltration, runoff and soil moisture), which in turn affect vegetation growth patterns.

# CHAPTER: 3

# FORM AND FUNCTION OF GRASS RING PATTERNS IN ARID GRASSLANDS: THE ROLE OF ABIOTIC CONTROLS

(This chapter is in review for publication in *Oecologia*)

## Abstract

Ring shaped growth patterns commonly occur in resource-limited arid and semiarid environments. The spatial distribution, geometry, and scale of vegetation growth patterns result from interactions between biotic and abiotic processes, and, in turn, affect the spatial patterns of soil moisture, sediment transport, and nutrient dynamics in aridland ecosystems. Even though grass ring patterns are observed worldwide, a comprehensive understanding of the biotic and abiotic processes that lead to the formation, growth and breakup of these rings is still missing. Our studies on patterns of infiltration and soil properties of blue grama (*Bouteloua gracilis*) grass rings in the northern Chihuahuan desert indicate that ring patterns result from the interaction between clonal growth mechanisms and abiotic factors such as hydrological and aeolian processes. These processes result in a negative feedback between sediment deposition and vegetation growth inside the bunch grass, which leads to grass die back at the center of the grass clone. We summarize these interactions in a simple theoretical and conceptual model that integrates key biotic and abiotic processes in ring formation, growth and decline.

## 1. Introduction

Vegetation patterns such as bands [*Leprun*, 1999; *Valentin and d'Herbes*, 1999; *Yizhaq et al.*, 2005], stripes [*White*, 1971; *Janeau et al.*, 1999; *Ludwig et al.*, 1999], spots [*Couteron and Lejeune*, 2001] and rings [*Cosby*, 1960; *Lewis et al.*, 2001; *Sheffer et al.*, 2007] are a recurrent characteristic of resource limited arid and semi-arid landscapes [*Greigsmith*, 1979; *HilleRisLambers et al.*, 2001; *Rietkerk et al.*, 2002]. Interactions between surface soil moisture, erosion processes, and vegetation are thought to be the major factors responsible for the formation of these patterns [*Valentin et al.*, 1999]. The geometry, spatial distribution and scale of vegetation pattern, which result from interactions between biotic and abiotic processes, affect the spatial patterns of soil moisture, sediments and nutrients in these landscapes [*Puigdefabregas*, 2005; *Bautista et al.*, 2007; *Ludwig et al.*, 2007]. The spatial distribution of water and sediments, in turn, determine plant growth, root biomass and species composition [*Valentin et al.*, 1999]. Thus, vegetation patterns can be considered as biological indicators of abiotic processes such as runoff and infiltration, and of source-sink areas for sediments in dryland landscapes [*Imeson and Prinsen*, 2004]. Further, changes in vegetation patterns are thought to be easily recognizable signs of environmental change (e.g., desertification) in degraded arid landscapes that are sensitive to climate fluctuations and prone to anthropogenic disturbances [*von Hardenberg et al.*, 2001; *van de Koppel et al.*, 2002; *Scanlon et al.*, 2007]. On the other hand abiotic controls, such as hydrologic [*Reid et al.*, 1999; *Neave and Abrahams*, 2002] and aeolian processes [*Ravi and D'Odorico*, 2005; *Okin et al.*, 2006; *Li et al.*, 2007], determine the conditions favorable for the establishment and growth of vegetation, with consequent impacts on the structure and

function of these resource-limited ecosystems [*Bhark and Small*, 2003; *D'Odorico et al.*, 2007; *Ravi et al.*, 2007]. Hence, information on the formation, structure and growth of these vegetation patterns and the analysis of their interactions with abiotic controls can improve our current understanding of important processes underlying the dynamics of arid and semi-arid ecosystems [*Turner*, 1989].

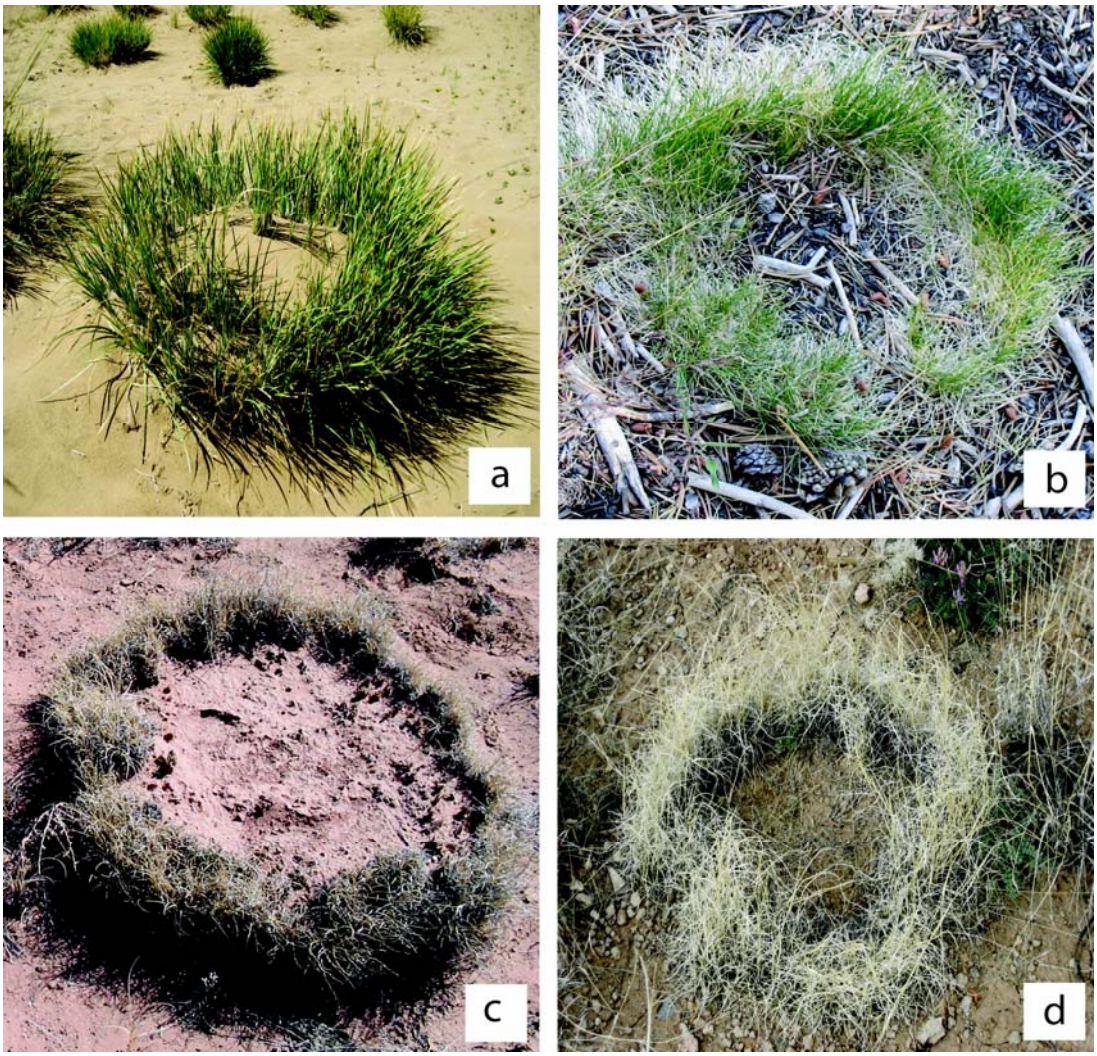


**Figure 3.1** Ring patterns in arid regions: (a) *Achnatherum splendens (Trin.) Neveski* in Inner Mongolia, China (b) *Carex spp. in* Yosemite National Park, California, USA (c) *Bouteloua gracilis* and (d) *Muhlenbergia arenicola* in Sevilleta Wildlife Refuge, New Mexico, USA. These rings are approximately 30-60 cm in diameter.

Ring patterns (Figure 3.1) of varying sizes are formed by clonally reproducing grasses, sedges and even shrubs growing in resource (i.e., water and/or nutrient) limited environments [*Cosby*, 1960; *Lewis et al.*, 2001; *Sheffer et al.*, 2007]. Even though grass ring patterns are observed worldwide [*Watt*, 1947; *Cosby*, 1960; *Danin and Orshan*, 1995; *Adachi et al.*, 1996; *Wan and Sosebee*, 2000; *Lewis et al.*, 2001; *Wikberg and Svensson*, 2003; *Bonanomi et al.*, 2005; *Sheffer et al.*, 2007], a comprehensive understanding of the biotic and abiotic processes that lead to the formation, growth and breakup of these patterns is still missing. Several theories have been put forward to explain the formation of grass ring patterns such as those based on changes in plant growth architecture or developmental morphology [*Danin and Orshan*, 1995], negative soil-plant feedbacks [*Bonanomi et al.*, 2005], the effect of soil borne pathogens [*Packer and Clay*, 2000] and external disturbances such as fires [*Lewis et al.*, 2001]. Negative soil-plant feedbacks (i.e., the negative interactions between plant growth and soil resource distribution that locally inhibit vegetation growth), are examples of mechanisms contributing to plant-induced soil heterogeneity. The negative feedbacks invoked to explain grass ring patterns include mechanisms of resource depletion at the center of a grass clump caused by interspecific competition patterns [*Bonanomi et al.*, 2005], changes in abiotic factors [*Castellanos et al.*, 1994], release of allelopathic compounds by grasses [*Gatsuk et al.*, 1980; *Wikberg and Mucina*, 2002] and litter accumulation in the center of a vegetation patch [*Wan and Sosebee*, 2000]. However few studies have addressed the negative plant-soil feedbacks resulting from the interaction between vegetation and hydrological-aeolian processes [*Ravi et al.*, 2007]. Recent studies on spatial patterns of infiltration and soil properties in Chihuahuan Desert mesquite

shrublands [*Ravi et al.*, 2007] indicated that differential rates of soil deposition and removal by aeolian processes result in differential rates of hydrological processes, such as infiltration and runoff, with important implications on the formation and expansion of coppice dunes [*Ravi et al.*, 2007]. Even though several studies have investigated soil moisture and infiltration patterns in blue grama grasslands [*Rauzi and Smith*, 1973; *Wood et al.*, 1986; *Vinton and Burke*, 1995; *Hook and Burke*, 2000; *Pierson et al.*, 2002;], little is known about the spatial and temporal variability of infiltration inside a grass ring. In this paper we aim to describe a negative soil-plant feedback associated with grass ring patterns resulting from the three-way interaction among vegetation, hydrological and aeolian processes. Further, a simple theoretical model is developed to explain the role of abiotic factors such as soil erosion and sediment deposition in ring initiation and growth. To date, such feedbacks between vegetation and soil erosion processes have not been fully accounted for by existing models of pattern formation in dryland vegetation.

## 2. Materials and methods

The study site was a blue grama (*Bouteloua gracilis*) dominated grassland at the Sevilleta National Wildlife Refuge, located in the northern Chihuahuan Desert, near Socorro, New Mexico, USA (N 34$^{o}$ 23.961$^{'}$, W 106$^{o}$ 55.710'). Blue grama is a long-lived, grazing-tolerant, native, perennial $C_4$ bunchgrass characterized by a shallow fibrous root system [*Bowman et al.*, 1985; *Weaver*, 1958]. Foliage height ranges from 15-30 cm and root depth ranges from 1-2 meters. Soil nitrogen (N) and carbon (C) availability and soil moisture infiltration are greater beneath clumps of blue grama than under adjacent patches of soil (*Vinton and Burke*, 1995; *Hook and Burke*, 2000). In arid

regions, as seed propagation is limited, vegetative reproduction by way of tillers is common, subject to resource (moisture) and "bud bank" limitations [*Hyder et al.*, 1971; *Briske and Wilson*, 1977; *Dalgleish and Hartnett*, 2006; *Lauenroth et al.*, 1994]. The grass rings in the study sites were unevenly distributed with soil interspaces of 0.2 to 0.5 m separating the rings.

More than one hundred infiltration tests were performed inside and at the outer edges of a total of 40 grass rings and interspace soils at three selected sites (more than one kilometer apart) during dry periods of the year (April and July 2007). Infiltration rates were measured using a mini disk infiltrometer (Decagon Devices, Pullman, Washington), which measures the amount of water infiltrating into the soil in a given time interval. This infiltrometer, with an adjustable suction (0.5 to 7 cm), consists of a 32.7 cm long water reservoir with a porous stainless steel disc (4.5 cm diameter and 3 mm thick) at the base. The minidisk infiltrometer is ideal for measuring the variability of infiltration rates and hydraulic conductivity within a grass ring because of its small size and very small water requirement for its operation (135 ml). Infiltration was measured using a suction of 2 cm in the center and near the outer edges of a ring, and in the soil interspaces between plants. The infiltration data were used to calculate the saturated hydraulic conductivity ($K_{sat}$) of these dryland soils following the methods of Zhang (1997), which is ideal for dry soils [*Zhang*, 1997].

Volumetric soil moisture was measured inside and outside the grass ring using a Hydrosense water content meter (Decagon Devices, INC, Pullman, USA). This instrument calculates volumetric soil moisture content using dielectric permittivity measurements of the soil around its probe rods (12 cm long), which can be directly

related to water content. Diameter and height of the rings (compared to interspaces) were also measured. Soil samples (top 5 cm) were collected from the center and outside edge of the ring and also from interspace soil between rings.

Soil texture (percentage of sand, silt and clay) was determined using the standard hydrometer method [*ASTM*, 1981]. A dispersed soil sample (40g of oven dried soil) was mixed with water in a graduated glass cylinder (1000ml) and allowed to settle. A soil hydrometer (Fisher brand Specific Gravity Scale Soil Hydrometer) was calibrated to measure the specific gravity of the soil suspension. The size fractions were calculated based on the settling time of the suspended particles. The percentage by weight of sand, silt and clay in the solution was determined by taking hydrometer readings at 3 seconds and 2 hours after the onset of the sedimentation process. Subsamples of soils were analyzed for total organic Carbon (TOC) and total Nitrogen (TN). These subsamples were oven dried at 60$^{o}$C in the laboratory, sieved to 2 mm and homogenized using a mortar and pestle. TOC and TN, expressed as percent by mass, were measured using an Elemental Analyzer (EA, Carlo Erba, NA1500, Italy) [*Wang et al.*, 2007]. To investigate how differences in infiltration rates and particle size distribution change with the development of the grass rings, the results of all these measurements are reported separately for small (0.1 to 0.3 m), medium (0.4 to 0.6 m) and large (0.7 to 1.0 m) diameter rings.

Statistical tests (using SAS v. 9.1, SAS Institute Inc, Cary, NC) were used to determine if hydraulic conductivity, particle size distribution, soil moisture, TOC and nutrient contents differed between the inside and outer edges of grass rings. A Kolmogorov-Smirnov test [*Jackson and Caldwell*, 1993] was used to determine if soil

variables differed among ring size groups (e.g., large rings vs. small rings). Soil texture differences between inside and outside of small, medium and large rings were tested using single factor ANOVA. The significance level used for all statistical tests was $\alpha$=0.05.

**3. Results**

The infiltrometer measurements showed that overall the infiltration rates were higher at the edges of the grass rings compared to interspace soils between the rings. This result was consistent irrespective of the size of the ring. The hydraulic conductivity (saturated) values were much lower in the soil interspaces (avg 0.0019 cm/sec) compared to outer edges of the rings (avg 0.006 cm/sec). However, the infiltration rates varied within the rings, with the center of the rings having lower infiltration rates compared to the outer edges (Figure 3.2). This heterogeneity in infiltration rates was stronger in medium sized rings compared to small and large rings. Infiltration rates inside and outside of large rings were comparable. Hydraulic conductivity values calculated from the infiltration data indicated that hydraulic conductivity was higher at the outer edges of the rings compared to the centers (Figure 3.3). The hydraulic conductivity values between the center and outer edges of the rings were significantly different (using KS test) in small ($p$-value = 0.006) and medium sized rings ($p$-value = $8.2 \times 10^{-5}$), but not in large rings ($p$-value = 0.14). In addition, soil moisture content was significantly higher in the outer edges of the rings compared to the center (Figure 3.4) for both medium and large sized rings in both April ($p$-value = 0.0091) and July ($p$-value = $5.83 \times 10^{-4}$).

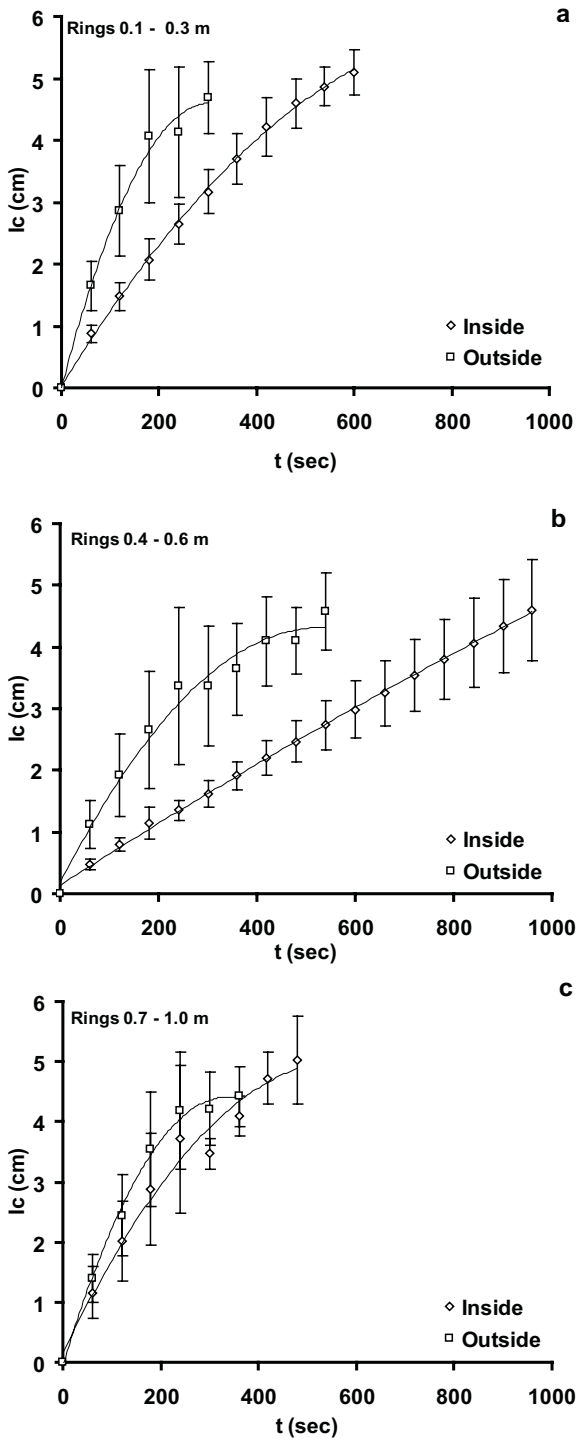


**Figure 3.2** Average infiltration rates at inner side and outer edges of the grass rings in three size classes: Small rings (0.1 to 0.3 m), medium rings (0.4 to 0.6 m) and large rings (0.7 to 1.0 m). Error bars indicate the standard deviation of cumulative infiltration within each time interval.

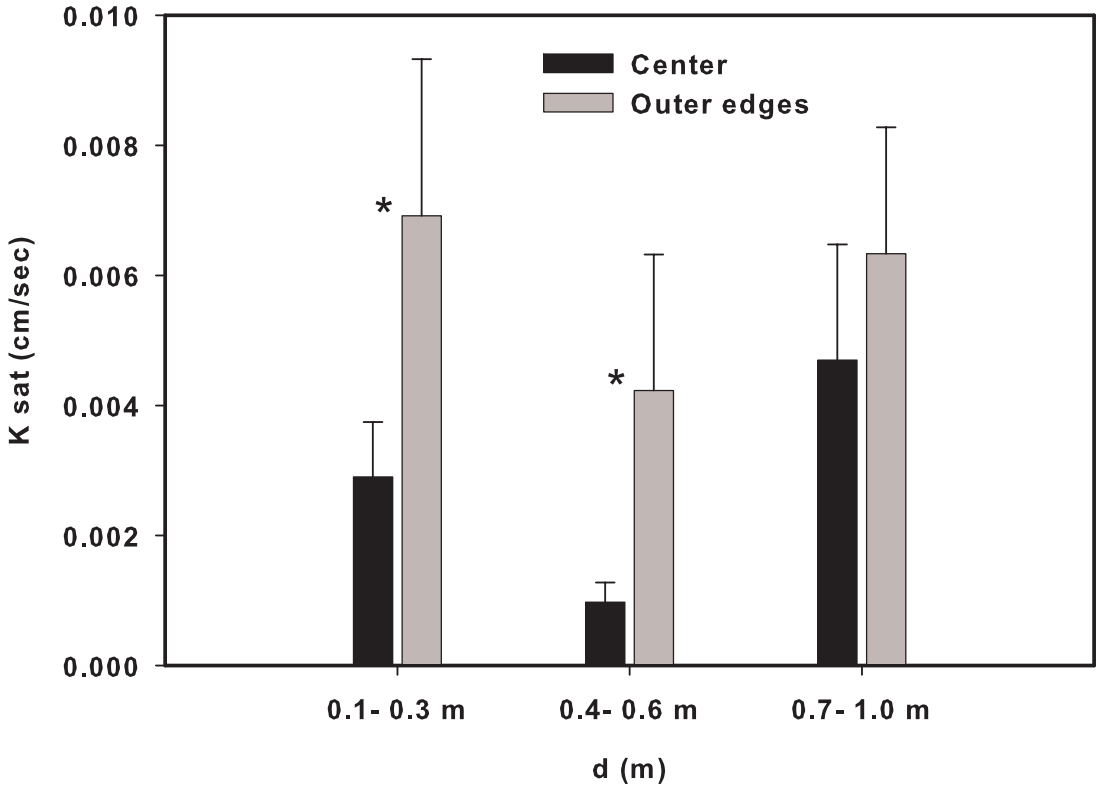


**Figure 3.3** Soil hydraulic conductivity ($K_{sat}$) at the center and outer edges of three ring classes. Error bars represent the standard deviation of hydraulic conductivity in each size class. The " * " indicates that the $K_{sat}$ value at the center and at the outer edges are significantly different based on a Kolmogorov-Smirnov one sample test within each grass ring diameter class.

The height of the grass ring center relative to the adjacent soil interspace between rings decreased as ring diameter increased (Figure 3.5). Particle size analysis showed that the difference in fines (silt and clay) between the center and at the outer edges increased with ring diameter between small and medium sized rings, whereas it decreased in large rings (ANOVA, F=61.48, df = (2, 13), *p*-value < 0.0001, Figure 3.6). The TOC and TN were significantly higher inside medium sized grass rings compared to the outer edges (*p*-

value = 0.02 for TOC and *p*-value = 0.0082 for TN, Figure 3.7), but not in large rings (*p*-value = 0.930 for TC and *p*-value = 0.999 for TN).

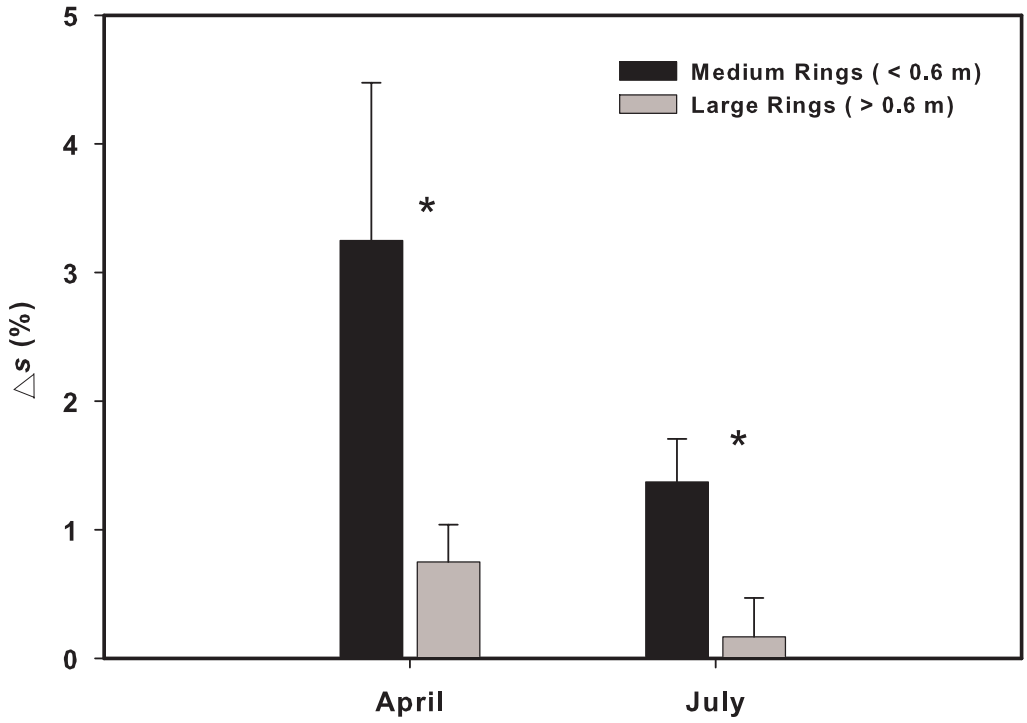


**Figure 3.4** Average difference in soil moisture (Δs) between inside and outer edges of medium and large ring size classes in April and July 2007. The error bar represents standard deviation of soil moisture differences within each ring diameter class. The " * " indicates that the difference in soil moisture (s) at the center and outer edges are significantly different for the medium and large rings based on a Kolmogorov-Smirnov one sample test.

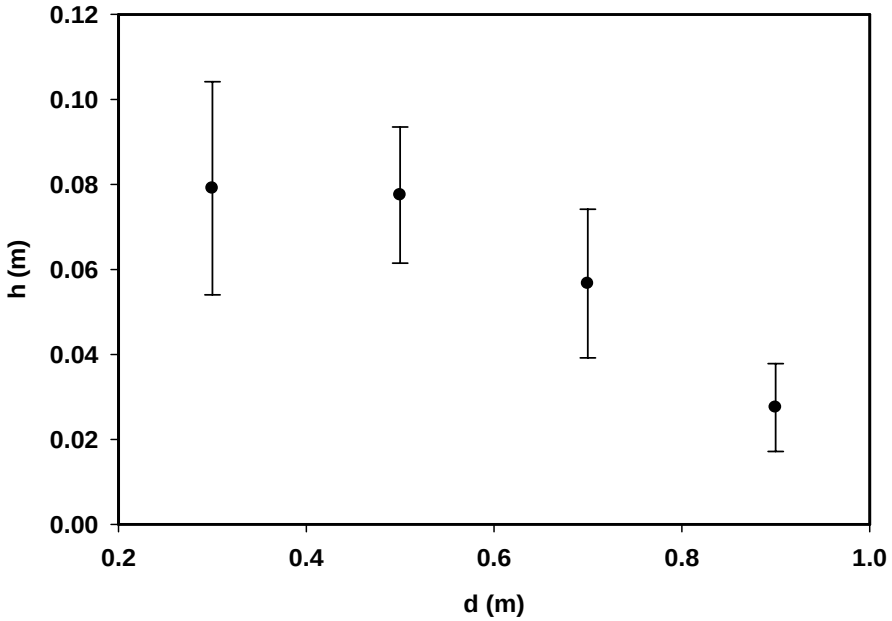


**Figure 3.5** Relationship between height (h) and diameter (d) of the grass rings. The error bars represent the standard deviation of height in each size class.

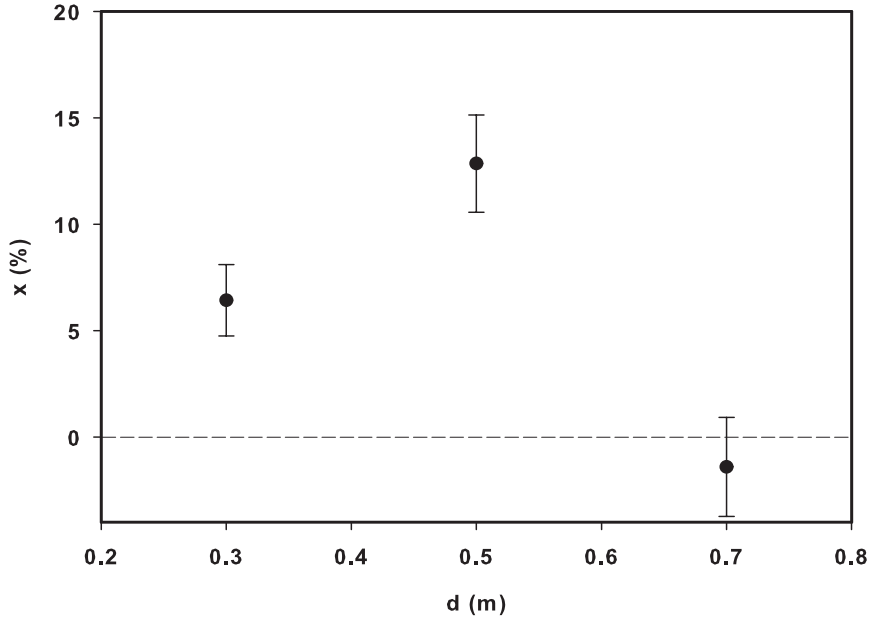


**Figure 3.6** Difference in fines (X) between inside and outside of grass rings in three ring diameter classes. The error bar represents the standard deviation of the differences in each size class.

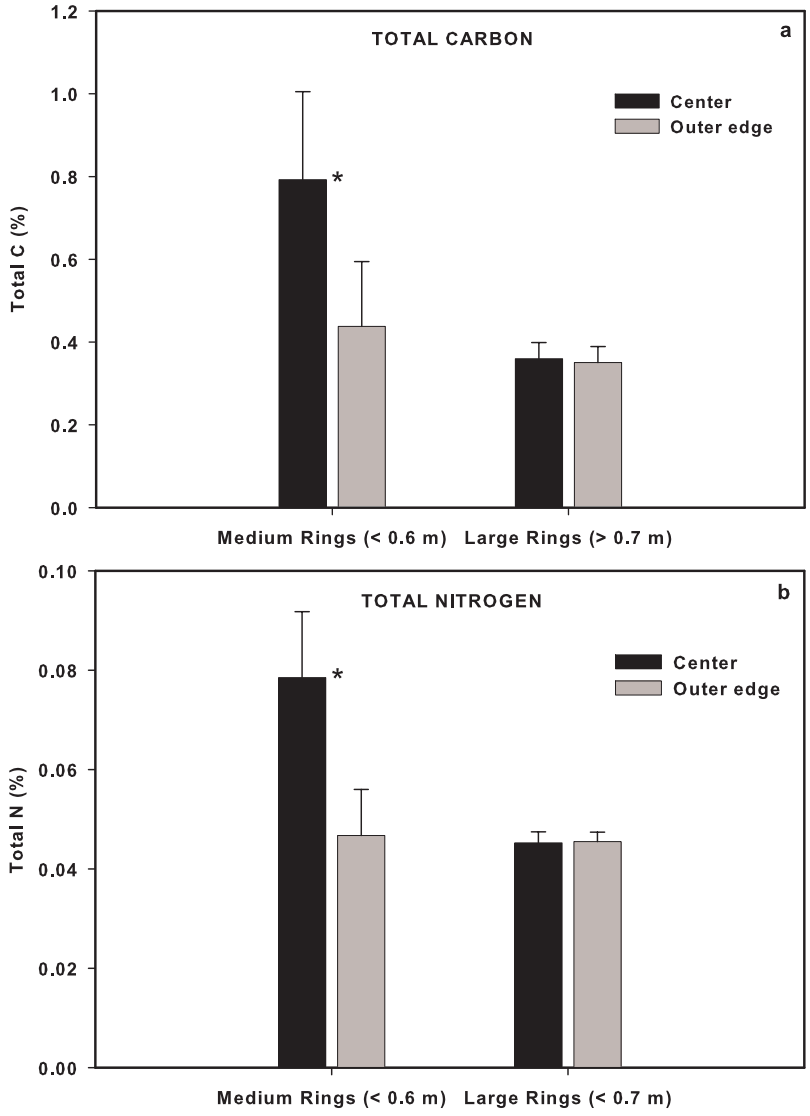


**Figure 3.7** Total carbon and nitrogen at the center and outer edges of the medium and large diameter rings. Error bars represent the standard deviation within each size class. The "*" indicates that total C and total N at the center and outer edges of medium sized rings are significantly different based on analysis of variance.

## 4. Discussion

Results from the infiltration experiments indicate that infiltration rates are higher at the outer edges of the grass rings compared to the center and bare interspaces (Figure 3.2). The difference in infiltration rate between the center and outer edges was larger for

small and medium sized rings compared to large rings. The corresponding hydraulic conductivities calculated from the infiltration data showed a similar trend (Figure 3.3). This pattern is explained by the variations in the fraction of soil fines between the center and outer edges of the grass rings (Figure 3.6), as soil infiltration is directly related to soil texture [*Wood et al.*, 1987; *Bestelmeyer et al.*, 2006]. Consistent with previous studies [*Wikberg and Mucina*, 2002], nutrient content (total C and N) in the medium sized rings was higher at the center of the rings compared to the outer edges (Figure 3.7), indicating that nutrient resource depletion was not the reason for grass mortality at the center of the rings. Rather, our results indicate that moisture limitations may explain grass mortality at the center of the rings and soil moisture also may limit ring growth at the outer edges.

How do the shape and function of grass rings change with time? We noticed that the heterogeneity in infiltration rates (and corresponding $K_{sat}$ values), soil particle size distribution and nutrient content increased with ring growth, and then decreased after reaching a critical ring size (Figures 3.2 - 3.4, 3.6, and 3.7). Aeolian processes are responsible for depositing fines on to grass clumps [*Hook and Burke*, 2000], leading to the development of a relatively thick layer of fines inside the grass, which decreases the soil infiltration capacity (Figure 3.2). This canopy trapping, which is a function of vegetation structure [*Raupach et al.*, 2001], increases with increasing ring diameter at the initial stages of ring development (i.e., for small to medium size rings) leading to accumulation of more fines inside the grass canopy, which further increases the heterogeneities between the inside and the outer edges of the rings. The deposited fines typically have high nutrient concentrations [*Li et al.*, 2007], which explains the higher C and N content inside the rings (Figure 3.7). The accumulation of fines (Figure 3.5) results

in considerable changes in soil texture [*Fearnehough et al.*, 1998; *Ravi et al.*, 2007], which in turn affects soil moisture dynamics inside the grass rings. These processes result in a decrease in infiltration rates (and hydraulic conductivity) and subsequent increase in runoff rates from the center to the outer edges. This altered pattern in surface soil moisture distribution is correlated with patterns in plant growth, especially in the case of blue grama, in which most of the root biomass is generally distributed very close to the surface and more or less directly beneath the plant. In fact, studies on root distribution of blue grama have shown that about 80% of the root biomass is distributed in the top 5- 15 cm of the soil [*Weaver*, 1958; *Bowman et al.*, 1985]. The retention of available soil moisture at the soil surface by the fine-textured sediments deposited at the center of the rings combined with development of biological and physical crusts [*Singer and Shainberg*, 2004; *Belnap et al.*, 2005; *Collins et. al.,* 2008] limit water infiltration, thereby inhibiting grass development in the central part of the ring. The medium size rings exhibited the optimum clay content (10-20% clay) for the formation of physical crusts, as crust formation is inhibited at low (< 10%) and high (> 30%) clay contents [*Singer and Shainberg*, 2004].

Grass mortality caused by aeolian deposits was reported as early as in the 1930s in shortgrass steppe ecosystems in the Great Plains (United States) where 2.5 cm of soil deposition from dust storms was observed to cause mortality of blue grama [*Weaver and Albertson*, 1936; *Mueller*, 1941]. In some cases, field observations have indicated that in years of high moisture availability, the growth patterns of the recovering grasses were strongly affected by these aeolian deposits [*Robertson*, 1939]. Similar processes are also

observed in desert shrubs [*Fearnehough et al.*, 1998; *Ravi et al.*, 2007] where aeolian deposits caused vegetation dieback at the center of revegetated dunes.

Grasses use resources (i.e., soil moisture) from a larger area outside the ring, while due to the limited infiltration capacity the soils at the center of the rings remain relatively dry and unable to provide sufficient soil moisture for grass growth. As the ring grows in size the volume of soil accessible by grass roots inside the ring decreases as the access to soil resources outside the ring is cut-off by the growth of new tillers at the periphery [*Wikberg and Svensson*, 2003]. This causes a decrease in plant density and increased tiller mortality in the inner areas of the ring. However, as ring size increases and tiller density decreases in the center of the ring the canopy trapping efficiency of grasses decreases, leading to wind- and water-induced loss of fine sediments that accumulated in the center during the earlier stages of ring development (Figure 3.5). The loss of fines from the central area is enhanced by high runoff rates from the center to the outer edges of the ring, where water is able to infiltrate at a higher rate. This loss in fine sediment in the center of the ring is indicated by the decrease in ring height of the center relative to the adjacent interspaces, as the ring diameter increases (Figure 3.5), as well as by changes in the fine soil fractions with ring size (Figure 3.6). The runoff from the center to the outer edges of the rings also supplies resources (water and nutrient-rich fine soil particles) to the edges. The edges of the rings receive resources also as aeolian deposits and runoff from bare interspaces between rings. Hence, the outer edges are preferential sites for the establishment and growth of new tillers as they have loose soil structure and higher moisture contents, both of which are ideal for the clonal growth of these grasses (Figure 3.8). In fact, low clay content and loose soil structure prevent crust

development, thereby favoring the emergence of new grass. Moreover, the vegetation growing at the outer edge of a ring can enhance soil infiltration capacity. These findings are supported by experiments on root development of ring forming grasses, which demonstrated with non-radioactive tracers [*Bonanomi et al.*, 2005] that the active roots in these rings are found at the outer edges rather than inside the rings. Indeed, roots extending outside the rings were found to be functional while roots found inside the rings where almost all dead [*Bonanomi et al.*, 2005].

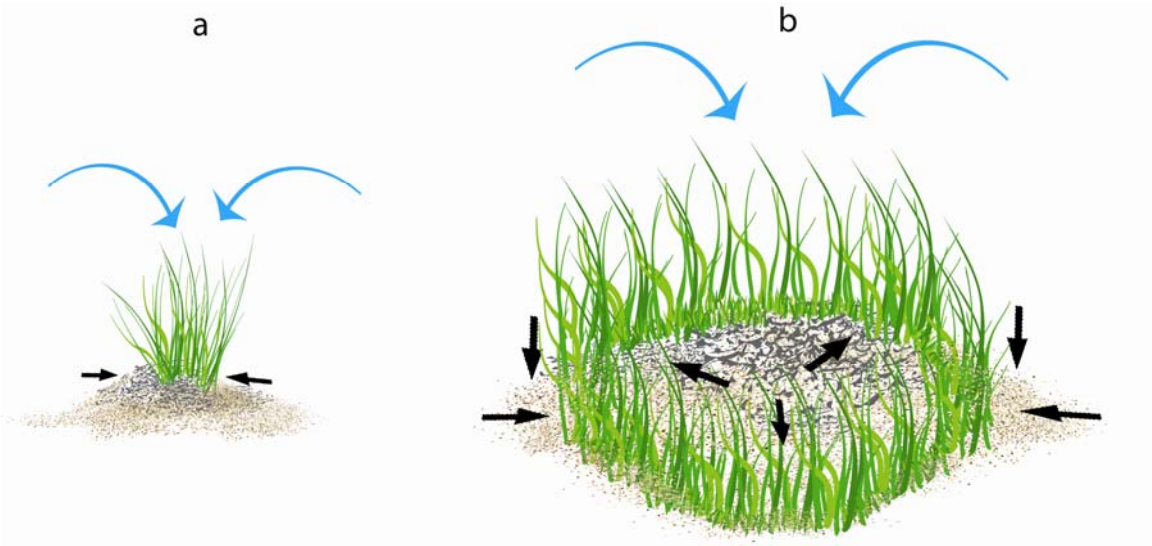


**Figure 3.8** Conceptual diagram showing the interaction of hydrological and aeolian processes resulting in the formation and expansion of grass rings. The straight black arrows indicate hydrological processes (infiltration and runoff) and curved grey arrows indicate aeolian processes (deposition and erosion)**.**

## 5. A conceptual model of grass ring dynamics

The previous discussion suggests that to some extent the dynamics of ring formation and growth resemble those of banded vegetation on sloping terrain [*Valentin et al.*, 1999]. In fact, in both cases vegetation growth is facilitated on one side of the band and inhibited on the other side. Moreover, one can argue that the formation of the barren

area at the center of a grass ring is due to limitation in the availability and access to soil water. We summarize the dynamics of grass ring development in four relatively distinct stages:

i) *Grass clump*: at this stage an almost uniform clump of grass is surrounded by bare soil. The clump is a preferential microsite for the trapping and deposition of fine wind-borne soil particles. As a result, infiltration rates are lower in the middle than at the edges of the clump. Thus, optimal conditions for rainfall infiltration, soil water storage and grass growth are found at the outer edges of the clump.

ii) *Ring formation*: As the clump radius, $r$, increases, the grass in the middle of the clump has reduced access to soil water resources at the edge of the clump. Eventually, tillers in the center of the clump die and the soil is exposed. This process, which leads to ring formation, can be mathematically demonstrated by showing that in the case of uniformly vegetated clumps grass biomass increases proportionally to clump area (i.e., proportionally to $r^2$) while the resources available through the edges for the clump increase proportionally to the perimeter of the clump (i.e., to $r$). Thus, as $r$ increases, grass biomass increases faster than the resources accumulate at the clump edge until carrying capacity is reached. At this point a further increase in $r$ leads to an increase in the grass-covered area proportional to $r$ instead of $r^2$ because otherwise the increase in grass biomass would not be balanced by an equal increase in accessible resources. Thus, in the case of circular clumps a constant area, $A$ (i.e., biomass) to circumference, $C$ (i.e., accessible resources) ratio is achieved with a ring shape with constant ring width

$$\frac{A}{C} = \frac{\pi(r_e^{\,2} - r_i^{\,2})}{2\pi r_e} \approx (r_e - r_i) = const \qquad (3.1)$$

where $r_e$ and $r_i$ are the ring's external and internal radius, respectively, and the approximation holds when $r_e \approx r_i$. The previous equation shows that for the grass-covered area, $A$, to grow proportionally to the circumference, $C$, the width of the ring, $r_e$-$r_i$, must remain constant.

iii) *Early ring stage*. A small to medium-size ring (see Section 2) is able to effectively trap and retain fine sediment particles (Figure 3.6), thereby maintaining low infiltration rates (Figures 3.2 - 3.3), and inhibiting grass growth in the barren soil at the center of the ring. Crust formation may further reduce the infiltration rates and enhance runoff generation in the middle of the ring. Runoff diverges from the center to the (lower elevation) outer edge of the ring, where infiltration occurs. In the absence of a slope the ring expands symmetrically in the direction of the outer edge of the ring, where favorable conditions exist for infiltration and soil water storage, and bud bank formation for future growth (*Dalgleish and Hartnett*, 2006). Due to the limitations in resource availability/accessibility expressed by equation (3.1), the ring expansion at the outer edge of the ring occurs at the expense of the tillers in the inner side of the ring, similar to the case of tiger-brush banded vegetation [*Valentin et al.*, 1999].

iv) *Late ring stage*. As the ring grows in size its trapping efficiency decreases. The sediments in the middle are less effectively sheltered by the surrounding tillers, and the fine-textured bare soil accumulated inside the ring is eroded (Figure 3.5). Moreover the loss of fine sediments leads (Figure 3.6) to an increase in infiltration rates (Figures 3.2 - 3.3) in the bare soil enclosed by the ring. In these conditions two major processes determining the ecohydrologic functioning of grass rings are

either weakened or altered: a) grass growth at the inner edge of the ring is no longer inhibited by limitation in infiltration rates; and b) the effect of runoff concentration from the poorly drained soils in the middle to the outer edges of the rings disappears. As a result the ring becomes less resilient and drought or another type of disturbance may cause the grass ring to break apart. Ring fragments may then serve as nuclei for the formation of new rings, via steps 1 through 4.

## 6. Conclusions

Ring formation in blue grama is best explained by the differential deposition of wind borne fines on to the bunch grass, which changes soil texture inside the grass clump. Runoff contributes to redistribution of water and nutrients from the central areas of the ring, which are characterized by low infiltration rates and high nutrient content, to the outer edges. This explains the preferential establishment of new vegetative growth at the outer edges of the ring and low plant density and mortality of grass tillers in the central areas of the ring. After the ring reaches a certain critical size, the differences in properties between the inside and outside of the ring diminish and the advantage of ring formation is lost. At this critical size the ring breaks into separate parts and at least some of these ring fragments become independent plants, thereby contributing to the vegetative regeneration and complex dynamics in aridland plant communities [*Lewis et al.*, 2001].

# CHAPTER: 4

# POST-FIRE RESOURCE REDISTRIBUTION IN DESERT GRASSLANDS: A POSSIBLE NEGATIVE FEEDBACK ON LAND DEGRADATION

(This chapter is in review for publication in *Ecosystems*)

## Abstract

The grasslands at desert margins, which are very sensitive to external drivers like climate change, are areas affected by rapid land degradation processes. In many regions of the world the common form of land degradation at the desert grasslands is the rapid conversion of vegetation from grasses to woody plants, or in other words, shrub encroachment. This process, thought to be irreversible and sustained by biophysical feedbacks of global desertification results in the formation of "islands of fertility" scattered among patches of grasses and nutrient-depleted bare soil. The emerging two-phase landscape which exhibits a more heterogeneous distribution of soil resources is considered to be a sign of land degradation. Most of these shrub-grass transition systems at the desert margins are affected by disturbances such as fires which affect the interactions between ecological, hydrological and land surface processes. Here we show that prescribed fire can counteract the hetereogeneity-forming dynamics of land degradation associated with shrub encroachment by enhancing local-scale soil erodibility by aeolian and hydrological processes, potentially reversing the early stages of land degradation.

## 1. Introduction

Drylands cover 41% of the earth's surface and support over 2 billion inhabitants [*MEA*, 2005], mainly in the developing world. According to the United Nations Convention to Combat Desertification [*UNCCD*, 1994], 70% of the drylands globally are affected by land degradation, due to the combined effects of regional or global climate change and anthropogenic disturbances, such as overgrazing, changes in fire pressure, and land cultivation without adequate soil conservation [*Archer et al.*, 1995; *Nicholson*, 2000; *Nicholson et al.*, 1998; *Van Auken*, 2000]. Land degradation is a major contributor to the expansion of desert margins [*Nicholson et al.*, 1998; *Reich*, 2000], with important impacts both on regional climate [*Dregne*, 2002; *Nicholson*, 2000; *Nicholson et al.*, 1998; *Rosenfeld et al.*, 2001] and on the loss of ecosystem functioning and services [*Daily*, 1995; *Hibbard et al.*, 2001]. This process often occurs in conjunction with the encroachment of shrubs in regions historically dominated by grasses as observed in North America [*Archer*, 1989; *Buffington and Herbel*, 1965; *Van Auken*, 2000], South America [*Cabral et al.*, 2003], Africa [*Roques et al.*, 2001] and Australia [*Fensham et al.*, 2005] (Figure 4.1). Shrub encroachment typically involves an increase in bare soil, the removal of nutrient-rich soil by wind and water from unvegetated areas, and its partial redeposition in shrub-dominated soil patches through mechanisms of canopy trapping [*Charley and West*, 1975; *Schlesinger et al.*, 1990]. These processes trigger a self-sustained cycle of erosion, depletion of soil resources, and vegetation loss in grass-dominated areas [*Archer et al.*, 1995], while the encroachment of shrubs is favored by the deposition of nutrient-rich sediments transported by wind and water [*Breshears et al.*, 2003; *Ravi et al.*, 2007], and the subsequent accumulation of fertile soils beneath the

shrubs [*Charley and West*, 1975; *Schlesinger et al.*, 1990]. At the same time, loss in grass fuel decreases the pressure of fires on shrub vegetation thereby further enhancing woody plant encroachment [*Archer et al.*, 1995; *Van Auken*, 2000; *van Langevelde et al.*, 2003]. The resulting landscape exhibits a mosaic of nutrient-depleted barren soil bordered by nutrient-enriched shrubby areas known as "islands of fertility" [*Charley and West*, 1975; *Schlesinger et al.*, 1990]. Even though shrub encroachment is considered as a major contributor to the desertification of several regions around the world [*Okin*, 2002; *Schlesinger et al.*, 1990] with important environmental and socio-economic implications [*MEA*, 2005; *UNCCD*, 1994], little is known about mechanisms that could counteract this process.

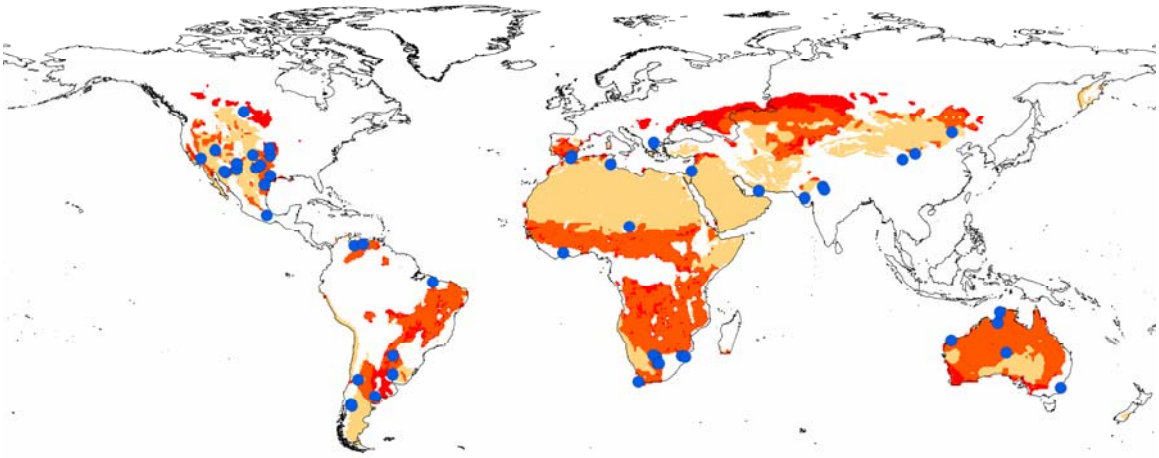

**Figure 4.1** Global map of woody plant encroachment. Map showing locations (blue points) where encroachment of woody plants has been reported. Colors: Red indicates fire, Yellow represents desert vegetation and orange represents areas where they overlap (see the Appendix B).

Is this land degradation process irreversible? Here we demonstrate that at the early stages of shrub encroachment fire can play an important role in the local-scale redistribution of soil resources within the landscape. This process generates a more

homogeneous distribution of soil resources, providing some form of reversibility to the dynamics of land degradation. The grasslands at desert margins are affected by fire occurrences, suggesting that a sufficient amount of grass biomass exists in these transitional zones to carry the fires from the points of ignition and through the surrounding vegetation (Figure 4.1). In these conditions fires short-circuit the processes that reinforce heterogeneity by activating the transport of nutrient-rich soil from islands of fertility to the adjacent bare soils. Using microtopography measurements, $\delta^{15}N$ isotope tracers, and quantifying post fire erosion processes we show that in a landscape covered by a mixture of native grasses and invading shrubs fires change the spatial patterns of soil erosion, favoring the local scale redistribution of soil nutrients from the islands of fertility beneath the burned shrubs to the adjacent bare interspaces.

## 2. Materials and methods

The global map of woody plant encroachment (Figure 4.1) was prepared using MODIS land cover product (desert vegetation), Terra MODIS fire data (global annual burned area estimates [*Giglio et al.*, 2006]) and locations where woody plant encroachment has been studied in the past. The desert vegetation map was derived from the MODIS land cover product. The fire data was taken from the global annual burned area estimates from *Giglio et al.*, 2006, using Terra MODIS fire data and ancillary vegetation cover information. The woody plant encroachment locations were collected from around two hundred published studies on woody plant encroachment around the world. (See Appendix B for more details).

The field experiments were conducted at the Sevilleta National Wildlife Refuge (New Mexico, USA) in the northern Chihuahuan Desert, in a transition zone where creosote bush is now invading black grama dominated grassland (N 34$^{o}$ 20 17.0$^{'}$, W 106$^{o}$ 43 3.0‘). The field sites were in a heterogeneous landscape with a mosaic of grass (*Bouteloua eriopoda, Sporobolis spp.*) and shrub (*Larrea tridentata* and *Gutierrerzia spp*) cover with bare interspaces. The grass cover was minimal at the shrub base but provided enough connectivity among shrubs to allow for the spread of fires in the presence of strong winds. The soil is a sandy loam.

Three treatments (cleared, burned, and unmanipulated control plots), with three replicates each were used for this study. The plots were circular (6 meters in diameter) and laid out in such a way that each plot captured the heterogeneous nature of this landscape, with at least 2-3 shrub patches in each plot. Each set of replicated plots was more than 50 m from the others, while treatments within a replicated set were approximately 20 m apart. In the cleared plots, shrubs and grasses were cut close to the soil surface and removed without disturbing the soil surface using a system of platforms to walk over the plots. For the second treatment, prescribed burns were done, which were confined inside the circular plots. During the burns, soil surface temperature around the shrub and grass patches were measured.

In the cleared plots, shrubs and grasses were cut close to the soil surface and removed without disturbing the soil surface using a system of platforms to walk over the plots. For the second treatment, prescribed burns were done, which were confined inside the circular plots. The wind speeds measured over burned and cleared plots were not significantly different from a 1:1 dependence ($R^2$=0.83). However, the relation between

wind speed on the cleared and control plots deviated significantly from a 1:1 dependence ($R^2$=0.52), due to the different surface roughness.

In each plot wind-blown sediments were collected using dust samplers (BSNE isokinetic dust samplers by Custom Products, TX, USA installed at 5 cm and 30 cm from the surface). The saltation activity (i.e., soil movement close to the surface) was measured using SENSIT wind eroding mass sensors (SENSIT Company, ND, USA) buried in the ground and with the sensitive part of the sensor at a height of 2 cm from the soil surface. Wind velocity was measured with an array of cup anemometers installed at four heights (0.2 m, 0.6 m, 1.2 m & 2 m). Both wind speed and saltation activity were monitored in each plot for a continuous 10-day period after the manipulation. Statistical tests (ANOVA) were done to show that the amount of samples collected from the different treatments were significantly different.

Locations were established in each plot to measure with a soil bridge, the small scale changes (microtopography) in soil elevation over time [*White and Loftin*, 2000]. The soil erosion bridges used in the study were 1.5 m long with 31 measuring points, and were oriented from the center of a shrub towards adjacent grass patches and bare interspaces. Soil microtopography measurements were conducted in all plots both one month and four months after the experimental manipulation. To estimate the elevation loss from the shrub islands, only the microtopography measurements near the shrub islands were considered.

To trace the post-disturbance redistribution of soil nutrients, a $^{15}N$ tracing experiment was conducted [*Wang et al.*, 2006]. Labeled ammonium nitrate ($NH_4{}^{15}NO_3$, ~200‰) mixed with 500 ml water was uniformly applied within 10 cm of the shrub base

beneath two randomly selected shrubs in each plot. In the burned plots the tracer was applied two days before the prescribed burn to provide insight into the processes occurring during and following the burn. Two weeks after the application, 2-cm deep surface soil samples were collected from shrub islands, within 10 cm of the shrub base, and bare interspaces, more than 100 cm from shrub base. In each plot, soil samples were collected from under the two labeled $^{15}N$ shrubs and three adjacent bare interspaces. Samples of the new grass growth in the interspaces were collected from each plot two weeks after the fire. Leaf and soil samples were dried at 60º C for 72 hours and then ground and homogenized using a mortar and pestle. Stable nitrogen ($^{15}N$) isotope analysis was performed using a Micromass Optima Isotope Ratio Mass Spectrometer (IRMS) (GV/Micromass, Manchester, UK) coupled to an NA1500 elemental analyzer (EA) (Carlo Erba, Italy). The $^{15}N$ compositions are reported in the conventional form (‰):

$$\delta^{15}N\ (‰) = [(^{15}N/\ ^{14}N_{sample} / \ ^{15}N/\ ^{14}N_{standard}) - 1\ ] \times 1000 \qquad (4.1)$$

where $(^{15}N/\ ^{14}N)_{sample}$ and $(^{15}N/\ ^{14}N)_{\ standard}$ are the respective isotope compositions of a sample and the standard material. Reproducibility of these measurements is approximately 0.2‰. The interspace foliar $\delta^{15}N$ differences between burned, cleared and control plot were tested using one-way ANOVA and mean separations were calculated by a Tukey *post hoc* test at $\alpha = 0.05$ using SAS (SAS v. 9.1, SAS Institute Inc, Cary, NC). To quantitatively assess the $^{15}N$ source for the grasses growing in the interspaces, a mixing ratio calculation was performed using the initial shrub mound tracer level (the $\delta^{15}N$ value just after the $^{15}N$ application) and the initial concentration of $^{15}N$ in the interspaces as two end members. The calculation is as follows, $\delta^{15}N_{grass} = \delta^{15}N_{shrub\ mound} \times f_{shrub\ mound} + \delta^{15}N_{intersapce} \times f_{interspace}$, where $\delta^{15}N_{grass}$ is the $\delta^{15}N$ value of new-growth grasses

at the interspace microsites, $\delta^{15}N_{shrub\ mound}$ and $\delta^{15}N_{intersapce}$ are the two end-member values. The $f_{shrub\ mound}$ and $f_{intersapce}$, which must sum to one, are relative contributions of two end members to $\delta^{15}N$ in the grass. The plant nitrate uptake fractionation factors depend on species and location and 3‰ were used in the calculation [*Yoneyama et al.*, 2001]. The differences in soil $\delta^{15}N$ difference between $^{15}N$ labeled shrub mounds and interspaces for the three treatments (burned, cleared and control) were also compared using one-way ANOVA and Tukey *post hoc* test at $\alpha = 0.05$.

To investigate the effects of fire on soil properties such as hydrophobicity and infiltration capacity, an additional (~25 $m^2$) area was burned in the surroundings of the replicated treatment plots. In this burned area water repellency was quantified in terms of Water Drop Penetration Time [*Doerr*, 1998] (WDPT is the average time required for the drops to penetrate into the soil surface). To this end, a pipette was used to place uniformly sized water drops on the soil surface. The WDPT was measured in the shrub patches (30 cm around the shrub base), grass patches and bare interspaces in the burned, cleared and control areas. The fire temperatures were measured using temperature sensitive colors spread on ceramic tiles left in the plot during the control burn. Infiltration rates were determined using a mini disk infiltrometer (Decagon, Pullman, USA), which can be used to calculate the saturated hydraulic conductivity of the soil ($K_{sat}$). These measurements were compared to corresponding measurements in the adjacent control areas.

**3. Results**

Our field experiments at the shrub-grass transition zone of Northern Chihuahuan desert margin (New Mexico, USA) indicate that fires result in enhanced redistribution of soil resources (*e.g.* nitrogen) from the shrub islands ("Islands of fertility") to the interspaces, where they contribute to the post fire establishment and growth of grasses. The microtopographic measurements of small scale changes in soil elevation with time showed a post-fire decrease in soil surface height near the shrub islands and an increase in soil surface height in the bare interspaces (Figure 4.2a). This rapid microtopographic change was observed even just two weeks after the burn and continued in the following weeks. Further, comparing microtopography measurements from burned areas, areas cleared of the aboveground vegetation and undisturbed control areas, we found that the overall changes in soil surface height were stronger in the burned areas than in the cleared and control areas of this replicated field experiment. In fact, the soil loss from shrub islands in the burned areas (8.25 mm) was 5 times higher than in the cleared areas (1.63 mm), while in the control areas the microtopographic changes were negligible (Figure 4.2b). Moreover, changes in soil surface elevation near the shrub islands were significantly different from those in cleared and control plots ($p = 0.01$). In fact, one of the control plots showed an increase in the elevation near the shrub micro-sites over time, indicating soil accumulation by canopy trapping. Further, the $^{15}N$ tracer study also indicated a post-fire redistribution of soil resources. The signature of $^{15}N$ initially applied on shrub islands was detected in new grass growth collected two weeks after the fire up to 150 cm away from the pre-burn island of fertility (Figure 4.3a). The redistribution of $^{15}N$ was also observed in the cleared areas, but redistribution rates were higher in the

burned areas, as indicated by the more elevated interspace grass foliar $\delta^{15}N$ values in the burned areas compared to cleared and control areas( $p<0.05$) .

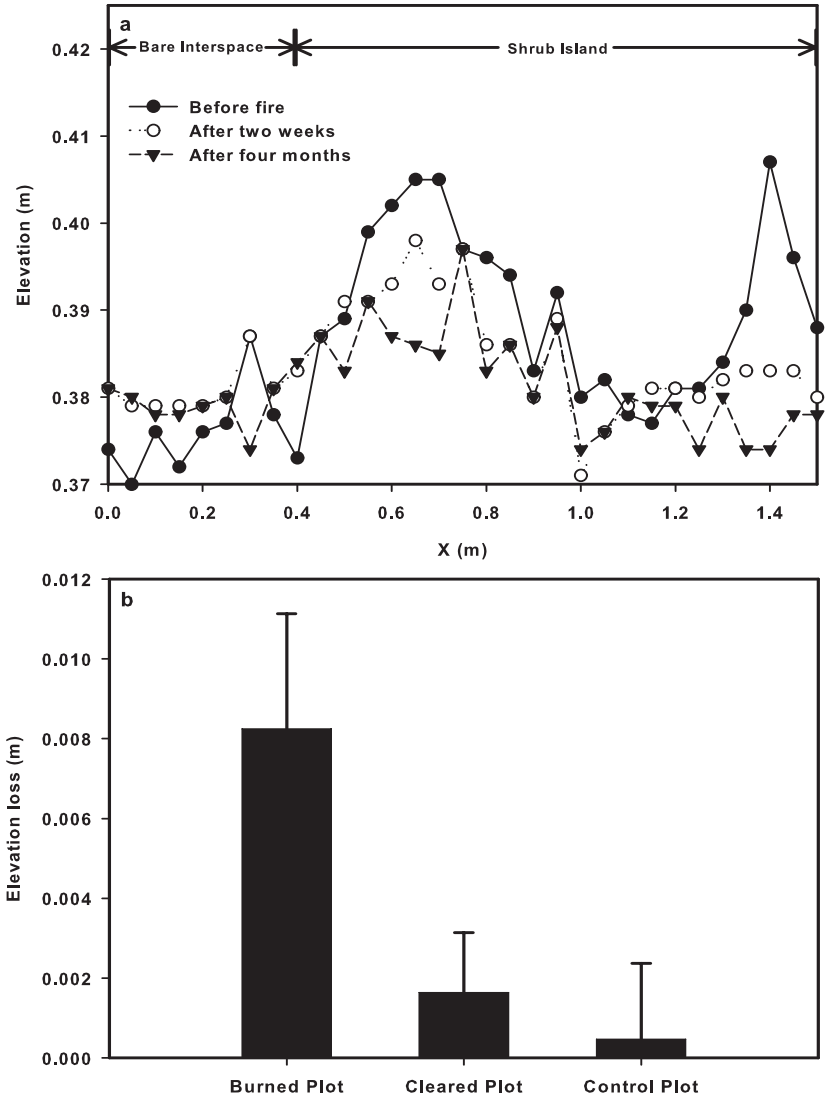


**Figure 4.2** Changes in soil microtopography **(**a) Redistribution of soil resources from around the shrub islands to bare interspaces with time following the fire as measured by repeat measurements with a soil microtopography bridge in one replicate of the burned treatment. (b) Average elevation loss around the shrub islands following fire in all treatments when only the microtopography measurements near the shrub islands were considered. Error bars represent the standard deviation of elevation loss between all the replicates of each treatment.

Mixing ratio calculations show that 45%, 19% and 1% of the grass foliar $^{15}N$ came from the $^{15}N$-labeled shrub mounds for the grass in burned, cleared, and control areas respectively. The post-fire redistribution of soil resources is further evidenced by the observed decrease in differences in soil $\delta^{15}N$ between $^{15}N$-labeled shrub mounds and interspaces. Two weeks after the fire these differences were found to be significantly lower ($p<0.05$) in the burned areas, while in the cleared and control areas these differences were not significant (Figure 4.3b).

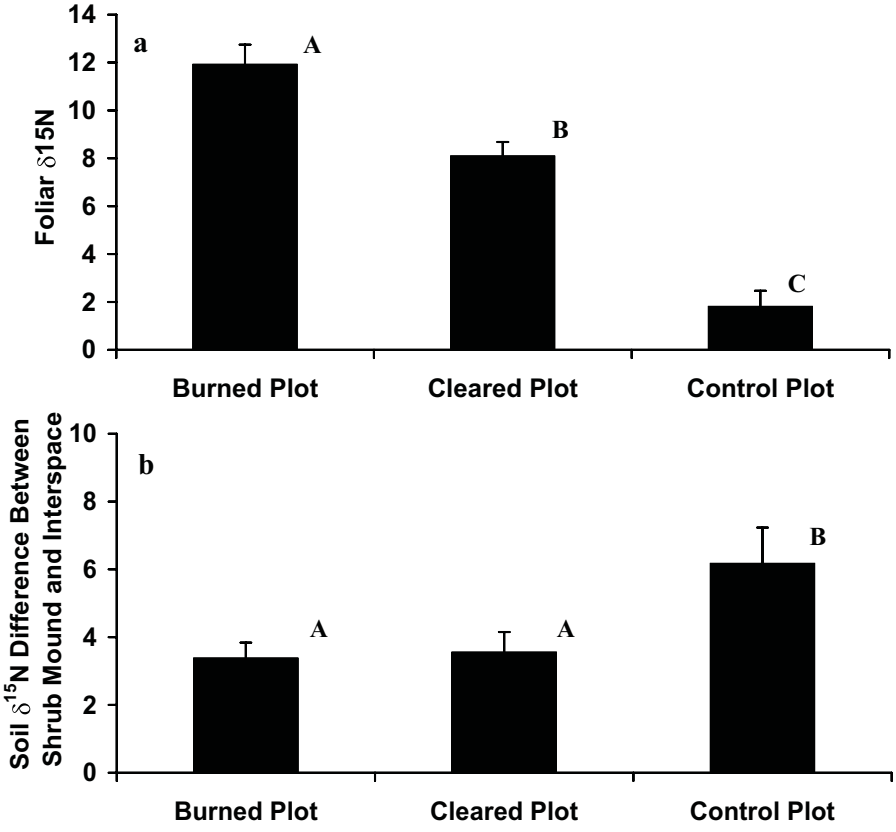


**Figure 4.3** The $^{15}N$ isotope tracer experiment**.** (a) The interspace grass foliar $\delta^{15}N$ values from burned, cleared and control plot and (b) the soil $\delta^{15}N$ difference between $^{15}N$ labeled shrub mounds and grasses growing in shrub interspaces for the three treatments (burned, cleared and control). The results are from one-way ANOVA and Tukey *post hoc* test at $\alpha = 0.05$. The same capital letters indicate the same mean values.

The enhancement of resource redistribution in the burned areas can only be attributed to an increase in the rates of post fire soil erodibility by wind and water, as the burned and cleared plots had comparable surface roughness and experienced the same wind shear. Two weeks after the burn the sediment samplers in all the burned areas collected significantly more wind-blown sediments ($p<0.05$) than on the other two treatments (Figure 4.4a). Even though the overall dust collection in all plots decreased in the following weeks, the samplers collected significantly more sediments ($p<0.05$) in the burn plots even three months after the fire (Figure 4.4b).

The records from particle impact sensors indicate that the frequency and intensity of saltation (indicator of soil movement at the surface) were higher in the burned areas than in the cleared and control areas. The number of erosion events (number of 5 minute data collection intervals with soil particle movement at the surface) in the burned areas (234 events per month) were three times more compared to the cleared plots (79 events per month). These results clearly show that in the burned areas, saltation events are more frequent, indicating the occurrence of a post-fire enhancement in soil erodibility in the burned plots compared to the cleared and control areas.

Fire induced water repellency was observed in the burned areas (Figure 4.5), and the impact of fire on soil properties differed among shrub, grass and bare soil microsites (Figure 4.6a). Fire temperatures were higher beneath the shrubs (average temperature 260 °C) compared to grass patches (average temperature 120 °C) and bare interspaces ($< 90^0$ C), whereas no difference in temperature was detected at 3-5 cm depth regardless of the above ground vegetation.

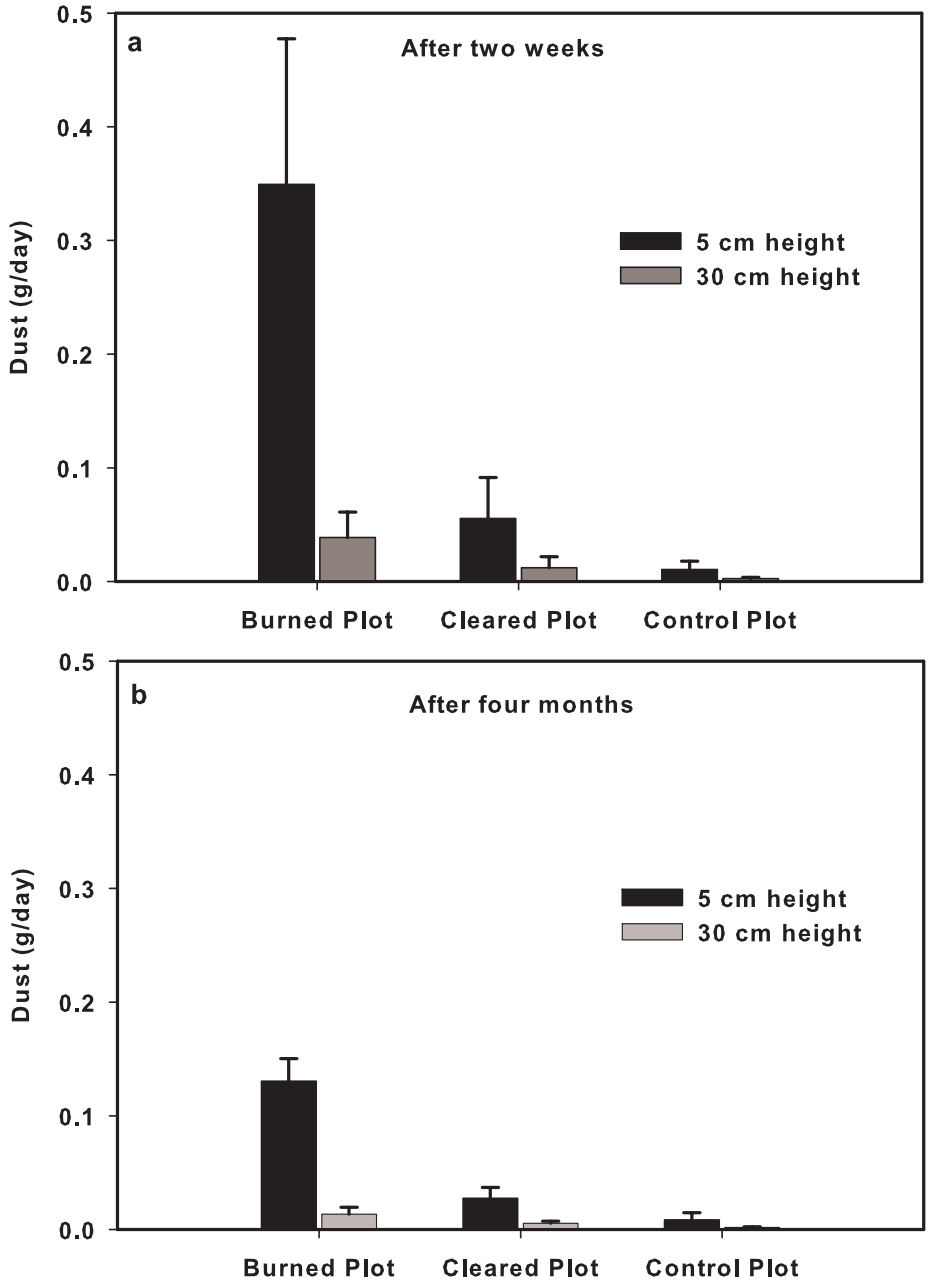


**Figure 4.4** Enhancement of post fire aeolian processes**.** Amount of dust collected by the BSNE dust samplers (at 5 cm and 30 cm height) (a) two weeks and (b) four months after the fire. Error bars represent the standard deviation of dust collected in three replicates of each treatment.

Measurements of Water Drop Penetration Time (WDPT; i.e., the time needed for a water drop to penetrate the soil [*Ravi et al.*, 2006a; *Ravi*, 2007]) along a transect from a burned area to a control (unburned) area indicated that the fire-induced soil water repellency was higher within the burned shrub islands (WDPT Avg ~ 120 sec and Max ~ 270 sec) compared to burned grass patches (WDPT Avg ~ 7 sec & Max ~11 sec), whereas no soil water repellency was observed in the bare interspaces (WDPT ~ 0 sec).

**Figure 4.5** Post-fire water repellency around a burned creosote bush in the Sevilleta National Wildlife Refuge, NM. (The scale on the right hand side is in centimeters)

The decrease in infiltration rates beneath and around burned shrubs compared to unburned shrubs indicate that fire induced water repellency resulted in the altered hydrological response of the surface soil (Figure 4.6b).The infiltration rates in the shrub islands were higher than in the bare interspaces before the fire. However, following the prescribed burn, the infiltration rates around the shrub islands and the bare interspaces were comparable. The corresponding hydraulic conductivity values ($K_{sat}$) were

significantly lower ($p$<0.05) under the burned shrubs (0.0011 cm/s) when compared to unburned shrubs (0.128 cm/s).

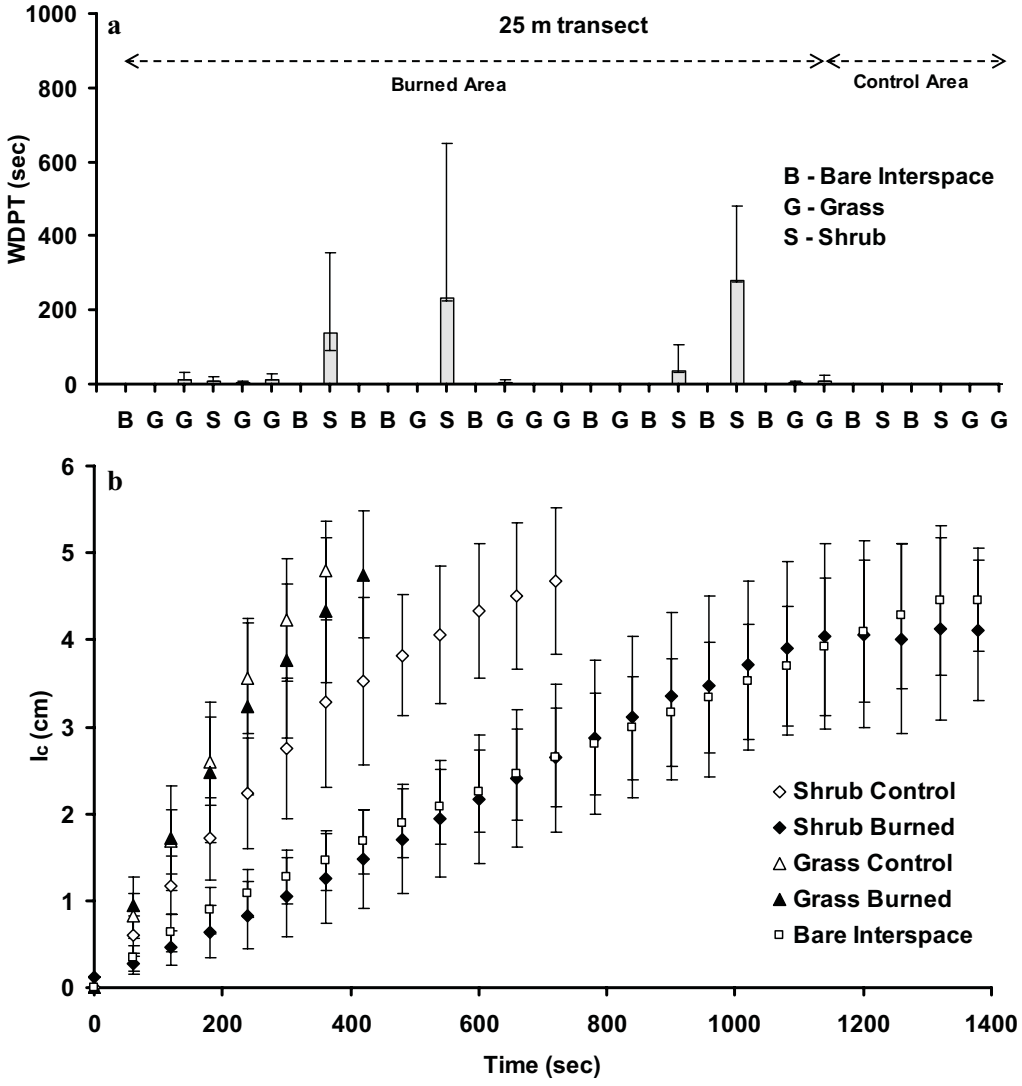


**Figure 4.6** Fire induced water repellency and infiltration (a) Soil water repellency (quantified using WDPT) along a transect from burned area to control (unburned) area. The error bars represent the 80$^{th}$ percentile and 20$^{th}$ percentile values of WDPT (b) Infiltration rates (measured using a Mini disk infiltrometer) in the shrub patches and grass patches before and after the prescribed burns. The infiltration rates in the bare interspaces were unaffected by the fire. The error bars represent the standard deviation of replicates of infiltration in each class.

Differences in hydraulic conductivity values and infiltration rates were negligible between burned and unburned grass patches as well as in the bare interspaces. The post-fire decrease in infiltration rates combined with the higher soil elevation of the fertility islands resulted in increased runoff from these soil mounds to the interspaces, and in the enhancement of sediment redistribution by water erosion. Further, field measurements one month after the prescribed fire showed no traces of water repellency in the burned plots, which indicate that the fire induced water repellency in theses systems are short-lived.

**4. Discussion**

Overall, the enhancement of soil erosion in the fertile islands remobilized nutrient-rich sediments that were trapped in the sheltered area beneath the shrub canopy. This sediment was redistributed by wind and water; the $^{15}N$ tracer indicated that the interspaces receive a significant amount of nutrients, including nitrogen, from the nearby fertile islands, and that some of these nutrients are taken up by grasses (Figure 4.3a), which recovered quickly after a burn. Recent studies have shown that post fire enhancement of soil erosion can be induced by the increase in soil hydrophobicity caused by the burning vegetation [*Doerr et al.*, 2000]. Fire temperatures were highly heterogeneous, with higher surface soil temperature beneath the shrubs (average temperature 260 °C) than in grass patches (average temperature 120 °C) and bare interspaces ($< 90^0$ C), whereas no difference in temperature was detected at 3-5 cm depth regardless of the above ground vegetation. The higher contents of hydrophobic compounds and the higher fire temperatures of shrub vegetation led to the development

of stronger post fire soil-water repellency in and around shrub patches. Here we explain the post fire enhancement in wind and water erosion as an effect of fire induced water repellency. Soil erodibility was found to significantly increase in the microsites affected by the burning of shrub biomass. These microsites were also the areas, which developed a higher soil water repellency, presumably due to the higher fire temperatures and the more hydrophobic compounds released by the burning of shrub vegetation. Thus, by altering soil surface physical and chemical properties for a short period, fires can counteract the hetereogeneity-forming dynamics of land degradation associated with shrub encroachment. Further, our experimental findings indicate that the post fire resource homogenization in these degraded landscapes is a rapid process occurring in the time frame of weeks. Due to this effect of fires, "islands of fertility" can be dynamic rather than static features of these landscapes.

In this study we compared processes occurring in burned and vegetation denuded areas (i.e., areas with similar roughness and experiencing same wind shear) to show that the post fire enhancement of soil erodibility in the fertility islands is not a mere result of the higher topography of the shrub mound. We also avoided confounding factors, such as the activity of small mammals and fire effect on microbial crusts, which could affect the stability of the surface soil in these landscapes. In our field sites we eliminated the effects of small mammals by selecting undisturbed study sites where no detectable signs of small mammal activity was observed. Further, the effect of fires on microbial crusts cannot have enhanced soil erodibility beneath the shrubs, as the microbial crusts were observed only in the bare interspaces and not directly under the shrub patches, consistently with the findings from other arid systems [*Schlesinger and Pilmanis*, 1998].

## 5. Conclusions

Our findings demonstrate the potentially important role of fire as a management strategy to reverse the early stages of land degradation associated with the encroachment of woody plants in arid and semi arid ecosystems. It is expected that the consequent enhancement of ecosystem functioning and services at the desert margins may contribute to counteract or limit desert expansion.

# CHAPTER: 5

# ENHANCEMENT OF WIND EROSION BY FIRE-INDUCED WATER REPELLENCY

(This chapter is published in *Water Resources Research*)


## Abstract

The occurrence of fire and the subsequent increase in wind erosion are known to affect vegetation dynamics in dryland landscapes. Fires act as a disturbance on shrubs and trees and expose the soil surface to the erosive action of wind, thereby affecting the loss and redistribution of soil nutrients. Despite the relevance of wind erosion and fires to the dynamics of arid ecosystems, the interactions between these two processes remain poorly understood. We have investigated how a representative water repellant organic compound released by burning biomass and absorbed in the soil may enhance soil erodibility. To this end, we carried out a series of wind tunnel experiments, laboratory tests, and theoretical analyses to assess the effect of fire-induced water repellency on the soil susceptibility to wind erosion. The experiments were carried out using clean, well-sorted sand which was artificially coated with palmitic acid, a common water repellency inducing fatty acid found in most plants. The results indicate that fire-induced water repellency enhances soil erodibility, causing a drop in wind erosion threshold velocity. The results are explained by the effect of water repellent compounds on soil-water contact angle and on the strength of interparticle wet-bonding forces.

## 1. Introduction

The occurrence of fire and the subsequent increase in wind erosion are known to affect the composition and structure of vegetation in dryland landscapes. Fires contribute to determine the dominance or co-dominance of woody plants (trees and shrubs) and grasses in arid and semiarid ecosystems [e.g*., Scholes and Archer*, 1997; *Higgins et al*., 2000; *Van Langevelde et al*., 2003; *Sankaran et al*, 2004]. Vegetation, in turn, affects the fire regime, in that both fire intensity and frequency depend on the relative abundance of trees and grasses [e.g., *Anderies et al.*, 2002; *van Wilgen et al.*, 2003]. Fire suppression and overgrazing have been conjectured to be able to trigger a sequence of processes – known as "bush encroachment" -leading to the conversion of desert grasslands into shrublands [e.g., *Archer et al*., 1988; *Archer*, 1989; *Van Auken*, 2000]. Bush encroachment is often associated with the formation of vegetation patterns characterized by patches of woody vegetation separated by bare ground. The emergence of this two-phase landscape [e.g., *Schlesinger et al.,* 1990] may result from the positive feedback inherent to the removal of nutrient-rich soil from the intercanopy areas, to its deposition onto vegetated patches, and to the consequent formation of "islands of fertility" [*Schlesinger et al*., 1990]. Wind erosion is often invoked as a major factor causing soil removal from intercanopy areas and deposition in shrub patches [*Okin and Gillette*, 2001]. Thus, by exposing the soil surface to the erosive action of winds [*Zobeck et al*., 1989; *Okin and Gillette*, 2001], disturbances - such as fires, grazing, and climate fluctuations - act as initiators of grassland-to-shrubland conversions, while wind erosion maintains and enhances these local heterogeneities in

nutrient and vegetation distribution [*Schlesinger et al*., 1990; *Schlesinger and Gramenopoulos*, 1996].

Despite the relevance of wind erosion and fires to the dynamics of arid and semiarid ecosystems, the interactions between these two processes remain poorly understood. Recent experimental evidence [*Whicker et al*., 2002] suggests that fires enhance soil susceptibility to wind erosion: the erodibility of burned and adjacent bare unburned soil plots was found to be significantly different in the desert shrublands of the American Southwest. The burned sites were observed to exhibit lower threshold velocities for wind erosion and higher volumes of soil loss. This finding remains partly unexplained, in that it is unclear why adjacent sites, with similar surface roughness and exposure to winds, should have differing susceptibility to wind erosion. Here we show that, by affecting the strength of interparticle wet-bonding forces, fire-induced water repellency enhances soil erodibility, causing a drop in wind erosion threshold velocity (the minimum velocity for erosion to occur). Thus, the mechanisms causing the enhancement of post-fire soil erodibility are associated with post-fire soil hydrophobicity.

Fires are known for having a major impact on infiltration, runoff and water erosion [e.g., *DeBano*, 2000]. The post-fire increase in runoff and soil erosion is caused by the decrease in infiltration capacity resulting from fire-induced water repellency [*Krammes* and *DeBano*, 1965; *DeBano*, 1966]. Organic compounds of chaparral and other vegetation types are volatilized by the fire and transported into the soil by the strong temperature gradients existing through the soil profile. The condensation of these vapours develops a hydrophopic coating of fatty acids around the soil particles [e.g., *DeBano,* 2000]. This effect depends on the fire regime, in particular on fire temperature

[e.g., *DeBano*, 2000; *Doerr et al.*, 2000]. The fatty acids affect the physical-chemical properties of the grain surfaces: in particular, they increase the contact angle formed by the air-water interface with the soil grains. When this angle exceeds $90^{o}$, the capillary pressure becomes positive [e.g., *Letey,* 2001] preventing the adsorption of moisture onto the soil grains. Further, in the case of porous materials like soil grains some other effects exist which are associated with the roughness of the soil surface and the existence of air-filled pore spaces and air-water interfaces beneath water droplets reaching the soil surface (e.g., rainfall). These effects result in enhanced repellency of the soil, referred to as super repellency [*McHale et.al.* 2005] and further limit the infiltration of rainfall or dew.

While the effect of post-fire water repellency on runoff and water erosion is relatively well-understood [e.g., *Doerr et al.,* 2000] its impact on wind erosion has never been assessed before. This is quite surprising, in that soil stabilization treatments with polysaccharides have been extensively studied in the recent past [e.g., *Saleh and Letey*, 1989; *Ben-Hur and Letey*, 1989; *El-Morsy* et al., 1991], while the enhancement of erodibility due to the release fatty acids from burning biomass has remained unexplored. In this paper we test through a number of wind tunnel experiments the hypothesis that fire-induced water repellency indeed increases soil susceptibility to wind erosion.

## 2. Materials and methods

### *2.1. Soil Type and treatments*

Three treatments of clean, well-sorted sand from the Ottawa, Illinois facility of US Silica (ASTM 20/30 Unground Silica) were used for this study. Ottawa sand is used in many experimental situations because its grains are uniform in size and with small surface area

($0.007 m^2/g$, e.g. *Lee,* 1999), are spherically shaped and hence they can be modeled as uniformly sized spheres. This sand has 97% of grain sizes between 0.85 and 0.60 mm. Further, the water repellency formed as a result of fires is known to be more severe in coarse-textured sandy soils because of their smaller specific surface area compared to fine-textured soils.

The compound used for the treatment, Hexadecanoic acid (Common name: Palmitic acid), is a common fatty acid found in most plants. Palmitic acid ($CH_3 (CH_2)_{14}$ ) is also able to cause water repellency in soils after heating by fire [*Letey, et al*, 1975; *Ma'shum, et al*, 1988; *Morley,* 2005]. Different concentrations of Hexadecanoic acid (HAD) were applied to sands to represent varying intensities of soil heating. To identify the appropriate treatments for this study, small samples (20g) were initially treated with different concentrations of HAD. Concentrations of 0.01% and 0.1% of HAD were found to be adequate for our purposes, as treatments with higher concentrations (i.e., > 0.1%) were causing the presence of clods and aggregates preventing the sand from being uniformly treated and well-mixed. Further, at higher concentrations (i.e., >1%) fatty acids were observed to coat the walls of the container used for treating the soil samples. Three concentrations of HAD were thus selected: 0.1% HAD (treatment #1), 0.01% HAD (treatment #2), and the control (i.e. untreated Ottawa sand). In each treatment, 45 kg of Ottawa sand was used.

The treated soils were prepared as follows: 2000g of Ottawa sand was placed in a heat resistant plastic container (0.25 m diameter, 0.1m height) and heated for 10-15 minutes in a high power microwave. Powdered HAD (96%) was added to the sand (2 g of fatty acid in 2000 g of sand for the 0.1% treatment and 0.2 g in 2000 g of sand for the

0.01% treatment), the container was closed and the contents were mixed thoroughly by shaking the container. The heating process was continued with mixing in between (by shaking the closed container) every 3-4 minutes. The heating and mixing processes were continued until the compound melted completely and mixed uniformly with the sand without forming aggregates. The sample was removed from the microwave and the mixing was continued until the sample reached room temperature. The same procedure was repeated several times until 45 kg were treated. The treated sands were stored (at ambient laboratory conditions) in a container and the contents were mixed thoroughly to ensure a uniform lot.

*2.2. Contact angle and hydrophobicity measurements*

The HAD (96%) crystals were melted in a small beaker. The end of a thin glass slide was dipped into this melted compound to obtain a uniform coating on the slide surface. The slide was taken out and the thin film coating of the melted compound was allowed to crystallize. Using this slide the contact angle between water droplets and the fatty acid coating was measured using a contact area measuring instrument (Cahn Dynamic Contact Angle Analyzer DCA-315). The average contact angle was found to be approximately equal to $90^{o}$ (average $89.4^{o}$ and standard deviation of 0.27) which indicates a water repellent surface.

The water drop penetration method was adopted to quantify the water repellency produced in the treated sands. The samples of each treatment were taken in a plastic cup (5 cm diameter and 5 cm deep). Using a pipette a drop of water was placed carefully on the surface of the soil. The time required for the drop to penetrate the surface was noted

down. The water drop penetration time (WDPT) for a sample was taken as the mean WDPT for 10 droplets.

*2.3. Wind tunnel tests*

The non-recirculating wind tunnel (Figure 5.1) used for this study (USDA-ARS Wind Erosion and Water Conservation Research Unit in Lubbock, Texas) is 10.0 m long, 0.5 m wide, and 1.0 m high; the test section has Plexiglas windows and is equipped with removable metal trays (1.5 cm x 46.0 cm x 100.0 cm). A fan at the end of the tunnel, powered by an electrical motor, generates the air stream by drawing air through the working section of the tunnel [e.g., *Orozco*, 2000].

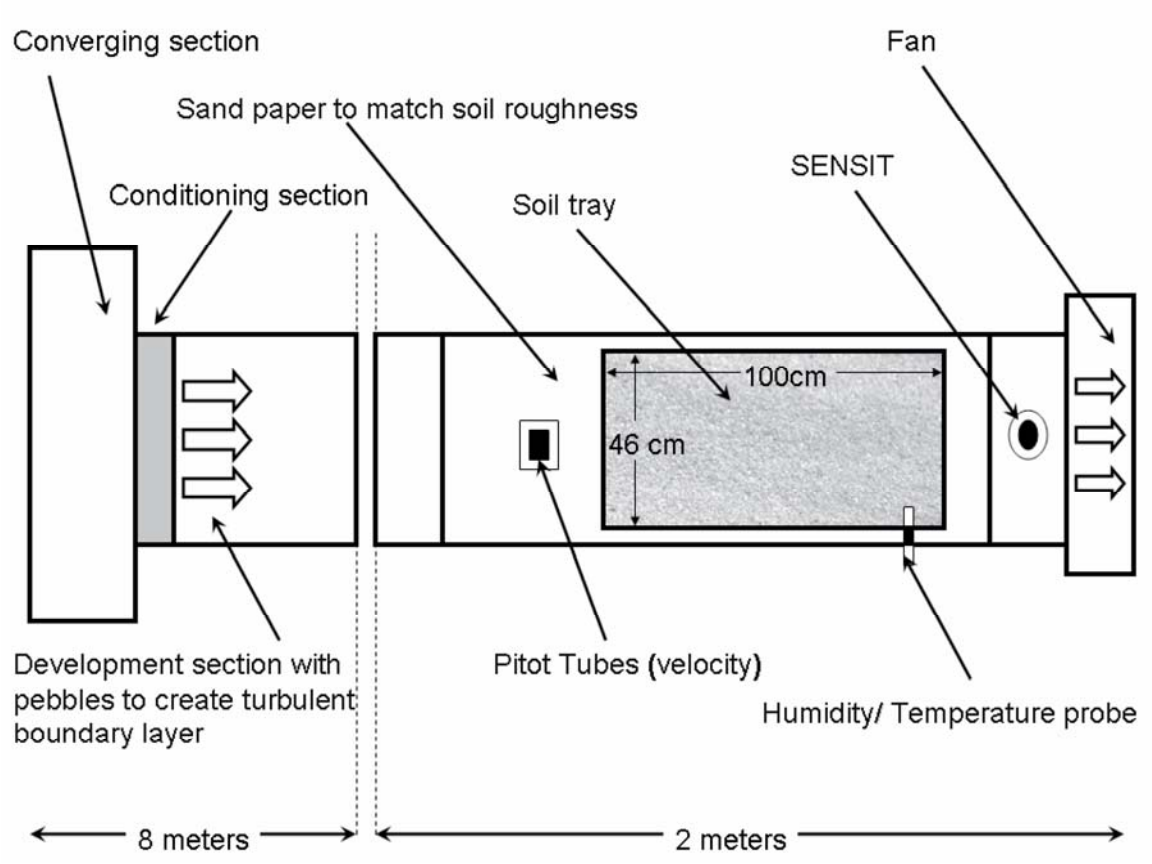


**Figure 5.1** Schematic representation of the wind tunnel

The wind velocity was measured using a SCANIVALVE pressure transducer connected with a Pitot tube installed upwind from the soil tray at a height of 60 cm above the bottom surface of the tunnel. The bottom of the tunnel was covered with a sand paper lining with the same roughness as the soil surface in the tray. The wind profile was measured using six Pitot tubes at different heights in the tunnel connected to different ports of the SCANIVALVE pressure transducer. These velocity values were used to calculate the parameters of the wind profile (roughness height = 0.0012 m, calculated by fitting the Prandtl-von Karman logarithmic law to the wind profile data) and to express the wind speed in terms of shear velocity ($u*$). Saltation was measured using a SENSIT impact sensor [e.g., *Stout and Zobeck*, 1997] mounted in the wind tunnel with the sensitive part at a height of 2 cm from the surface and 45 cm downwind from the soil tray. Air temperature and relative humidity were recorded by a probe (Vaisala, Inc. Humitter 50U) placed 2 mm above the soil surface and did not significantly change in the course of single experiments. Soil temperature was measured using an infrared thermometer (Exergen Corp. IRT/C.2 with Type K Germanium lens) mounted 90 cm above the soil surface. A handheld relative humidity/temperature probe (Testo, Inc. Model 610) was also used to determine ambient room temperature and relative humidity. The climatic parameters like atmospheric humidity and temperature were not controlled for these wind tunnel experiments. The air in Lubbock is generally dry and the stronger variability is due to the diurnal cycle more than to seasonal fluctuations. In order to cover a fairly broad range of relative humidity., the experiments were repeated on different days with different ambient conditions.

Three treatments of Ottawa sand (US Silica) were used for this wind tunnel study: 0.1% and 0.01% treatment with HAD and the no-HAD control. Each wind tunnel test consisted of three replicates of each treatment. The sands were kept on trays and allowed to equilibrate with the ambient atmospheric humidity for 8-12 hours before each wind tunnel test. The sands were not artificially wetted or dried and the wind tunnel tests were done at a range of atmospheric humidities (10 – 90 %). Hence for all these experiments, the only source of surface soil moisture was from the atmospheric humidity. Before each wind tunnel test the Pitot tube and its transducer were calibrated and corrections were made for changes in atmospheric temperature. The trays were then placed in the wind tunnel and the motor was activated. The air flow was initially increased stepwise to attain a wind speed just below the threshold value and then increased slowly until the particle impact sensor indicated particle movement. The threshold velocity was determined as the velocity at which an abrupt increase from zero to more than 100 particle impacts per second was observed. Statistical analysis (ANOVA) were done to show that the threshold velocity values were significantly different for the control and the treated soils.

*2.5 Estimating the moisture content of the water repellent soils*

The water repellency in the treatments was induced by mixing the Ottawa sand with HAD at the required concentrations as described in section 2.1. Soil from the top 2 mm was sampled from the controls and the treated soil trays after the each wind tunnel test, and the soil moisture from each sample was measured gravimetrically. In our previous studies done under same range of ambient conditions (10-90 % RH) it was shown that the wind tunnel experiments were not affected by soil drying during the tests [*Ravi et al*, 2004, *Ravi et al,* 2006b]. The melting point of HAD is approximately 63° C;

thus, the standard procedure to calculate gravimetric soil moisture by oven drying cannot be followed because a considerable amount of organics would be lost along with the soil moisture in the course of the drying process. To account for this loss of organics during oven drying and to accurately measure the moisture content of these treated soils, the palmitic acid concentrations (from total carbon content) of each treatment and of the control were measured before and after oven-drying using a CN analyzer (Carlo Erba Elemental Analyzer NA1500). The soil treated with 0.01% concentration of organics was found to be extremely heterogeneous, i.e., with a non-uniform coating of the sand grains with HAD. Hence the carbon and moisture content (not shown) were found to be extremely heterogeneous in the 0.01% treated sand. Statistical analyses (ANOVA) were done to test the significance of the variations in surface soil moisture between the control and the treated soils for the four classes of relative humidity considered in this study.

*2.6 Water retention curves*

The moisture retention curves (Figure 5.2) for the control and treatments were determined by measuring the water potential values (using a water activity meter, DECAGON AquaLab Series 3T) and moisture content (gravimetrically, with adjustment to account for the loss of organics during oven drying). The water activity meter used in this study can determine soil matric potentials above –300 MPa with an accuracy of +/- 0.003 water activity units [*Gee et al.,* 1992]. Water activity readings, $a_w$, were converted into matric potential values as $\psi_m = \frac{RT}{M}\ln(a_w)$, where $\psi_m$ is the matric potential, $R$ is the gas constant, $M$ is the molecular mass of water and $T$ is the Kelvin temperature.

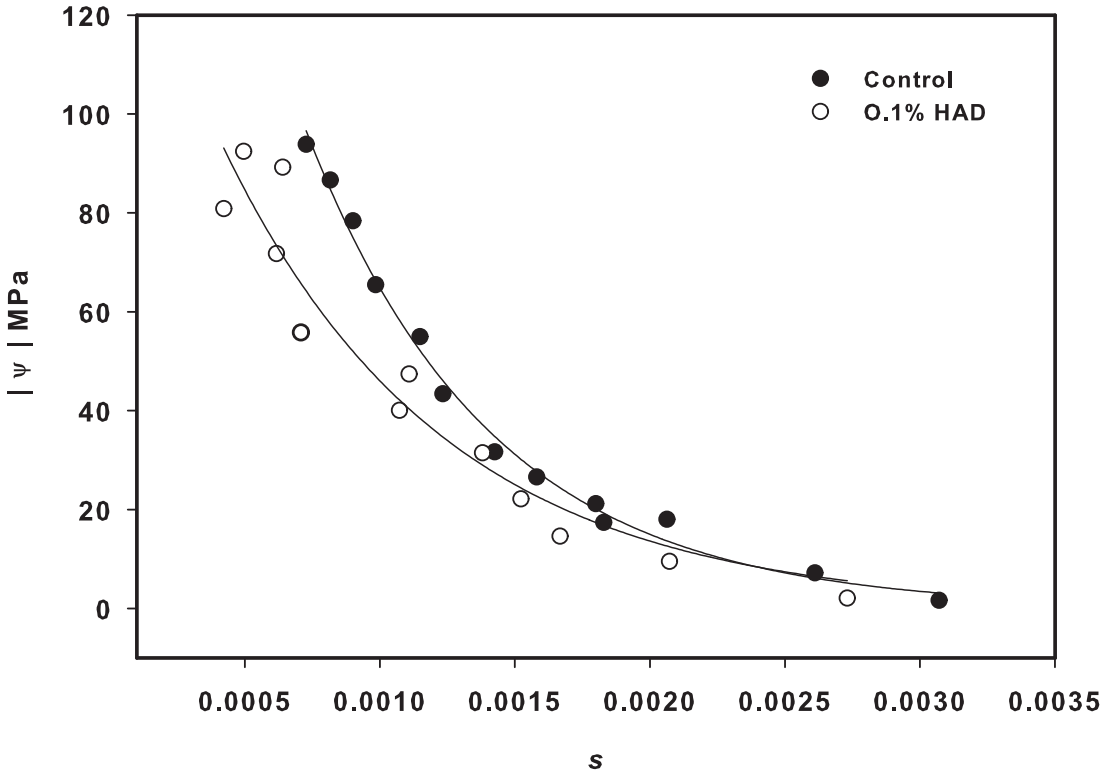


**Figure 5.2** Water retention curves for the control and the repellent soil (0.1%) used in this study. *s* represents gravimetric soil moisture and |ψ| is the absolute value of matric potential.

## 3. Results

### *3.1 Water Drop Penetration Time*

The repellent soils made in the laboratory were tested for the extent of water repellency induced by the organic coatings using the water drop penetration method. This analysis showed that the organic coatings on the soils grains were able to induce water repellency in both the HAD treated sands. The control sand was perfectly wettable, with water drops penetrating the soil surface instantly. The repellent soil treatments were not easily wettable: the water drop penetration time (WDPT) for the samples treated with 0.01% of

palmitic acid ranged between 5-6 hours, while for soil treated with 0.1% of the same compound the WDPT was 8-9 hours. These results indicate that the organic coating did induce water repellency and that this hydrophobicity was stronger in soils treated with higher concentrations of HAD.

*3.2 Wind tunnel experiments*

The effect of water-repellent coatings on wind erosion threshold velocity was assessed under different levels of atmospheric humidity through wind tunnel tests carried out on three soil treatments. The primary experimental result of this study is that in each of the four different humidity ranges considered (i.e., 10-30%, 30-50%, 50-70%, and 70-90%) the threshold velocity was highest for the control sand (Figure 5.3) and decreased with increasing concentrations of fatty acid. The differences between the threshold velocity values of control and 0.01% treated sand and between 0.01% and 0.1% treated sand were found to be significant ($p<0.0001$) in all the humidity classes, while the surface moisture content of the control and 0.1% treated sands were found to be not significantly different for all the humidity classes ($p>0.05$). Thus, the statistical analyses show that the threshold velocity values were significantly different for the control and the treated soils even though the surface moisture contents were not significantly different. Moreover, for each treatment the threshold values increased with increasing air humidity, indicating the existence of a clear dependence of threshold velocity on air humidity (Figure 5.3). In this case, due to the absence of clay fractions the effect of absorbed moisture on interparticle bonding was different from our previous findings [*Ravi et al.* 2004; 2006b; *Ravi and D'Odorico,* 2005] in that the threshold velocity for wind erosion exhibited a monotonic increase with the humidity of overlying air.

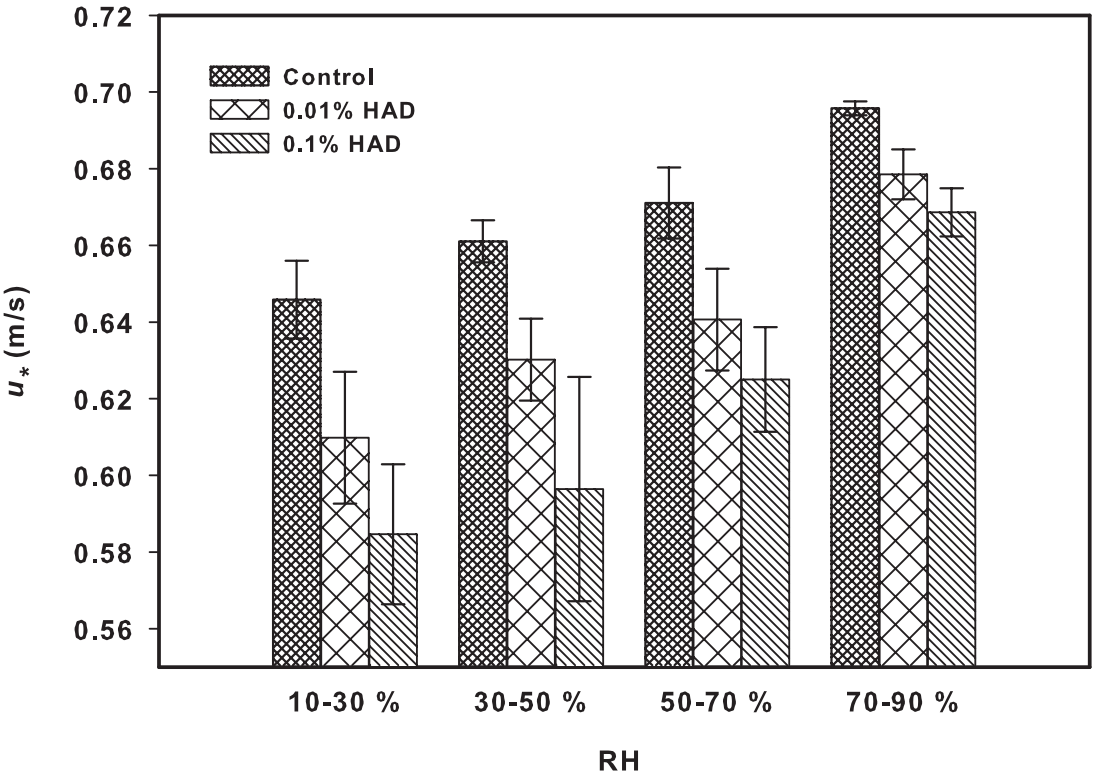


**Figure 5.3** Threshold shear velocity ($u_*$) as a function of atmospheric relative humidity (RH) as determined by wind-tunnel tests for three soil treatments. The error bars represent the standard deviation of threshold shear velocity within each class of relative humidity.

*3.2 Surface soil moisture and water retention curves*

Surface soil moisture of the control was observed to increase with increasing near-surface air humidity (Figure 5.4) consistently with our previous studies [*Ravi et al*., 2004; 2006b]. These results indicate that in the absence of other inputs of water, surface soil moisture (hence the threshold velocity) was controlled by near-surface atmospheric humidity. The sensitivity of surface water content on relative humidity was found to be stronger for the control soil than for the treatment #1 (0.1% of HAD). However, the

surface moisture content of the treatment with 0.1 % concentration of the HAD was also found to increase with increase in air humidity.

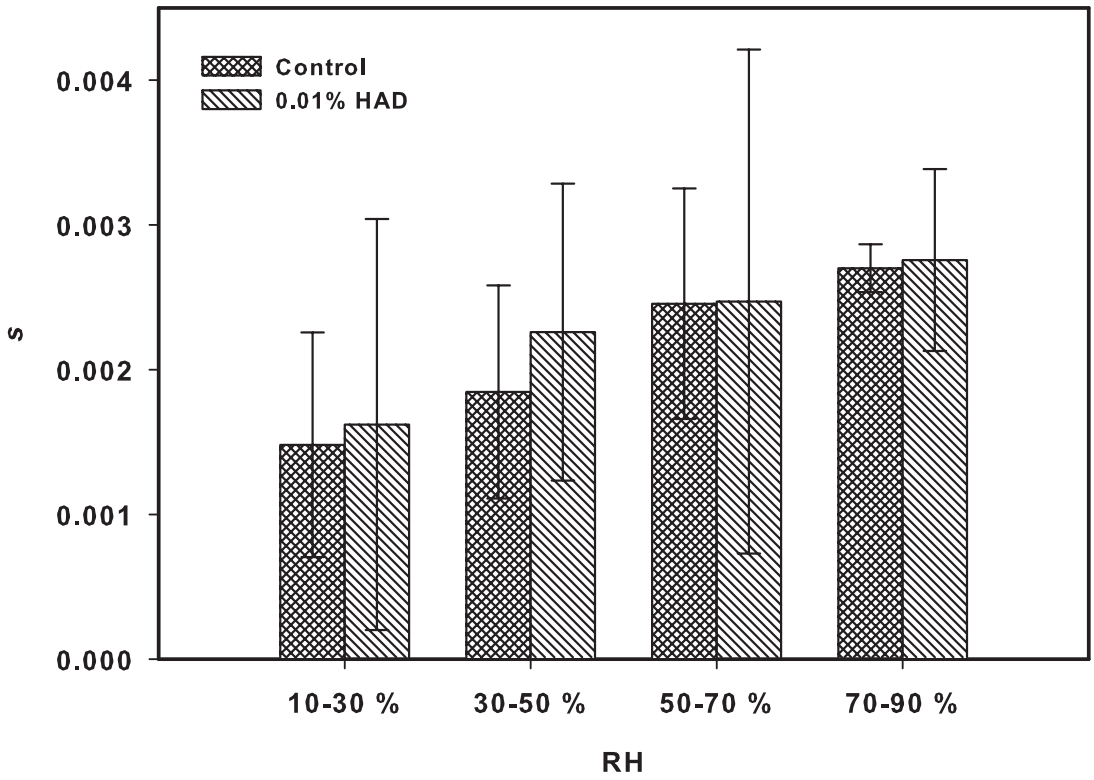


**Figure 5.4** Surface soil moisture (*s*) of the control and repellent soil (0.1%) at different atmospheric relative humidity (RH) ranges. The error bars represent the standard deviation of surface soil moisture within each class of relative humidity.

The moisture content of the treatment was consistently (slightly) higher than the control for the different humidity ranges considered for this study, though for some of them the differences in moisture content between treated and untreated soils were found not to be significantly different (Figure 5.4). The water retention curves (Figure 5.2) were almost similar for the control and the treated soil (0.1%) which indicated that these soils did not differ significantly in moisture retention properties.

## 4. A theoretical framework for the modeling of liquid-bridge bonding

Theories for the estimation of the threshold velocity for wind erosion generally do not account for the dependence on the contact angle, γ, which is usually taken equal to zero [*Fisher*, 1926; *McKenna-Neuman and Nickling*, 1989; *Cornelis et al.*, 2004]. This angle expresses the effect of the physical-chemical properties of soil grains and liquid (i.e., water) on the interaction between the grain surfaces and the fluid (Figure 5.5), while the surface tension is a property of the fluid only.

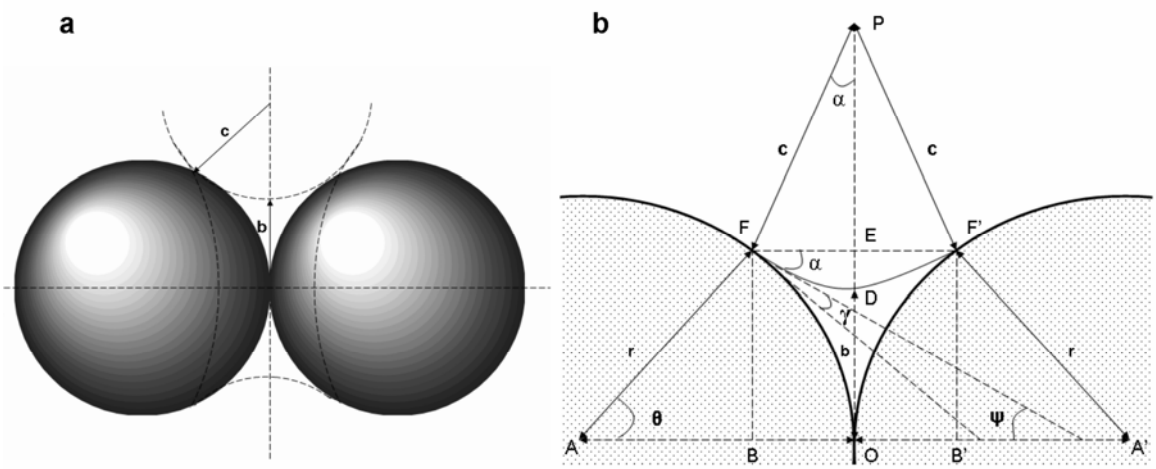


**Figure 5.5** (a) Shows the liquid bridge between two uniform spherical soil grains (b) Shows the contact angle (γ) between two uniform spherical soil grains with radius r. From simple geometric consideration we have that $\psi = \alpha = \frac{\pi}{2} - (\theta + \gamma)$.

The organic coating changes the contact angle in the treated soils thereby affecting the interparticle force due to liquid bridges between the adjacent soil particles. We adopt the theoretical framework developed by Fisher [1926] to show the impact of contact angle on interparticle forces ($F_i$) associated with liquid-bridge bonding between spherical particles. Liquid bridge bonding consists of capillary forces associated with (a) the tension due to the curvature of the air water interface and (b) the pressure deficit

between the pore air and the water in the liquid bridge [e.g., *Cornelis et.al.*, 2004]. In the case of spherical soil grains [Fisher, 1926] the interparticle force is

$$F_i = 2\pi bT\cos\psi + \pi b^2 T\left(\frac{1}{c}-\frac{1}{b}\right) \tag{5.1}$$

where $T$ is the surface tension of water, $b$ is the radius if the fluid neck connecting two spherical grains, $c$ is the radius of the meridian curve and $(\frac{1}{c}-\frac{1}{b})$ represents the total curvature of the surface at this point (see Figure 5.5).

In non-repellent soils the contact angle is γ=0°, while the maximum hydrophobicity is attained when γ=90°. We generalize Fisher's theory to account also for the dependence on the contact angle. From simple geometric considerations (Figure 5.5) we have that $\psi = \frac{\pi}{2} - (\theta + \gamma)$ and

$$c = \frac{r(1-\cos\theta)}{\cos(\theta+\gamma)}\,, \qquad b = r\sin\theta - c\left[1-\cos\left(\frac{\pi}{2}-(\theta+\gamma)\right)\right] \tag{5.2}$$

Expressing the interparticle force given by equation (5.1) in terms of contact angle γ, $F_i$ becomes

$$F_i = 2\pi bT\sin(\theta+\gamma) + \pi b^2 T\left(\frac{1}{c}-\frac{1}{b}\right) \tag{5.3}$$

with $b$ and $c$ depending on $\gamma$ (equation (5.3)).

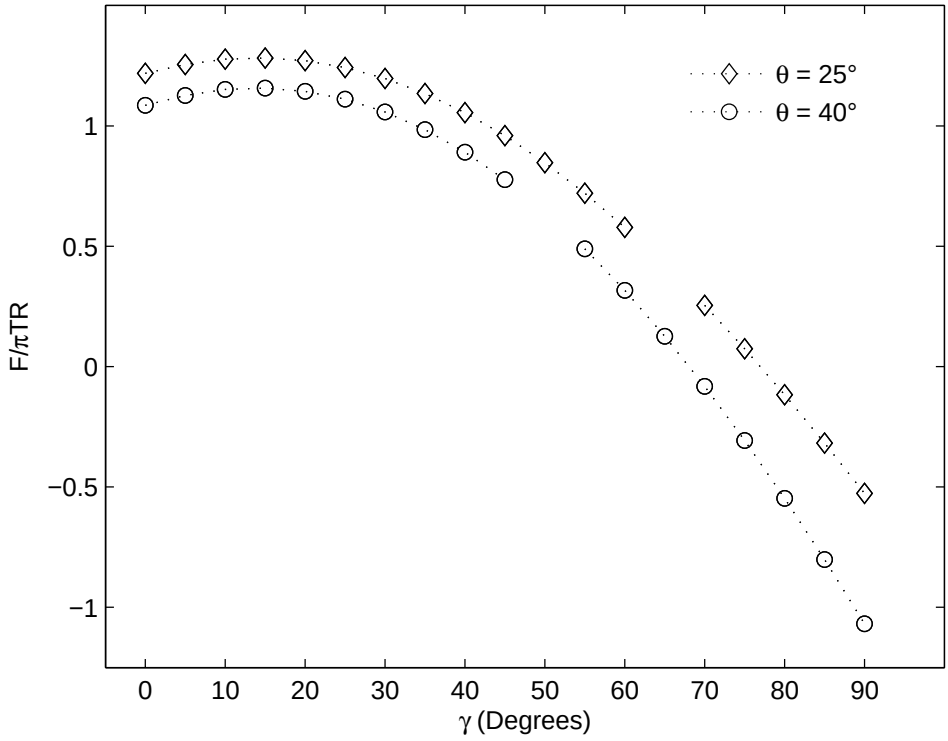


**Figure 5.6** Dependence between inter particle force and contact angle, γ, (equation 5.2) for a close packing (circles) and open packing (diamonds) systems with 12.5 % moisture content (expressed as % of pore space, *i.e.*, *s*=0.125). The angle θ (Figure 5.5) depends both on moisture content and on soil packing.

The value of θ was given by Fisher [1926] as a function of the moisture content for open packing and closed packing systems. In our case we found that the moisture content (hence, the angle θ) remained about the same between treated sands and the control. In the numerical calculations shown in figure 5.6 we use a value of relative soil moisture, s=12.5% (expressed as percentage of pore space). The corresponding values of θ are 40° and 25° for the open and close packing, respectively [*Fisher*, 1926, Table. I]. Equation (5.3) can be rewritten in dimensionless form as,

$$\frac{F_i}{\pi r T} = \left( \frac{b-c}{c} + 2\sin(\theta + \gamma) \right) \frac{b}{r} \tag{5.4}$$

where the right-hand-side is a function only of the moisture content (through the angle θ) and of the contact angle, γ. Figure 5.6 shows a plot of $\frac{F_i}{T\pi r}$ calculated using equation (5.4) as a function of the contact angle γ for the cases of close and open packing.

## 5. Discussion

The existence of higher moisture contents in water repellent soil seems to be counterintuitive, as water repellent soils are expected to adsorb less moisture from the overlying atmosphere. However, these results confirm the findings by Barrett and *Slaymaker* [1989], who observed that water repellent soils can absorb water. These authors suggested that water can move more freely as vapor in a water repellent soil than in a normal soil, allowing soil water to be redistributed even though the adsorption capacity of water repellent soil grain surfaces for water molecules is small. *Vermeire et al*, [2005] observed, in field plot experiments, that the repellent soils had about the same moisture contents compared to control soils. *Doerr et al* [2000] reviewed three different mechanisms that can be invoked to explain this counterintuitive behavior. In summary, a conclusive theory for water absorption by hydrophobic soils is still missing.

The results from the wind tunnel tests indicated that the water repellent sands were more susceptible to wind erosion compared to the control sand. The statistical analyses show that the threshold velocity values were significantly different for the control and the treated soils even though the surface moisture contents were not significantly different.

Three possible mechanisms may (in general) explain the decrease in threshold velocities for water repellent soils: (a) the effect of hydrophobicity on moisture adsorption on treated soils; (b) the geometry of the adsorbed layers, and (c) the effect of water repellent coatings on the contact angle. In the following discussion we will show to what extent these mechanisms can be invoked to explain the effect of water repellency on soil erodibility.

The condensation of water in the form of droplets adsorbed onto surfaces of water repellent grains is, in general, limited in hydrophobic soils [*Osmet*, 1963; see also Figure 5.7]. At lower humidities (before the formation of liquid bridges) moisture content could affect the threshold velocity through an "added gravity effect" (i.e. these soils might be expected to retain less adsorbed water and to be consequently lighter and with a lower threshold velocity, e.g. *Gregory and Darwish,* 1990). However, in our case, the fact that both the moisture content and the water retention curves (Figure 5.2) were about the same for the control and the treated soil (0.1%) suggests that these soils did not differ significantly in moisture retention properties. Thus the lower threshold values observed for water repellent soils in our study cannot be attributed to weaker moisture adsorption on the grain surface than in the control. However, the more irregular geometry of the adsorbed layers formed on HAD-treated soil grains (Figure 5.7) might have affected the strength of the adsorbed-layer forces by reducing the contact area between adjacent adsorbed layers. This reduction would be similar to the effect of surface roughness on the soil grains investigated by *Harnby* [1992].

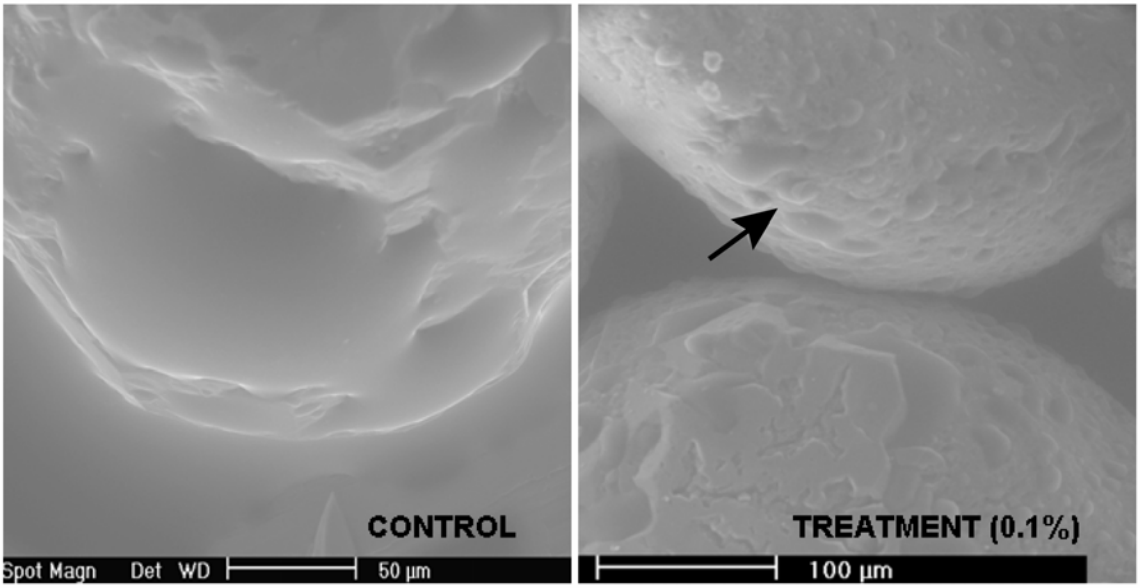


**Figure 5.7**. Photos taken with Environmental Scanning Electron Microscope of treated and untreated soil grains (at RH 80-90%). There is a clear difference in moisture adsorption onto grain surfaces for the control and repellent soil. The control soil has grains with a uniform coating of adsorbed water, while moisture is adsorbed onto the 0.1% treated soil with an irregular distribution of water droplets condensing on grain surfaces (indicated by the arrow).

As the atmospheric humidity increases, the thickness of the adsorption film increases and eventually reaches a stage when condensation starts to occur in the contact points between the particles, thereby forming a liquid bridge [*Harnby*, 1992]. The repellent coatings on the soils can delay the formation of liquid bridges, or even prevent their formation in cases of extremely water repellent soils. In such cases, i.e. when the contact angle exceeds $90^{o}$, the capillary pressure becomes positive [e.g., *Letey,* 2001] preventing penetration of moisture in the interstices between soil particles. This limitation on moisture penetration significantly reduces the interparticle forces associated with moisture bonding. Two different mechanisms contribute to wet-bonding forces in soils [e.g., *Ravi et al.*, 2006b], namely adsorbed-layer bonding in relatively dry soils, and

liquid-bridge bonding in wetter soils. In our previous work we have indicated RH≈60% as a reference threshold value for the formation of liquid bridges. We have also shown that for RH<60% - i.e., when the effects of adsorbed-layer bonding are stronger - the threshold velocity decreases with increasing values of RH (hence with increasing moisture contents [*Ravi et al.*, 2004; 2006b]. This effect was not observed in the soils used in this study (not even in the control), probably due to the low adsorptive capacity of these sandy soils, with no clay fractions. Thus, we argue that adsorbed-layer bonding was weak both in the control and in the treated soils. The dependence of threshold velocity on moisture content (i.e., on RH) was probably due to capillarity and to early stages of liquid bridge formation even in air dry soils (i.e., RH<60%). Since the moisture absorption explanation does not appear to work (except for the likely effect of the treatment on the geometry of the adsorbed layer), due to the low adsorptive capacity of these soils and the insignificant differences in moisture content between treated soils and the control, let us explain the difference in soil erodibility for the three treatments as the effect of changes in the contact angle between liquid bridges and the soil grains. Liquid bridge-bonding is known for being the dominant interparticle bonding force [Cornelis et al., 2004] in relatively wet soils (e.g., RH>60%) and we argue that at the early stages of bridge formation it may limit the erodibility also of air-dry, clay-free sandy soils. Figure 5.6 shows the effect of the contact angle on interparticle forces due to liquid-bridge bonding. It is observed that a maximum can be observed, beyond which $\frac{F_i}{T\pi r}$ increases with contact angle. The $\frac{F_i}{T\pi r}$ values overall decrease when the contact angle increase from 0° (perfectly wettable soil) to 90° (perfectly water repellent soil). This result indicates that

the interparticle forces associated with wet-bonding effects decrease with increasing degrees of water repellency. The interparticle bonding force ($F_i$) is related to threshold velocity ($u*$) for wind erosion as [e.g. *McKenna Neuman,* 2003, *Cornelis et al.,* 2004].

$$u_* \propto \sqrt{1+\frac{F_i B}{8(\rho_s-\rho_a)gr^3}} \tag{5.5}$$

where $\rho_s, \rho_a$ are the densities of the soil grains and air, respectively, g is the acceleration due to gravity, and B is a constant (electrostatic forces between the soil grains are not considered in this expression as these forces are negligible for sandy soils) . Thus the decrease in interparticle forces explains the consistent decrease in threshold velocity that we found (Figure 5.3) with increasing concentrations of soil organic repellents (i.e. increasing values of γ) despite the fact that the moisture contents and water retention characteristics were comparable.

The effect of enhancement of soil erodibility by fires depends also on a number of factors that have not been addressed in this study. For example, the level of soil hydrophobicity developed by fires depends on fire intensity, vegetation cover, and soil texture. Other authors have already investigated how these factors affect the formation of water repellency at the soil surface [e.g., *Doerr* et al., 2000]. Our research focused directly on the effect of water repellency on soil erodibility. Thus, the results can be applied also to the case of water repellency produced by vegetation in the absence of fires. This non-pyrogenic repellency can be by itself significant, especially in coarse textured soils [*e.g., Bond,* 1964]. Further, this study focused only on post-fire enhancement of mineral soil erodibility, while other effects associated with the deflation of surface ashes and other light combustion products have not been investigated. This loose, nutrient-rich organic material is readily lost from the burned site by wind erosion.

The effect of soil water repellency on wind erosion is expected to come into play once most of the light, charred and burned surface material has been removed.

## 6. Conclusions

Our results experimentally support the hypothesis that fire induced water repellency in arid soils significantly affect the soil susceptibility to wind erosion. This study has shown that the 0.01% and 0.1% treatments with HAD were able to induce significant water repellency in soils. These repellent soils showed neither a significant change in moisture retention curves or in the moisture content. However water repellency was able to induce important changes in the threshold shear velocity for wind erosion, which was found to decrease with the increasing degrees of soil water repellency. The results were explained as an effect of the increase in soil-water contact angle (induced by the organic coating of the soil grains) on the strength of interparticle wet-bonding forces. Through a theoretical framework developed to express the wet bonding forces as a function of contact angle it was shown that water repellency weakens the interparticle forces, thereby enhancing soil erodibility by wind.

# CHAPTER: 6

# THE EFFECT OF FIRE-INDUCED SOIL HYDROPHOBICITY ON WIND EROSION IN A SEMIARID GRASSLAND: EXPERIMENTAL OBSERVATIONS AND THEORETICAL FRAMEWORK

(This chapter is in press for *Geomorphology*)

## Abstract

Arid land ecosystems are often susceptible to degradation resulting from disturbances like fires and grazing. By exposing the soil surface to the erosive action of winds, these disturbances contribute to the redistribution of soil nutrients associated with grassland-to-shrubland conversions and to the formation of a heterogeneous landscape. Wind erosion maintains the local heterogeneities in nutrient and vegetation distribution in arid landscapes through the removal of nutrient-rich soil from the intercanopy areas and the subsequent deposition of soil onto vegetation patches. Even though wind erosion and disturbances like fires strongly interact with each other and determine vegetation patterns in arid landscapes, very few studies have addressed these interactions. Using soil samples collected after a wildfire event at the Cimarron National Grasslands in southwestern Kansas, we demonstrate through a series of wind tunnel experiments, laboratory measurements and theoretical analyses how wind erosion can be enhanced by fire-induced water repellency. Results from the wind tunnel experiments show that in semiarid grasslands fires can cause a decrease in the threshold velocity of wind erosion, thereby enhancing the post-burn erosion of (hydrophobic) soils. Further, a generalized process-based theoretical equation was derived to explain the decrease in threshold

friction velocity in water-repellent soil for the case of soil particles modeled as asymmetrical cones.

## 1. Introduction

In arid and semiarid environments, aeolian processes redistribute soil particles and nutrients [*Schlesinger et al*., 1990; *Okin and Gillette*, 2001] thereby affecting soil surface texture, water holding capacity, and soil fertility [*Offer et al*., 1998; *Lyles and Tatarko*, 1986]. These changes in the characteristics and distribution of soil affect the productivity, composition and spatial patterns of vegetation in arid landscapes [*Schlesinger et al*., 1990]. Arid lands exhibit fragile ecosystems susceptible to degradation from disturbances like fires and grazing, which can modify the interactions among ecological, hydrological, and land surface processes [*Ludwig et al*., 1997]. These disturbances expose the soil surface to the erosive action of winds and consequently contribute to the formation of a heterogeneous landscape. In arid shrublands, soil erosion results mainly from aeolian, as opposed to fluvial, processes [*Breshears et al*., 2003], which maintain local heterogeneities in nutrient and vegetation distribution through the removal of nutrient-rich soil from intercanopy areas and subsequent deposition onto vegetation patches [*Schlesinger et al*., 1990; *Okin and Gillette*, 2001]. On the other hand, fires affect the abundance and distribution of shrubs and grasses in arid ecosystems [*Scholes and Archer*, 1997; *van Langevelde et al*., 2003; *Sankaran et al*., 2004]. Thus, wind erosion and fires influence the dynamics of dryland landscapes, and the interactions between these two processes play a major role in determining the composition and structure of vegetation patches.

The relevance of wind erosion and fires to the dynamics of dryland landscapes explains the need to investigate the interactions between these two processes. Even though interactions of wind erosion with disturbances such as fires are expected to affect the dynamics and spatial patterns of arid land vegetation, only a limited number of studies have investigated these interactions within a process-based framework. Recent studies [*Whicker et al*., 2002, *Ravi et al*., 2006a] have shown that fire increases the soil susceptibility to wind erosion in arid lands. Further, *Ravi et al*. (2006a) experimentally showed that the enhancement of post-fire erodibility was associated with soil hydrophobicity and explained these findings as the effect of water-repellent compounds released by burning plants. The condensation of these compounds onto the soil particles modifies the contact angle between soil grains and air-water interface in the soil pores with consequent effects on the strength of interparticle wet bonding forces.

The empirical relations between concentration of water-repellent compounds and the threshold velocity for wind erosion found by *Ravi et al*. [2006a] were determined using clean, uniform, and almost spherical sand grains treated in the laboratory, while to date these effects have not been tested using natural soils. Thus, it remains unclear whether the water repellency developed by real fires may indeed lead to a noticeable increase in soil erodibility in natural soils. Moreover, the theoretical framework developed by *Ravi et al*. [2006a] to show the dependence of interparticle bonding forces on the contact angle was derived in the idealized case of spherical soil particles and thus, it is not well-suited to explain the effect of repellency on capillarity in real soil, which generally consists of particles with relatively sharp edges. Here, we use soils from burned and unburned plots collected after a major fire event at the Cimarron National Grasslands

(KS) to demonstrate that wind erosion may be enhanced by fire-induced water repellency. Further, the theoretical expression developed by *Ravi et al*. [2006a] to explain the decrease in threshold friction velocity in water-repellent soils is generalized to the case of more natural grain shapes.

## 2. Background

For the wind to cause soil erosion, its speed must exceed a certain threshold value that depends on field surface conditions, size and shape of the aggregates, clay content, near surface soil moisture, and other physical and biotic factors [*Bagnold*, 1941; *Belly, 1960*]. Surface soil moisture is an important factor controlling changes in soil erodibility at relatively short (e.g., diurnal) time scales [*Gregory and Darwish*, 1990; *McKenna Neuman and Nickling*, 1989; *Fecan et al*., 1999; *Ravi et al*., 2004]. Laboratory tests [*Ravi et al*., 2004, 2006b] have shown that atmospheric humidity plays a major role in determining the moisture content of the soil-surface. Indeed, air humidity has been used as a proxy for surface soil moisture in some recent studies on soil moisture controls on threshold velocity [*Ravi et al*., 2004; *Ravi and D'Odorico*, 2005].

Soil water is stored in the soil matrix below field capacity in two ways: as liquid-bridges formed around contact points between adjacent grains, and in the thin film of water adsorbed on the grain surface [*Hillel*, 1980]. Whether adsorbed onto grain surfaces or stored in liquid-bridges, moisture significantly affects the entrainment of soil particles by wind [e.g., *McKenna Neuman and Nickling*, 1989; *Fecan et al*., 1999; *Ravi et al*., 2006b] by introducing wet-bonding forces between the grains. Capillary forces are significant under relatively large soil moisture conditions when a liquid-bridge exists

between the soil grains. In these conditions the interparticle forces are contributed mostly by capillarity, especially in sandy soils, where only a small water fraction is retained in the adsorbed layer. In air-dry soils at low humidity the adsorptive (i.e., hygroscopic) forces dominate the wet-bonding forces because soils are too dry for the formation of liquid-bridges, thus no liquid-bridge bonding (i.e., capillarity) occurs. The amount of water adsorbed on the grain surface depends on hygroscopic properties of the soil particles, and it increases with clay content. At relatively large values of atmospheric humidity, water vapor condenses close to the contact point between soil grains and leads to the formation of liquid-bridges [*Harnby*, 1992]. Liquid-bridge bonding consists of capillary forces associated with (a) tension because of the curvature of the air-water interface and (b) the pressure deficit between the pore air and the water in the liquid-bridge [e.g., *Fisher*, 1926; *Cornelis et al*., 2004].

During fires, organic compounds released by burning biomass are volatilized and transported into the soil by the strong air pressure gradients that are set up by strong temperature gradients existing within the soil. The condensation of these organic vapors around the soil grains may create a hydrophobic coating depending on the nature of the parent fatty acid [e.g., *DeBano*, 2000]. The severity of this hydrophobic effect depends on the fire regime, in particular on fire temperature, soil properties, moisture content, type of vegetation and other factors [*e.g.*, *DeBano*, 2000; *Doerr et al*., 2000]. The presence of these hydrophobic coatings increases the contact angle ($\gamma$) formed by the air-water interface with the soil grains. When the contact angle, which is an indicator of the free energy of the solid-gas interface in soils, is less than $90^{o}$, water displaces air in the soil pores and spontaneously wets the soil; conversely, when the contact angle exceeds $90^{o}$,

an external force is required to wet the soil by forcing the displacement of air within the interspaces between grains. When this angle exceeds $90^o$, the capillary pressure becomes positive [*e.g.*, *Letey*, 2001] and prevents the wetting of the soil grains. As the aeolian erosion process affects the top few millimeters of the soil, the moisture content of the surface soil needs to be considered to investigate its effect on the intergrain bonding forces. At the same time water retention properties at the soil surface may be significantly affected by hydrophobicity induced by fires.

The threshold velocity ($u_t$) for wind erosion depends on the interparticle bonding force ($F_i$) as [*e.g.*, *McKenna- Neuman*, 2003, *Cornelis et al*., 2004]

$$u_t \propto \sqrt{1+\frac{F_i B}{8(\rho_s-\rho_a)gr^3}} \tag{6.1}$$

with $\rho_s, \rho_a$ being the densities of the soil grains and air respectively, $g$ the acceleration of gravity, $r$ radius of the grain and $B$ a constant. Existing theories for the estimation of the threshold friction velocity for wind erosion generally do not account for the dependence of the interparticle force on the contact angle, $\gamma$, which is usually taken as being equal to zero [*Fisher*, 1926; *McKenna Neuman and Nickling*, 1989; *Cornelis et al*., 2004]. *Ravi et al*. [2006a] developed a theory that accounts for this effect by modifying the theory by *Fisher* [1926] to express the interparticle force because of liquid-bridge bonding between spherical particles of radius $r$ as a function of the contact angle. *Ravi et al*. [2006a] showed that the interparticle bonding force first increases and then decreases when the contact angle increases from 0° (perfectly wettable soil) to 90° (water-repellent soil). The theoretical equation developed by *Ravi et al*. [2006a] expressing the decrease in threshold friction velocity in water-repellent soils is generalized in this paper (see Appendix C) to the case of more irregular soil grains (*i.e.*, with sharper edges) by

assuming the contact areas between the soil grains to be approximated as asymmetrical cones rather than spheres, as suggested by *McKenna Neuman and Nickling* [1989].

## 3. Materials and methods

### *3.1 Soil sampling and study site*

In the midst of an extended drought associated coincidentally with many large grassfires throughout a large portion of the US Southern Great Plains [*National Climatic Data Center*, 2006] on February 5, 2006, a large fire spread through part of the Cimarron National Grassland near Elkhart in the southwest corner of Kansas (Figure 6.1).

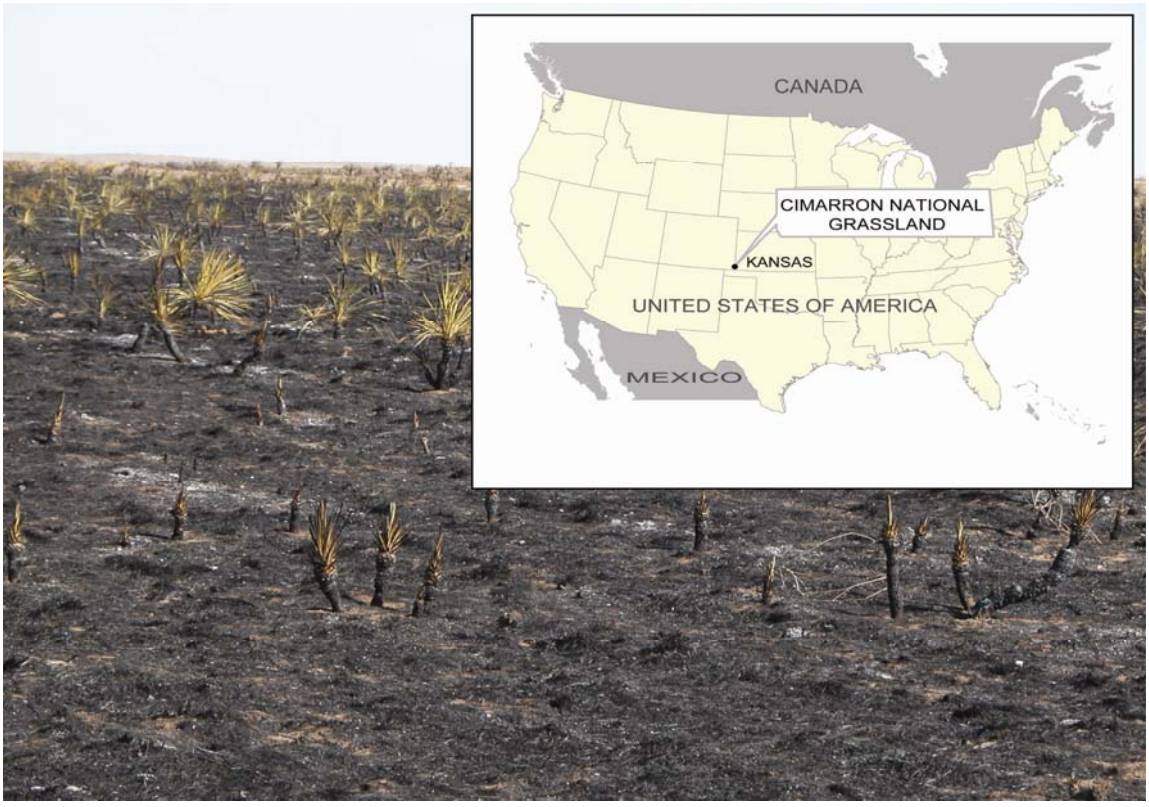


**Figure 6.1** A photo of the burned field at the Cimarron National Grassland (the burned Yuccas in the picture are approximately 0.5 m tall). Inset shows the location of study area.

This fire was termed the “Steeler Fire” by US Forest Service personnel and it burned an area of approximately 1700 ha [*US Forest Service*, 2006]. This human-caused fire happened at the beginning of the windy season. After all of the above-ground vegetation had burned, the soil surface was left exposed to strong winds resulting in rapid erosion. Ten days later on February 15, soil samples were collected from a burned short-grass prairie ecosystem affected by significant shrub encroachment (Figure 6.1). Surface soil (top 5 cm) was collected from three replicate plots from the burned area and adjacent unburned area separated by the fire line. Most of the burned vegetation debris and black carbon had been blown off of the soil surface during the ten days since the fire. Water drop penetration tests carried out in the field showed that significant water repellency existed in the burned plots (Figure 6.2).

**Figure 6.2** Water Drop Penetration Test (WDPT) on the burned plot indicating a water repellent soil (the water drop in the picture has a diameter of approximately 1 centimeter).

*3.2 Characterization of soil hydrophobicity*

The severity of fire-induced water repellency of the soil samples was measured in the laboratory by two methods: the water drop penetration time (WDPT), and the molarity of an ethanol drop (MED) instantaneously infiltrating into the soil [e.g., *Doerr*, 1998]. The samples of each treatment were transferred to metal cups (5 cm diameter and 5 cm deep). For the WDPT test, a pipette was used to carefully place water drops on the soil surface. The time required for the drop to penetrate the surface was noted. The time for the water drop to penetrate (WDPT) for a sample was taken as the mean penetration time for ten droplets. In the MED test, standardized solutions of ethanol in water of known surface tensions were used to characterize the water repellency in the soil [*Doerr*, 1998; *Roy and McGill*., 2002]. Drops of the ethanol-water solutions with increasing molar concentrations are placed on the surface of the water-repellent soil sample. As the molarity of the solution increases, the surface tension decreases and at a certain critical concentration (designated the 'critical surface tension') the drop penetrates the soil surface instantaneously (*i.e*., within 2 seconds). The MED test results were used to calculate the initial advancing contact angle $\theta$ [*Roy and McGill*, 2002] using the equation

$$Cos\,\theta = \left(\frac{T_c}{T_w}\right)^{\frac{1}{2}} - 1 \qquad (6.2)$$

where $T_c$ is the surface tension of the ethanol water solution that instantaneously wets the water repellent soil and $T_w$ is the surface tension of water.

*3.3 Soil texture analysis and soil moisture retention curves*

The fractions of sand, silt, and clay in each soil sample were measured using the standard hydrometer method [*ASTM*, 1981; *Liu et al*, 1984]. A hydrometer (Fisherbrand Specific Gravity Scale Soil Hydrometer) was used to measure the specific gravity of the soil suspension; the size fractions were then calculated based on the settling time of the suspended particles. The values of soil water potential were determined using a chilled mirror potentiometer (DECAGON, AquaLab series 3T) and the corresponding gravimetric values of soil wetness were used to plot the water retention curves for the burned and unburned soil samples. To account for the very small soil moisture contents, a high-precision weighing balance (i.e., providing measurements in grams with 4 decimal digits) was used to determine the gravimetric soil moisture.

*3.4 Wind tunnel tests*

A non-recirculating wind tunnel at the Wind Erosion and Water Conservation Research Unit of the US Department of Agriculture, Agricultural Research Service, located in Lubbock, Texas, was used for this study [see description in *Ravi et al*., 2006b],. This wind tunnel is 10.0 m long, 0.5 m wide and 1.0 m high, while the test section is 1.2 m long. The soils were kept in removable metal trays (1.5 cm deep by 46.0 cm wide by 100.0 cm long) that fit in the test section of the wind tunnel. Wind velocity was measured at different heights inside the tunnel using a series of Pitot tubes (ten in total) connected to pressure transducers. These velocity values were used to calculate the surface roughness ($Z_o$ = 1.17 mm) and to express the wind speed (v) in terms of shear velocity ($u*$). During the tests for threshold velocities, the wind speed was measured with a single Pitot tube at 60 cm above the bottom of the tunnel. A particle impact sensor

(SENSIT) was used to measure the onset of saltation 45 cm downwind from the edge of the soil tray. Soil temperature was measured using an infrared thermometer (Exergen Corp, IRT/C.2 with Type K Germanium lens) and the near soil surface temperature and relative humidity (2mm from surface) were measured using a probe (Vaisala, Inc. Humitter 50U). A handheld relative humidity/temperature probe and a wire thermocouple were used to monitor the ambient temperature and humidity outside the wind tunnel. Before each test in the wind tunnel, the Pitot tube and its transducer were calibrated and corrections were made for changes in atmospheric temperature. The trays were then placed in the wind tunnel and the motor was started. The air flow was initially increased stepwise to attain a wind speed just below the estimated threshold value and then increased slowly until the particle sensor indicated particle movement. The threshold velocity was determined as the velocity at which an abrupt increase from zero to more than 10 particle impacts per second was consistently observed for more than 3 seconds.

Three replicates of the control and burned soils were used for this wind tunnel study. The soil samples were passed through a 2 mm sieve and kept in the metal trays for 5-6 hours before each wind tunnel test to equilibrate with the ambient atmospheric humidity and temperature. Our previous studies [*Ravi et al*., 2004, 2006b, *Ravi and D'Odorico*, 2005] have shown that atmospheric humidity is a major factor controlling the moisture in the surface soil for air dry soils. To account for this, the wind tunnel tests were repeated at two ranges of relative humidity: low range (10-40%) and high (50-80%). Climatic parameters such as atmospheric humidity and temperature cannot be controlled in this wind tunnel facility, and thus, were determined by the ambient weather conditions. The air in Lubbock is generally dry and greater variability in humidity results from the

diurnal cycle than as a result of seasonal fluctuations. To cover a broad range of relative humidity, the experiments were repeated on different days with different ambient conditions. One advantage of this approach is that because the soils are neither artificially wetted nor dried, significant changes in soil moisture during the experiments are eliminated. Under these conditions, changes in surface soil moisture are only due to fluctuations in air humidity.

## 4. Results

The burned and control soils collected from the field were tested for the extent of water repellency in the laboratory by WDPT and MED tests. In the laboratory, the burned soils had a WDPT of 2-5 minutes; however, when tested in the field the WDPT was much longer (5-10 minutes). The soil samples from the control plots had no water repellency as measured by the WDPT test (*i.e.*, the drops were absorbed instantaneously). The ethanol concentration required for "instantaneous" absorption of drops on the burned soil was 3 molar, corresponding to a critical surface tension of $4.2 \times 10^{-4}$ N/cm, (surface tension (at $20^{o}$ C) of water being $7.2 \times 10^{-4}$ N/cm and ethanol $2.2 \times 10^{-4}$ N/cm) indicating the existence of relatively high levels of water repellency in the soil [*Roy and McGill*, 2002]. The initial advancing contact angle of the burned soils calculated using the MED test results was around $103^{o}$. The textural analysis done using the hydrometer method indicated that the soil from Cimarron grassland was sandy in nature with 82% sand, 10% silt, and 8% clay content.

The dependence of soil moisture on near-surface air humidity for the Cimarron control soil sample (8% clay) and untreated clean, round, well-sorted Ottawa sand (US

Silica ASTM 20/30 unground silica), which was used in our previous study [*Ravi et al*., 2006a], is shown in Figure 6.3.

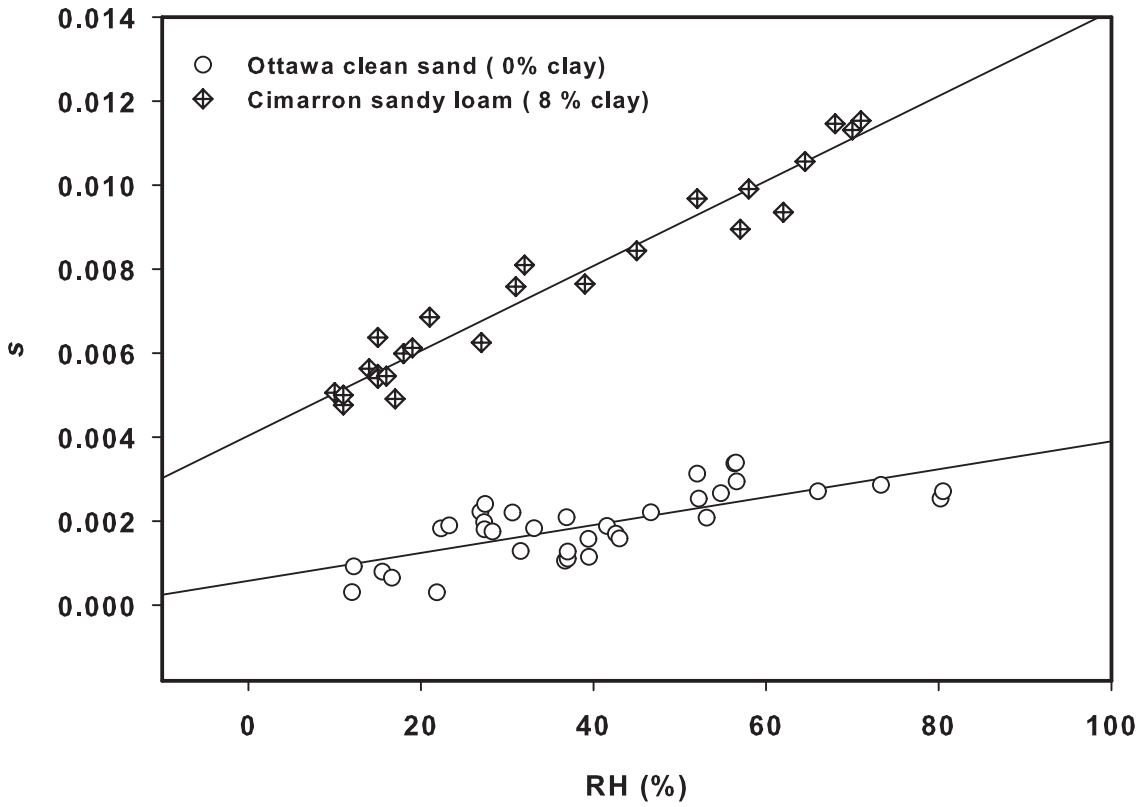


**Figure 6.3** Surface soil moisture (*s*) as a function of relative humidity (RH) for clean untreated sand (Ottawa sand) and a natural unburned sandy loam (Cimarron soil).

The wind tunnel tests showed that the threshold friction velocities of burned soils were significantly less than the control soil samples in the two humidity ranges considered for the study (Figure 6.4). This was consistent with the results obtained using the Ottawa sand treated with a hydrophobic compound (hexadecanoic (palmitic) acid) to simulate fire-induced water repellency using the methods detailed in *Ravi et al.* [2006a]. Even though the curve for water retention for the burned soil shows a slight change from

the control soil, the surface soil moisture of the burned and control soils were not significantly different at the different humidity ranges considered (Figure 6.5).

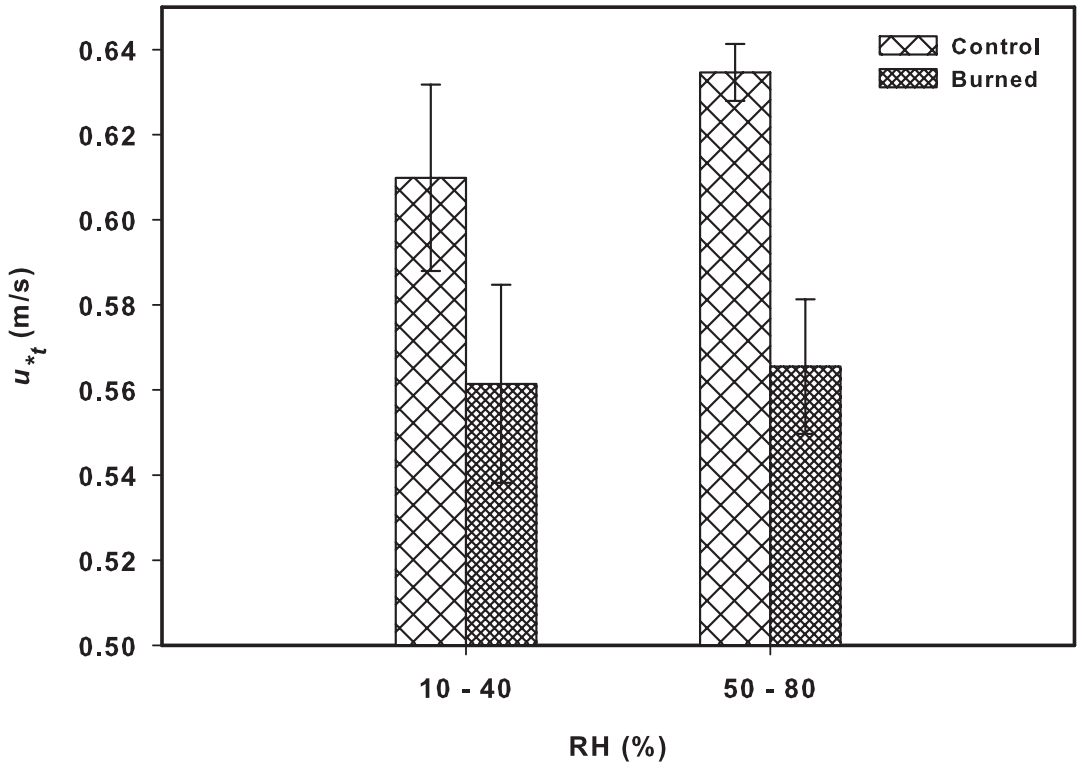


**Figure 6.4** Threshold friction velocity ($u_{*t}$) as a function of atmospheric relative humidity (RH) as determined by wind-tunnel tests for control and burned Cimarron soil. The error bars represent the standard deviation of threshold shear velocity within each class of relative humidity.

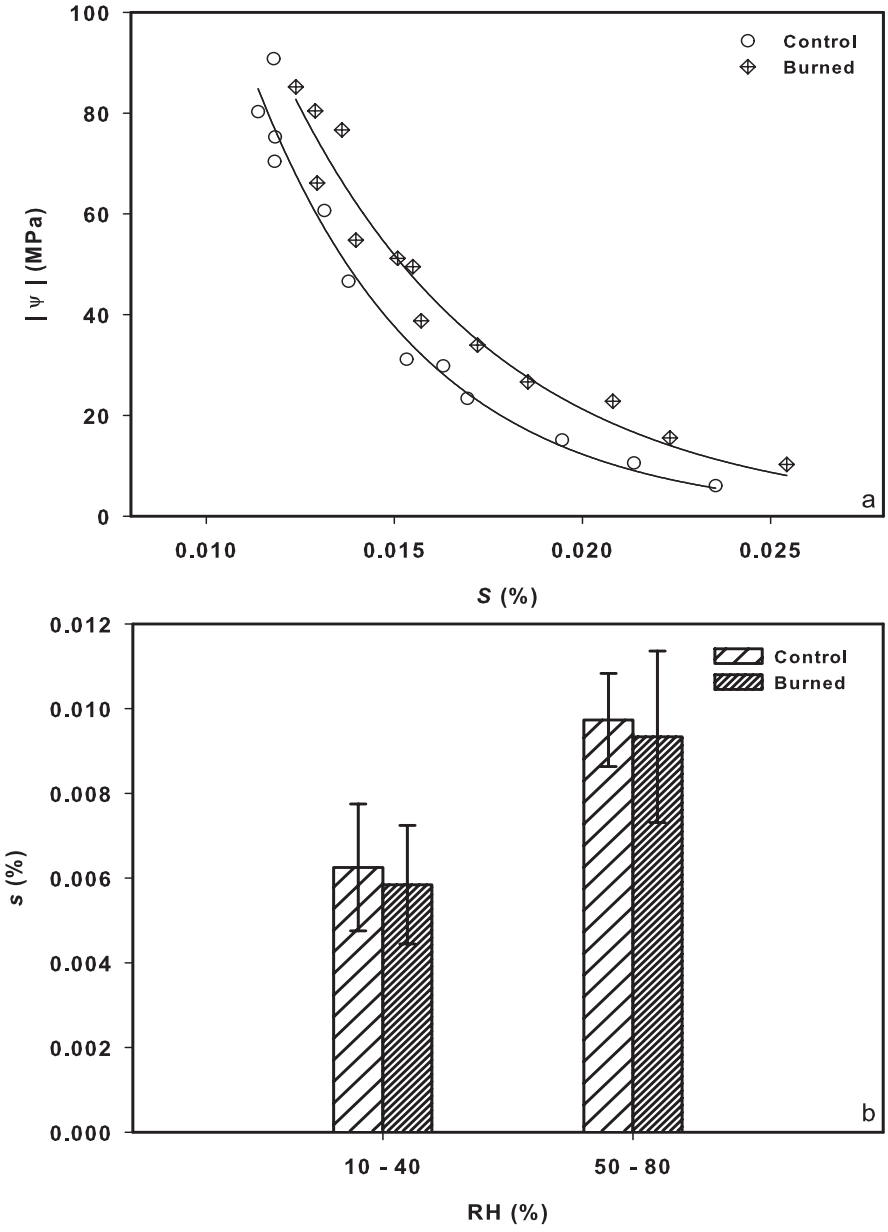


**Figure 6.5** (a) Water retention curves for the control (i.e., unburned) and the burned soil from Cimarron National Grassland used in this study. *s* represents gravimetric soil moisture and |ψ| is the absolute value of matric potential (MPa). (b) Surface soil moisture (*s*) as a function of relative humidity for the control and burned soil. The error bars represent the standard deviation of soil moisture within each class of relative humidity.

**5. Discussion**

The results from the WDPT and MED tests indicate that the soils from Cimarron grasslands developed water repellency as a result of the fire. By contrast, the soil from the control plots showed no water repellency. The soil moisture content did not significantly change after the fire as shown by the moisture content of the surface soil for the control and burned soils (Figure 6.5). The slight shift in the water retention curve might result from the changes in adsorption of moisture by the burned soils. These results are consistent with our previous study of clean sands treated in the laboratory with hydrophobic compounds [*Ravi et al*., 2006a]. The greater clay content (8%) of the soil samples from Cimarron Grasslands and differences in particle size in the silt-sand fraction explain the stronger dependence of surface soil moisture on air humidity when compared to untreated Ottawa sand (Figure 6.3). Wind tunnel tests showed that, after burning, soils exhibited a significant decrease (Figure 6.4) in the threshold shear velocity for wind erosion (based on t-test of the mean at the 5% significance level). The decrease in threshold velocity was similar (in magnitude) to that found on sands treated with hydrophobic compounds [*Ravi et al*., 2006a]. Further, the threshold velocity of the unburned, but not the burned soil, was observed to increase with increasing air humidity (Figure 6.4). These results show that fire-induced water repellency significantly affects soil susceptibility to wind erosion, even though the soil moisture content remains generally the same before and after the fire.

To explain the results obtained with the treated Ottawa sand, *Ravi et al.* [2006a] developed a theoretical expression based on a modification of the analysis by *Fisher* [1926] to account for the effect of the contact angle on wet bonding forces between

spherical particles. Liquid-bridge formation because of the condensation of water vapor in the spaces between soil grains can be delayed or even prevented in the case of hydrophobic soils. Even when the liquid-bridges are formed, however, the observed decrease in threshold shear velocity for burned soils can be explained as the effect of changes in the contact angle caused by soil hydrophobicity. Here, we derive a more realistic expression to show the effect of water repellency on interparticle wet bonding forces for the case of soil grains with sharp edge contact points. To this end, we borrow from *McKenna Neuman and Nickling* [1989] the schematic representation of the interparticle contact areas given by two co-axial asymmetrical cones (Figure 6.6).

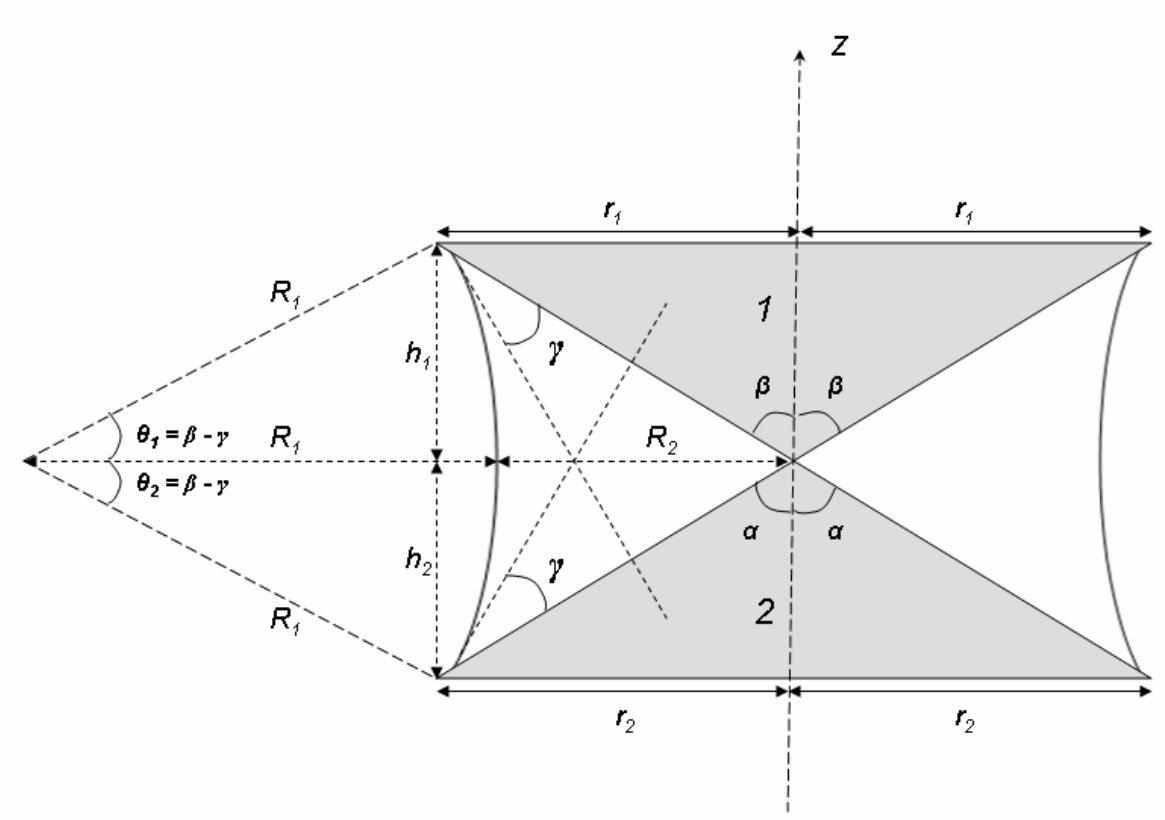


**Figure 6.6** Schematic representation of soil particles as coaxial cones.

The formal derivation of an expression for the interparticle wet bonding forces ($F_i$) presented in the Appendix C leads to an expression of $F_i$ as a function of the contact angle

$$F_i = \pi r_1 T \left[ \left( \frac{b_2 - b_1}{a_1 - a_2} \right) \sqrt{a_1} + \frac{b_1}{\sqrt{a_1}} \right] = \pi r_1 T \; G_1 , \tag{6.3}$$

where $T$ is the surface tension, $a_1$, $b_1$, $a_2$, $b_2$, and $G_1$ are parameters that depend on the contact angle and on the geometry of the cone-shaped soil contact areas (see Appendix C). $G_1$ modulates the dependence of $F_i$ on the contact angle, $\gamma$, and on the particle geometry. Figure 6.7 shows the effect of changes in contact angle ($\gamma$) on $G_1$.

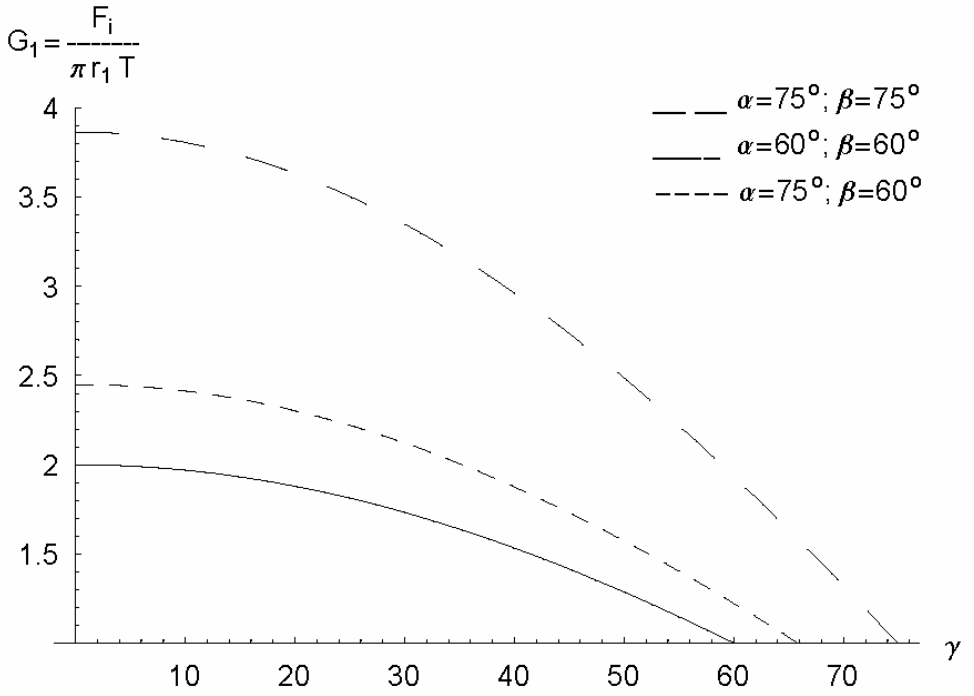


**Figure 6.7** Dependence of $G_1$ on the contact angle, $\gamma$, for different combinations of α and β. It is shown that the capillarity-induced interparticle bonding force decreases with increasing values of the contact angle (*i.e.*, with increasing degrees of soil water repellency).

It is observed that $G_1$ decreases with increasing values of $\gamma$, *i.e.*, increasing soil hydrophobicity. Thus, because in Equation (6.3), $G_1$ is proportional to the interparticle bonding force, $F_i$ decreases with increasing soil hydrophobicity. A comparison between Figure 6.7 and results from our previous study using Ottawa sand [*Ravi et al*., 2006a] shows that the dependence of the interparticle wet-bonding force on the contact angle given by these two models is qualitatively the same. The differences in the actual values of $F_i/ (\pi\ r_1\ T)$ between these two studies result from the different geometry used by the two models and to the values used for the parameters $\eta$, $\alpha$, $\beta$.

## 6. Conclusions

The results presented in this paper provide experimental evidence of the effect of post-fire enhancement of the potential for wind erosion in arid lands. This phenomenon results from an increase in soil erodibility, i.e., to a reduction in the threshold velocity for wind erosion. In addition to a higher susceptibility to wind erosion because of loss of vegetation cover, soils affected by biomass burning exhibit lower threshold velocities than unvegetated soil plots not exposed to fires. We interpret this phenomenon to be the result of fire-induced soil hydrophobicity generated by post-fire condensation of organic vapors on the soil grains. In a previous study, we demonstrated that water repellency induced artificially in soils by laboratory treatments may reduce the threshold velocity. This paper shows that real fires may indeed cause an enhancement in soil erodibility. Because significant levels of repellency were detected after the fire, we conclude that the observed reduction in threshold velocity was an effect of soil water repellency, consistent with our previous findings on laboratory-treated soils. We acknowledge, however, that

the enhancement of soil erodibility by fires also depends on factors like microbial crusts, organic matter and types of vegetation, which were not considered in this study. Our previous studies [*Ravi et al*., 2006a] using clean sands, without the above mentioned confounding factors have well established the role of fire induced water repellency on the enhancement of wind erosion after fires.

A theoretical expression for the wet-bonding force as a function of soil-water contact angle was developed to explain these results. To account for the sharp-edge shape of natural soil grains, we assumed the contact areas between soil grains to be asymmetrical cones and calculated the interparticle bonding forces as a function of grain geometry and of the contact angle. This theoretical analysis supports our experimental findings, and shows how soil hydrophobicity increases the soil susceptibility to wind erosion.

# CHAPTER: 7

# FEEDBACKS BETWEEN FIRES AND WIND EROSION IN HETEROGENEOUS ARID LANDS

(This paper is published in *Journal of Geophysical Research -Biogeosciences*)


## Abstract

Shrub encroachment, a widespread phenomenon in arid landscapes, creates “islands of fertility” in degraded systems as wind erosion removes nutrient-rich soil from intercanopy areas and deposits it in nearby shrub-vegetated patches. These islands of fertility generally are considered to be irreversible. Recently, fire has been observed to alter this pattern of resource heterogeneity through the redistribution of nutrients from the fertile islands of burnt shrubs to the surrounding bare soil areas. Despite the recognized relevance of both fires and wind erosion to the structure and function of arid ecosystems, the interactions between these two processes remains poorly understood. This study tests the hypothesis that fire-induced soil hydrophobicity developing in the soils beneath burned shrubs enhances soil erodibility by weakening the interparticle wet-bonding forces. To test this hypothesis, the effects of grass and shrub fires on changes in soil erodibility and on the intensity of fire-induced soil water repellency are compared at both the field and patch scales in heterogeneous arid landscapes. Higher water repellency was observed in conjunction with a stronger decrease in wind erosion threshold velocity around the shrubs than in grass-dominated patches affected by fire, while neither water repellency nor changes in threshold velocity was noticed in the bare soil interspaces. Thus, fires are found to induce soil hydrophobicity and to consequently enhance soil

erodibility in shrub-vegetated islands of fertility. These processes create temporally dynamic islands of fertility and contribute to a decrease in resource heterogeneity in aridland ecosystems following fire.

## 1. Introduction

In arid environments erosion processes redistribute soil particles and nutrients [*Schlesinger et al.,* 1990; *Okin and Gillette,* 2001], thereby affecting soil texture and soil water holding capacity [*Lyles and Tatarko,* 1986, *Offer et al*., 1998] with consequent effects on the productivity, composition and spatial patterns of vegetation [*Schlesinger et al.,* 1990]. In these landscapes soil erosion is mainly due to aeolian processes [*Breshears et al.,* 2003], which maintain the local heterogeneities in nutrient and vegetation distribution through the removal of nutrient-rich soil from intercanopy areas and the subsequent deposition onto vegetated areas [*Schlesinger et al.,* 1990; *Okin and Gillette,* 2001]. Thus, wind erosion is often invoked as a major factor enhancing and maintaining soil heterogeneity, particularly in shrub encroached arid landscapes [*Okin and Gillette,* 2001].

Dryland ecosystems are often prone to disturbances like fires and grazing, which may render soils more susceptible to wind erosion with important impacts on regional and global climate, human health, biogeochemical cycles, and desertification [*Nicholson,* 2000; *Rosenfield et al.,* 2001; *Fryrear,* 1985; *Whicker et al., 2006; Duce et al.,* 1991; *Schlesinger et al.,* 1990]. Fires modify the interactions between eco-hydrological and land surface processes [*Ludwig et al.,* 1997], expose the soil surface to the erosive action of winds, and affect the relative abundance and distribution of shrubs and grasses in arid ecosystems [*Scholes and Archer,* 1997; *van Langevelde et al.,* 2003; *Sankaran et al.,*

2004]. On the other hand, vegetation type and patterns affect both the intensity and frequency of fires [*Anderies et al.*, 2002; *van Wilgen et al*., 2003]. Although both wind erosion and fires play an important role in the dynamics of arid and semiarid ecosystems, the interactions between these two processes remain unknown. Fire is now a commonly used management tool in many aridland ecosystems to reduce shrub cover and to enhance grass growth. Thus, understanding how fire affects soil structure and resource heterogeneity is of fundamental and practical importance in systems where aeolian processes predominate.

Several studies have shown that fires in shrub-encroached grasslands favor grass regrowth and limit further shrub encroachment [*Van Auken*, 2000; *Van Wilgen* et al., 2003]. Recent studies [*White et al.*, 2006] have shown that, while the process of shrub encroachment favors the formation of a heterogeneous landscape with the concentration of resources beneath the shrub canopies and the formation of "fertility islands" (Figure 7.1a), fires tend to destroy this heterogeneity by enhancing wind-induced particle transport and erosion from fertile islands affected by the burning of shrub biomass. In fact, subsequent to fire occurrences, microtopographic differences between vegetated islands and bare interspaces decrease [*White et al*., 2006], indicating that the resources accumulated in the fertility islands are redistributed onto the interspaces, thereby reducing the spatial heterogeneity of the system (Figure 7.1b). In addition, soil organic matter increased in bare areas relative to vegetated patches, and in some sites, soil resources (*e.g.* nitrogen) were more homogeneously distributed for up to 22 months following fire [*White, in review*]. These findings are consistent with the observation that burned areas exhibit lower threshold velocities for wind erosion and higher volumes of

soil loss than in similar unburned areas [*Whicker et al.*, 2002]. This difference in soil erodibility determines important structural changes in the landscape through post-fire translocation of soil resources from burned “fertility islands” to bare soil areas. As a result, we hypothesize that fertility islands are not static, but rather dynamic features of the landscape. Thus wind erosion and fires influence the dynamics of dryland landscapes, and the interactions between these two processes play a major role in determining the composition and structure of vegetation.

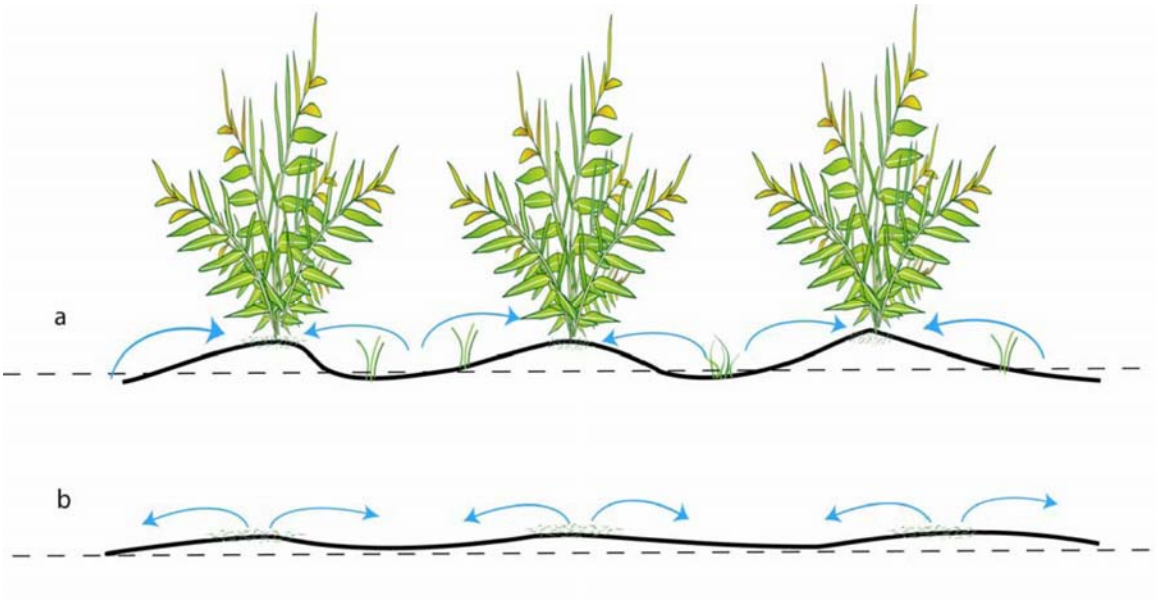


**Figure 7.1** (a) Diagram showing the formation of islands of fertility around the shrub patches and increase in microtopography. (b) Diagram showing post-fire enhancement of wind erosion leading to redistribution of resources to bare interspaces and reduction in microtopography.

However, an important component of these dynamics remains unexplained, as it is unclear why adjacent sites, with similar surface roughness and exposed to the same winds, should exhibit differing susceptibility to wind erosion [*Whicker et al.*, 2002]. Recent studies on soils treated in the laboratory with water-repellent compounds [*Ravi et*

*al.*, 2006a] have experimentally shown that soil hydrophobicity enhances soil erodibility. By affecting the strength of interparticle wet-bonding forces, fire-induced water repellency enhances soil erodibility, causing a drop in wind erosion threshold velocity, the minimum velocity for erosion to occur. In this study we show that fire-induced water repellency creates the same effect, and we provide the first experimental evidence that post-fire enhancement of soil erodibility is due to fire-induced soil hydrophobicity. Fires are known for having a major impact on infiltration, runoff and water erosion [e.g., *DeBano*, 2000]. The post-fire increase in runoff and soil erosion is caused by the decrease in infiltration capacity resulting from fire-induced water repellency [*Krammes* and *DeBano*, 1965; *DeBano*, 1966]. In fact, burning vegetation releases fatty acids onto the underlying soil, with consequent effects on the physical-chemical properties of the soil grain surfaces; in particular, these organic compounds increase the contact angle formed by the air-water interface with the soil grains, thereby affecting the dynamics of moisture retention and the strength of interparticle bonding forces [*Ravi et al.*, 2006a].

In this paper, a study of the soil hydrophobicity caused by fire in arid landscapes and the subsequent effect on wind erosion thresholds in two different arid ecosystems is presented. In the first part of the study, two systems with different land cover, an arid grassland and a shrubland, were compared. The second part of the study concerns a heterogeneous arid landscape with a mosaic of vegetated shrub and grass patches separated by bare interspaces. The first part of the study investigates the relative importance of plant communities on the enhancement of soil susceptibility to wind erosion. The second part concentrates on differences in soil erodibility within a heterogeneous ecosystem, i.e., in grass- and shrub-dominated soil patches. Here we

hypothesize that the post-fire enhancement of soil erosion is stronger in shrub-dominated than in grass-dominated soils and that this difference is the result of the different level of soil-water repellency developed by the burning of shrub versus grass vegetation [*Adams et al.*, 1970]. We argue that the stronger enhancement in soil erodibility induced by burning shrubs causes the observed decrease in soil heterogeneity. To test this hypothesis, we investigate, with field and laboratory measurements, changes in soil erodibility and other soil properties in soil plots affected by burning biomass.

## 2. Materials and methods

The burn experiments were conducted in two different ecosystems from the southwestern U.S which are prone to fires and wind erosion, namely, the Cimarron National Grassland (KS) and the Sevilleta National Wildlife Refuge (NM). The Cimarron National Grassland (37° 7.29'N, 101° 53.81'W) is a short grass prairie ecosystem (Blue grama), with significant shrub encroachment (Sage brush and Yucca) in some areas. On February 5, 2006, a large fire burned approximately 1700 ha in part of the Cimarron National Grassland [US Forest Service, 2006]. Thus, after all of the above-ground vegetation had burned, the soil surface was left exposed to high wind erosion activity. Two sites were chosen at Cimarron: a pure grassland site and a grassland encroached by shrubs. Two sets of soil samples were collected on burned and unburned soils across the fire line on three replicated pairs of (burned and unburned) plots at each site. The second set of experiments were conducted at the Sevilleta National Wildlife Refuge, located in the northern Chihuahuan Desert approximately 80 km south of Albuquerque, New Mexico (N $34^{o}$ 23.961` & W $106^{o}$ 55.710`). The site chosen for our study was a desert

grassland/scrubland with a mosaic of soil patches dominated by grasses (*Sporobolis*) and shrubs (Four wing saltbush and Snake weed) with bare interspaces. In the three field sites used for the study, grass cover was minimal near the base of the shrubs and the landscape was heterogeneous with distinct patches of grasses and shrubs with bare interspaces. This patchy landscape is typical for these arid shrublands [*Kurc and Small,* 2004]. Soil samples were randomly collected at each site from an area of about 5 $m^2$ before and after the prescribed burn. As the focus of this study is on wind erosion and fires, soil samples were taken only from the surface (top 2 cm) under the grasses, around the shrubs, and from the bare interspaces in the three replicated plots before and after the prescribed burning.

The soil samples were passed through a 2 mm sieve and kept in metal trays for 5-6 hours before each wind tunnel test to equilibrate with the ambient atmospheric humidity and temperature. Surface soil moisture changed only in response to fluctuations in ambient air humidity as there was no control on the atmospheric humidity and temperature, and the soil samples were not artificially wetted or dried [*Ravi et al.,* 2004, *Ravi and D'Odorico,* 2005]. To account for the effect of air humidity on surface moisture content, the wind tunnel tests were repeated at two ranges of relative humidity: 10-30% and 40-60%. A non-recirculating wind tunnel (10.0 m long, 0.5 m wide and 1.0 m high) was used for this study. The soils were placed in the wind tunnel on removable metal trays (1.5 cm x 46.0 cm x 100.0 cm). The wind velocity was measured at different heights inside the tunnel using a series of Pitot tubes connected to pressure transducers. These measurements were used to calculate the surface roughness ($Z_o$ = 1.17 mm) and to express the wind speed ($v$) in terms of shear velocity ($u_*$). Saltation was measured by a

particle impact sensor (SENSIT), soil temperature by an infrared thermometer (Exergen Corp, IRT/C.2 with Type K Germanium lens), near surface temperature and relative humidity (2 mm from surface) by a RH/T probe (Vaisala, Inc. Humitter 50U). For each wind tunnel test, the air flow was initially increased stepwise to attain a wind speed just below the estimated threshold value and then increased slowly till the particle sensor indicated particle movement, i.e., an abrupt increase from zero to more than 10 particle impacts per second. Three replicates of the control and burned soils were used for each set of wind tunnel tests and these sets were repeated at two different humidity ranges. Statistical tests (t-test) were carried out to assess the significance of the results.

Determination of several soil properties was needed for interpretation of the experimental results. These included particle size distribution and soil wettability (i.e., the degree of hygroscopicity/ hydrophobicity of the soil grains). Fire-induced water repellency was determined using both the water drop penetration time (WDPT) and the molarity of ethanol solutions (MED) instantaneously infiltrating into the soil [e.g., *Letey*, 2001]. For the WDPT (laboratory method) a pipette was used to place water drops on the soil surface. The time required for the drop to penetrate the surface was measured. The water drop penetration (WDPT) time was determined for each sample as the mean WDPT for 10 droplets. In the molarity of an ethanol droplet (MED) test, standardized solutions of ethanol in water of known surface tensions were used to characterize the severity of water repellency in the soil [*Doerr*, 1998; *Roy et al.*, 2002]. Drops of the ethanol-water solutions with increasing concentrations were placed on the surface of the water repellent soil sample. As the molarity of the solution increases, the surface tension decreases and at a certain critical concentration (or critical surface tension, CST) the drop

penetrates the soil surface instantaneously (with in 3 seconds). Values of WDPT and MED for the soils used in the study are reported in Table 7.1. Soil texture was determined using the standard hydrometer method [*ASTM*, 1981]. A soil hydrometer (Fisher brand Specific Gravity Scale Soil Hydrometer) was calibrated to measure the specific gravity of the soil suspension; the size fractions were calculated based on the settling time of the suspended particles (Table 7.1).

**Table 7.1** Textural and wetting properties of the soils used in this study

| Study sites | | | Particle size distribution | | | Soil Hydrophobicity* | |
|---|---|---|---|---|---|---|---|
| | | | Clay (%) | Silt (%) | Sand (%) | WDPT (Sec) | MED (Molarity) |
| Cimarron | National | Shrubland | 9 | 12 | 79 | 120 | 3 |
| Grassland, KS | | Grassland | 8 | 10 | 82 | 30 | 1 |
| Sevilleta | National | Shrub patch | 28 | 19 | 53 | 50 | 2 |
| Wildlife Refuge, NM | | Grass patch | 33 | 26 | 41 | < 10 sec | < 1 |
| | | Bare interspaces | 25 | 18 | 57 | 0 | 0 |

* Soil hydrophobicity was not observed in control soils

## 3. Results

The results from the wind tunnel tests on the soils from the Cimarron National Grassland show that the threshold friction velocity of burned soils from both the grass-dominated and shrub-dominated areas were significantly less than for the control soils collected from adjacent unburned areas. Moreover the threshold velocity values were significantly different for the soils from the burned and the control plots even though the surface moisture contents were not significantly different. These differences were

consistently observed for the two humidity ranges considered in this study (Figure 7.2a-b). The differences in threshold velocities between the soils from control plots and burned plots were found to be statistically significant both for the grassland ($p < 0.001$ in the 0-40% RH range and $p < 0.001$ in the 40-80 % RH range) and shrubland at ($p<0.001$ in the 0-40% RH range and $p<0.00001$ in the 40-80 % RH range). Further for each treatment, the threshold values increased with increasing values of air humidity, indicating a clear dependence of threshold velocity on air humidity as seen in our previous studies [*e.g.*, *Ravi et al.*, 2006a; *Ravi et al.*, 2006b].

Higher post-fire enhancement of soil erodibility resulted from the burning of shrubs than of grasses (Figure 7.2a-b) as evidenced by the results of the t-test which was carried out between the differences in threshold shear velocities of burned and control plots in the grassland and shrubland. The test clearly showed that - in both humidity ranges considered in this study - the differences between threshold shear velocities of control and burn plots were significantly higher in the shrubland sites compared to grassland sites ($p < 0.026$ in the 0-40% RH range and $p<0.005$ in the 40-80 % RH range). These results indicate that this difference is severe at higher humidity values. Further, the severity of fire-induced water repellency was higher for the shrubs than for grasses (Table 7.1). The surface soil moisture of the burned and control soils were not significantly different for both the humidity ranges considered, whereas the surface soil moisture increased with increasing air humidity as reported in previous studies on unburned soils treated in the lab with water-repellent chemicals [*e.g., Ravi et al.*, 2006a].

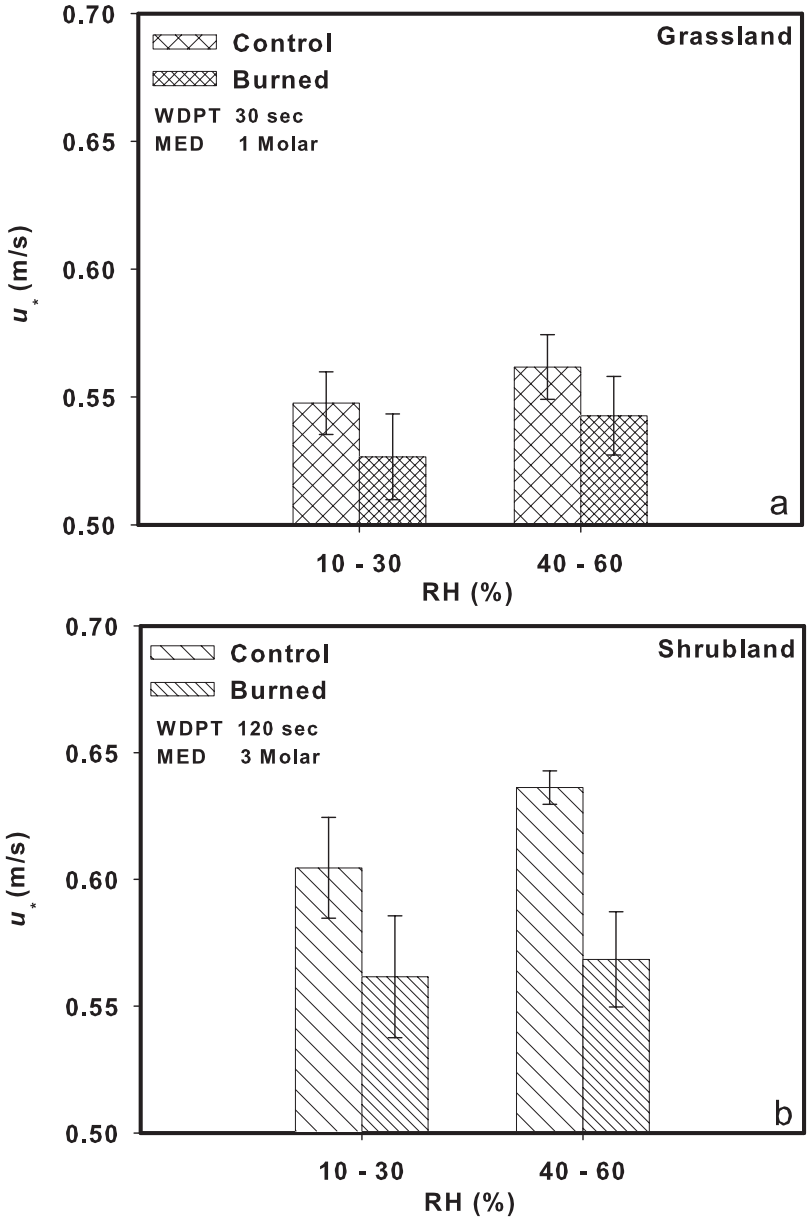


**Figure 7.2** Threshold friction velocity ($u_*$) as a function of atmospheric relative humidity (RH) as determined by wind-tunnel tests for control and burned surface soil from the Cimarron National Grassland. The error bars represents the standard deviation of threshold shear velocity within each class of relative humidity. The WDPT and MED values are for the burned soil.

The second part of the study focused on a heterogeneous arid landscape at the Sevilleta National Wildlife Refuge (NM), which exhibits a mosaic of patches dominated by shrubs, grasses and bare soil interspaces. In this system fires induced higher water repellency in the soils around the shrubs compared to grass-dominated patches, while no water repellency was noticed in the bare interspaces (Table 7.1). Laboratory wind tunnel tests showed that even before the burn experiment, different erosion thresholds existed in the same field due to the textural heterogeneity of soils sampled under shrubs, grasses and in bare soil patches (Figure 7.3). After burning, wind erosion thresholds decreased in the vegetated patches. The differences in threshold velocities between the soils from control plots and burned plots were found to be statistically significant both for the soils under grass patches ($p < 0.001$ in the 10-30% RH range and $p < 0.03$ in the 40-60 % RH range) and under shrubs at ($p < 0.0001$ in the 10-30% RH range and $p < 0.003$ in the 40-60 % RH range), while – as expected – this difference in threshold velocity was insignificant between the control and the burned bare interspaces($p > 0.40$ in the 10-30% RH range and $p > 0.49$ in the 40-60 % RH range).

Moreover, the decrease in threshold velocity was stronger in the case of soils affected by the burning of shrubs; in fact, in both the humidity ranges the difference between threshold shear velocities of control and burn plots were significantly higher in soils from burnt shrub patches compared to soils from burnt grass patches ($p < 0.003$ in the 10-30% RH range and $p < 0.013$ in the 40-60 % RH range). Thus, by decreasing the wind erosion thresholds in burnt shrub patches, fires enhance the erodibility of soils from beneath the burnt shrubs, thereby contributing to nutrient loss from the fertility islands and to the consequent reduction in landscape heterogeneities.

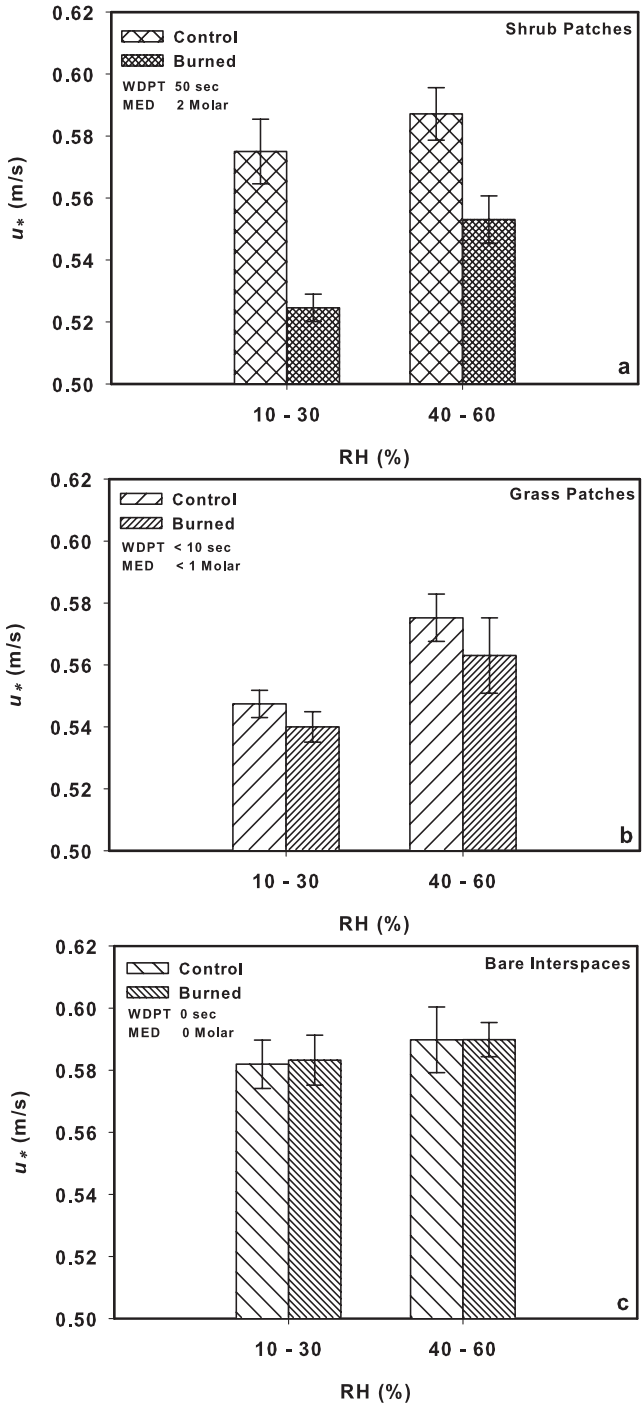


**Figure 7.3** Threshold friction velocity ($u_*$) as a function of atmospheric relative humidity (RH) as determined by wind-tunnel tests for control and burned soils from shrub patches, grass patches, and bare interspaces at the Sevilleta National Wildlife Refuge. The error bars represents the standard deviation of threshold shear velocity within each class of relative humidity. The WDPT and MED values are for the burned soil.

**4. Discussion**

The experimental results support the hypothesis that fires enhance soil susceptibility to wind erosion in areas affected by biomass burning and that this effect is more significant in the case of shrub-dominated compared to grass-dominated areas, both at the field (Figure 7.2 a-b) and at the patch scale (Figure 7.3 a-c). In the case of patchy landscapes, the post-fire redistribution of soil and nutrients from shrub patches to bare (or sparsely grass-covered) interspaces can occur only if the soils in and around the shrub patches become more erodible compared to the interspaces. Our results indicate that this effect can occur in the field due to the relatively higher fire-induced soil hydrophobicity occurring in and around the shrub patches, compared to either grass-dominated or bare soils. Hence, following fire events, shrub-dominated fertility islands exhibit lower erosion thresholds compared to grass patches and bare interspaces.

To assess the magnitude and significance of the enhancement of soil erodibility resulting from the post-fire decrease in threshold shear velocity , we used wind velocity records taken (at 2m height) from a bare soil plot at the Sevilleta site for a three-week period in the middle of the 2007 windy season (March - April). These velocity measurements were compared with the threshold velocity values determined in the wind tunnel. To this end, we used the Prandtl-von Karman logarithmic law [e.g., *Campbell and Norman*, 1998] to convert the threshold shear velocities measured for burned and control soils (Figure 7.3) into threshold wind speed values at 2 m height. The decrease in threshold velocity (at 2 m height) between burned and control soils was in the range of 1.0 – 1.5 m/s, which corresponds - in this short wind record - to a 70% increase in the number of occurrences with wind velocity exceeding the threshold velocity. This result

indicates that the decrease in threshold velocity observed in the burned soils can cause a significant increase in wind erosion activity after fires.

The level of soil hydrophobicity developed by fires depends on fire intensity, vegetation cover, and soil texture. The experimental results from our study show that a higher hydrophobicity develops in the soils beneath burning shrub vegetation (Table 7.1). This higher repellency found under the burnt shrubs is explained by the fact that shrubs typically contain more water-repellent organic compounds and are subjected to higher fire intensities compared to grasses [*Tyler et al.,* 1995; *Moreno et al.,* 1991]. Indeed, at the Sevilleta, fire temperatures beneath shrubs were 60-100 $^{o}$C higher than in grass patches. The shrub patches are also characterized by high surface accumulations of organic matter and leaf debris which can enhance the severity of water repellency induced by fire [*Pierson et al.,* 2001]. Further, the soil under shrub patches contained more sand (Table 7.1), and the severity of water repellency is higher in the case of sandy soils due to their relatively smaller specific surface area [*DeBano,* 2000].

The higher fire-induced hydrophobicity explains the stronger decrease in wind erosion threshold velocity observed in the soil patches that prior to burning were vegetated by shrubs, as compared to soils under burned grasses or in the bare interspaces. In the latter case no decrease in wind erosion threshold was observed, due to the limited effect of fires on the bare soil patches.

## 5. Conclusions

The enhancement of soil erodibility by fires may also depend on other factors in addition to soil water repellency, including the formation of cryptobiotic crusts by algae, fungi and soil bacteria, which may enhance the soil-water repellency [e.g. *Savage et al*., 1969] and are susceptible to destruction by fire. Previous laboratory studies showing the ability of soil hydrophobicity to weaken interparticle bonding forces [*Ravi et al*., 2006a] were carried out on clean sands treated with water repellent organic compounds and were not affected by confounding factors such as microbial crusts or organic matter. The effects of microbial crusts are not considered in this study because they are mostly found in the bare interspaces [*West,* 1990; *Schlesinger & Pilmanis*, 1998; *Stursova et al*., 2006] as they avoid competition with vegetation for resources [*Harper & Belnap,* 2001; *Li et al.*, 2002]. Although we acknowledge the role played by microbial crust in the process of soil erosion, it is not clear how they could contribute to the post-fire enhancement of soil erodibility from fertility islands. Conversely, the fact that fires induce soil-water repellency [e.g., *De Bano*, 2000; *Doerr et al*., 2000] is well-established, and the ability of repellency to enhance soil erodibility has been tested in the laboratory and mechanistically explained [*Ravi et al.,* 2006a].

In this study we also eliminated the effects due to the higher topography of shrub mounds and the soil disturbances caused by animals, by selecting study sites in areas where these effects were negligible. This study shows that the levels of soil hydrophobicity developed by typical rangeland fires are able to enhance soil erodibility. Moreover this effect is stronger in shrub than in grass patches, and non-existent in the bare interspaces. Thus, resource islands in aridland ecosystems are not static but rather

highly dynamic patch types in response to fire and perhaps other disturbances such as drought. These differences in the enhancement of soil erodibility provide the mechanism behind the recent observational evidence of loss in landscape heterogeneity subsequent to fires [e.g., *White et al*., 2006] and demonstrate the possible value of prescribed fire as a tool to mitigate the early stages of the processes of fertility island formation and desertification.

# CHAPTER: 8

# POST-FIRE RESOURCE REDISTRIBUTION AND FERTILITY ISLAND DYNAMICS IN ARID LANDSCAPES: A MODELING APPROACH


## Abstract

The common form of land degradation in desert grasslands is associated with the relatively rapid encroachment of woody plants, a process that has important implications on ecosystem structure and function, as well as on the soil hydrological and biogeochemical properties. Until recently this grassland to shrubland transition was thought to be highly irreversible. However recent studies have shown that there exists a very dynamic shrub-grass transition state, in which fire could play a major role in determining the dominance of grasses and their recovery from the effects of overgrazing. Fires tend to counteract the heterogeneity-forming dynamics of land degradation associated with the encroachment of shrub vegetation into desert grasslands. It has been shown that fires enhance soil erodibility under the burned shrub patches. This local scale enhancement of soil erosion decreases the spatial heterogeneity of resources created by wind and water, which remove nutrient-rich soil from bare interspaces and deposit them in "resource islands", beneath shrub canopies, thereby preventing grass regrowth. Here using a spatially explicit model, we show how the patch-scale feedbacks between fires and soil erosion processes affect resource redistribution and vegetation dynamics in a mixed grass-shrub plant community. The results of this study indicate that at its early stages, the grassland-to-shrubland transition can be reversible and fire-erosion feedbacks may play a major role in determining the reversibility of the system.

## 1. Introduction

The grasslands and rangelands at the desert margins are very sensitive to external drivers like climate conditions and disturbance regime, and can be affected by rapid land degradation induced by climate change, grazing, lack of proper management practices and changes in vegetation composition due to the introduction of invasive species or changes in the competitive pressure among native species [*Archer*, 1995, *D'Antonio and Vitousek*, 1992; *Nicholson et al*., 1998; *Asner et al*., 2004]. The common form of land degradation in these arid grasslands involves the relatively rapid encroachment of woody plants. Commonly referred to as "shrub encroachment" [*Buffington and Herbel*, 1965; *Archer*, 1989; *Van Auken*, 2000; *Roques et al*., 2001; *Cabral et al*., 2003; *Fensham et al*., 2005], this phenomenon is widespread globally and is usually thought to be highly irreversible, with important ecological and hydrological implications [*Archer*, 1989, *Huxman et. al*., 2005]. Triggering factors such as climate change, increase in atmospheric $CO_2$ concentrations, and anthropogenic disturbances, are often invoked to explain the initiation of the conversion of desert grasslands into shrublands, while aeolian and hydrologic processes tend to sustain this shift in plant community composition by enhancing and maintaining local heterogeneities in nutrient and vegetation distribution [*Reynolds et al*., 1996; *Okin*, 2002].

The persistent and catastrophic character of this land cover change, and of the associated process of land degradation, suggests that shrub encroachment may result from a self-sustained positive feedback loop, arising from the ability of shrubs to modify their physical environment creating a favorable habitat for their own survival [*Rietkerk and van De Koppel*, 1997; *Anderies et al.,* 2002*; Van Langevelde et al.*, 2003; Zeng *et al*.,

2004]. Thus, positive biophysical feedbacks would enhance and sustain the process of shrub encroachment, thereby explaining the rapid shift from grass to shrub vegetation. For example, in the case of the southwestern United States the introduction of cattle after European settlement led to an enhancement of mesquite seed dispersal, the degradation of the grass layer, and a reduction in fire frequency and intensity. These processes triggered a self-sustained cycle of erosion, depletion of soil resources, and vegetation loss in grass-dominated areas, while the encroachment of shrubs was favored by the deposition of nutrient-rich sediments transported by wind and water, and the consequent formation of fertile shrub patches or "Islands of fertility" [*Charley and West*, 1975; *Schlesinger et al*., 1990*; Okin and Gillette*, 2001]. These processes resulted in grass mortality and subsequent loss of fuel load and grass connectivity, which further suppressed or limited fires in the system. Further, as the grass cover decrease, wind and water erosion increase in importance [*Okin and Gillette*, 2001; *Breshears et al*., 2003], eventually driving landscapes with sandy soils into a coppice duneland state [*Ravi et al*., 2007]. Similar consequences of anthropogenic disturbances of dryland soils after the European colonization have also been reported in the case of Australia, Southern Africa, and South America where large scale commercial grazing in conjunction with management practices such as fire suppression led to an increase in woody plants (shrub encroachment), with negative impacts on ecosystem function and services [*Archer*, 1989; *Pickup*, 1998; *van Auken*, 2000; *Cabral et al*., 2003; *Fensham et al*., 2005].

The landscape-scale process of land degradation associated with shrub encroachment is manifested as an increase in the heterogeneity in the spatial distribution of soil resources. Thus the spatial and temporal distribution of soil nutrients is often used

as an indicator of changes in ecosystem processes in shrub–grass transition zones [*Schlesinger et al*., 1990; *Reynolds et. al*., 1996]. Soil erosion and deposition by wind and water, are the major factors responsible for the redistribution of soil resources in theses systems. Aeolian processes in particular, which dominate in these shrub encroached landscapes [*Okin and Gillette*, 2001; *Breshears et al*., 2003; *Ravi et al*., 2007], are responsible for the removal of soil and nutrients from the intercanopy areas and deposition onto vegetated patches which results in the emergence of a two-phased landscape with a mosaic of nutrient-rich soils bordered by nutrient-depleted bare soil. Until recently this process of grassland–shrubland conversion was thought to be highly irreversible. However recent studies [*Ravi et al*., in review] show that there exists a very dynamical shrub-grass transition state, in which fire plays a major role in determining the dominance of grasses. In many of these shrub-grass transition systems, there exists enough grass cover for the fire to propagate. Using a combination of replicated field experiments to monitor soil erosion processes, changes in microtopogrpahy and post fire nutrient redistribution (isotopic tracer experiments), *Ravi et al.* [in review] showed that in the early stages of shrub encroachment fires interact with soil erosion processes resulting in enhanced post fire redistribution of soil resources from the fertile shrub islands to the intercanopy areas. The post-fire enhancement of resource redistribution was shown to have an impact on the recovery of grasses following fires (Chapter 4). Overall the post fire resource redistribution results in a breakdown of heterogeneity induced by shrub-wind/water interactions and favors regrowth of grasses in the interspaces, which recover rapidly after fires.

**Figure 8.1** A heterogeneous landscape at the shrub-grass transition zone at the Sevilleta, National Wildlife Refuge, New Mexico showing patches of shrubs, grasses and bare (soil) interspaces. (Source: Sevilleta, LTER)

The enhancement of resource redistribution was attributed to an increase in local scale soil erosion processes, mainly aeolian [*Ravi et al*., 2007; *Ravi et al*. in review]. In fact, fires were found to enhance soil erosion in and around burned shrub patches, by inducing water repellency in the surface soil, and consequently increasing soil erodibility [*Ravi et al., 2006a*; *Ravi et al., 2007*]. Thus the field observations in the northern Chihuahuan desert reported in Chapter 4 have shown that, by favoring a more homogeneous redistribution of soil resources, fire dynamics provide some form of reversibility to the process of shrub encroachment. Since the spatial and temporal distribution of soil resources is a major determinant of ecosystem processes in shrub-grass transition zones [*Schlesinger et al*., 1990], the interactions between fires and soil

erosion processes - which contributes to resource redistribution - is hypothesized to have a crucial role in the dynamics of these ecosystems [*Ravi et al*., 2007; *Ravi et al*., review]. Under these circumstances, the islands of fertility can be considered as dynamic features on these landscapes in the early stages of shrub encroachment

Here we develop a process-based minimalist model of coupled vegetation-resource and fire dynamics to show the mechanistic relation between fire-soil resource redistribution and the reconversion to the arid grassland state. This framework is used to investigate the relative importance of fires and grazing in these transition systems, and their effect on the dynamics of islands of fertility. Spatially explicit cellular automata models are commonly used in the study of the spatial dynamics of these highly heterogeneous ecosystems [*Li and Reynolds*, 1997*; Hobbs*, 1994], as they can be modeled as a mosaic of patches, with each patch existing in a discrete state, with state changes depending on the frequency and intensity of disturbances (*e.g*, fires and grazing), as well as on the spatial dynamics of vegetation establishment. To this end, we developed a spatially explicit model to investigate how the feedbacks between fires and soil erosion processes acting at the patch scale may affect resource redistribution and vegetation dynamics at the landscape to regional scale.

The resulting modeling framework has the structure typical of a cellular automata model [*Wolfram*, 1984]. Cellular automata models have been widely used in ecology and ecohydrology to simulate the dynamics of spatially extended systems [e.g., *Silvertown et al*., 1992; *Colasanti and Grime*, 1993; *Jeltsch et al*., 1997; *D'Odorico and Rodriguez-Iturbe*, 2000*; van Wijk and Rodriguez-Iturbe*, 2002]. These models are not suitable to make quantitative predictions of ecosystem dynamics. Rather, they are commonly used to

investigate dynamical behaviors and emerging properties of spatially extended systems. Here, this modeling approach is used to investigate the combined effect of grazing, fires, and soil erosion/redistribution on the spatial dynamics of vegetation in systems affected by shrub encroachment. Particularly it will be investigated how the erosion and redistribution of soil resources subsequent to fire occurrence may counteract the process of shrub encroachment. Moreover it will be shown that the post-fire enhancement of soil erosion favors the recovery of grassland vegetation, when fires are re-introduced in the system before grasses are completely "lost" from the system.

## 2. Materials and methods

### 2.1 Model framework

A Spatially explicit cellular automation model was developed to model the vegetation structure and resource patterns, which account for the local interactions among nearest neighbors. The temporal dynamics are controlled by transition probabilities (change from one state - *e.g.* grass, shrub or bare states - to another) and the spatial dynamics are controlled by local rules of interaction, according to the cellular automation framework (i.e., assuming that interactions are localized). The model is implemented in a square lattice of 1000 x 1000 cells, which represents a surface area of about one square kilometer (i.e., each cell could represent a 1 x 1 $m^2$ soil plot) in a shrub-grass transition zone. A cell can exist in any of the following five possible discrete states: shrub, grass, bare soil, burned grass and burned shrub. Each cell interacts with its 8 nearest neighbors to account both for fire propagation and for vegetation encroachment. To avoid boundary effects due to the finite size of the domain, periodic boundary conditions are used. The

state of the system is expressed by two state variables: vegetation cover (V), and the level of soil resources (R). As noted, the vegetation cover is classified as bare soil (V=0), grass (V=1), shrub (V= 2), burned grass (V=3) and burned shrub (V=4). The model is initialized with a 75% grass cover, 5% shrubs and 20% bare interspaces. This land cover is typical of desert grasslands (*e.g* in the Northern Chihuahuan desert), which exhibit about 70 % grass cover, 20-30% bare interspaces, and a very low density of shrubs (e.g., *Báez et al*. 2006). The state variable R is normalized with respect to the resource level of the initial grassland state. Thus, R is initially set equal to 1.

The model is run with the time step of one year. At any time step, grazing may convert a grass patch to bare soil with a probability, $P_1$ ("grazing pressure"). The number of patches grazed (i.e., the number of grass to bare soil transitions) in each year depends on the number of existing grass sites and on the grazing intensity. The resulting bare patch loses resources (R) at a rate, $e$, of soil erosion rate for bare soil. This grazed (bare) patch has a small probability, $n_s P_2$, to be encroached by one of the shrubs in its $n_s$ shrub dominated nearest neighbors (with $0 \leq n_s \leq 8$ and $P_2$ representing the encroachment rate), provided that the resources (R) in that patch are above a certain threshold, $R_{th}=0$, required for shrub establishment. If no shrub encroachment occurs in that patch and the resources are above the threshold for grass growth, grass grows back. Shrub encroachment may result either from the nearest neighbor interaction described above, or randomly by seed dispersal (by grazing animals), with probability, $P_3$, which depends on the grazing intensity, $P_1$.

Fires start with the ignition of a grass patch with probability, $P_4$. The value of $P_4$ is chosen in a way that on average two separate fire events (i.e., two separate random

ignitions) occur in the whole domain. The fire spreads according to a nearest neighbor rule, which means that the fire spreads from the point of ignition (grass patch) to the nearby cells only if they are vegetated. Fire is let spread from neighbor to neighbor - depending on the connectivity of the vegetated patches – in a sub-yearly process throughout the lifetime of the fire. The lifetime is assigned in a way that each fire burns about 10 – 30% of the domain area. After fires, the burned vegetation is classified into two new states: burned grass and burned shrub states. The burned shrub patches erode at a higher rate (4*e*) compared to bare soil patches, due to the enhancement of soil erosion rate due to fire-induced water repellency. The eroded resources are equally redistributed to the neighbors of the burned shrub patch if these neighboring sites are either covered by burned grass or bare interspaces. Conversely, the erosion rates in the burned grass patches are much lower (0.2*e*) than the erosion rate of the bare soil since the surface soil is protected by unburned grass roots. Thus, the post-fire soil erosion rates are all expressed either as a multiple or as a fraction of the erosion rate for bare soil (*e*). The soil resources removed by erosion from the unvegetated soil patches is deposited onto vegetated (shrub and grass) patches, due to the mechanism of canopy trapping [*Charley and West*, 1975; *Schlesinger et al.*, 1990]. To this end, the total amount of soil resources removed by erosion from bare and burned sites is redistributed onto the vegetated patches in such a way that the shrub patches receive twice the amount of sediments due to the higher trapping efficiency. At the end of the each time step (i.e., year), all burned grass patches becomes grasses and the burned shrubs become shrubs with a 25% probability. The rate of grass seed dispersal ($P_5$) increases in the year following fire occurrence (doubled), due to weaker competition from shrubs, the post-fire homogenization of soil

resources, and the short-term fire-induced enhancement of available mineral nutrients (e.g., nitrogen). This increased rate of grass establishment is consistent with the field observations reported in chapter 4.

In this model we assume that no direct conversion occurs from shrub to grass and that the resources lost from the system are compensated by resource inputs into the system in the form of deposition from the surrounding areas. Further, we assume that no soil resources are lost from vegetated patches and no net deposition occurs on bare soil patches. Moreover, vegetated patches have only a limited capacity to trap and retain soil resources; thus, no further resources are deposited at any given site when the resource level exceeds a maximum value, $R_{max}$. Here we take $R_{max}$=2, based on our field observations in similar ecosystems (Sevilleta NWR, New Mexico) showing that the amount of nutrients (*e.g.* Nitrogen) trapped under shrubs is about twice that of the bare interspaces. It is also assumed that the climatic parameters remain unchanged through out the simulation period.

**2.2 Model parameters**

The model parameters are described in Table 8.1. The results from the field experiments discussed above (*Ravi et al*., in review) and from other studies in similar landscapes (Sevilleta LTER, NM) will be used to parameterize the model.

**Table 8.1 Model parameters**

| Sl. No | Parameter | Parameter values |
|---|---|---|
| 1. | Fire Frequency | 1. $P_4 = 2 \times 10^{-6}$ two ignitions per year (lightning)<br>2. Total burn area of 10-30% annually |
| 2. | Grazing Intensity | 1. Overgrazing rate of $P_1$=10%<br>2. Managed grazing rate of $P_1$=1% |
| 3. | Soil Erosion – Deposition | 1. Soil erosion of bare soil ($e$=0.1),<br>2. Post-fire enhancement of erosion in the burned shrub patch ($e_1$=5$e$)<br>3. Post-fire erosion in the burned grass patch ($e_2$=0.2 $e$)<br>4. Deposition is a function of eroded soil and the number of shrubs and grasses in the system<br>5. Post-fire resource redistribution equally to the neighboring bare, burned grass patches from burned shrub patches |
| 4. | Shrub Dynamics | 1. Shrub seed dispersal by cattle with probability $P_3$ = 0.01 over grazed situation and $P_3$ = 0.001 under managed grazing conditions.<br>2. Shrub encroachment probability into neighboring bare patches $P_4$ = 0.01<br>3. Shrub mortality after fire (0.75) |
| 5. | Grass Dynamics | 1. Probability of grass seed dispersal when no fire and over grazing $P_5$ = 0.25<br>2. Probability of grass seed dispersal following fire and controlled grazing $P_5$ = 0.5 |

**3. Results**

The model was first used to show that in the absence of periodic fires, overgrazed desert grasslands may shift towards a shrub land state over a period of 100-150 years (Figure 8.2a) consistently with historical records available for the southwestern United States [e.g., *Buffington and Herbel*, 1965; *Van Auken*, 2000]. Overgrazing and fire suppression lead to shrublands with around 70% bare interspaces and shrub cover of 30% after 300 years of simulation (Figure 8.2 a), in agreement with field observations from the northern Chihuahuan Desert [*Baez et al*., 2006]. The grassland to shrubland conversion results in the depletion of soil resources and an increase in resource heterogeneity (i.e., an increase in the spatial standard deviation, $\sigma_R$, of $R$, see Figure 8.2 a.2), a manifestation of land degradation resulting from the process of shrub encroachment. The resources decrease in time and the spatial heterogeneity increases and reaches a stable state when shrub islands are formed. In the resulting stable two phased landscape with shrub patches and bare interspaces fires cannot propagate due to limited connectivity (Figure 8.2 a.3), while shrubs cannot further encroach into the bare soil areas because they are depleted in soil resources. At this stage, even if we try to manage the system by introducing fires and reducing grazing intensity 100 years after the beginning of the grassland-to-shrubland conversion, the system cannot revert back to its initial state (Figure 8.2 b).

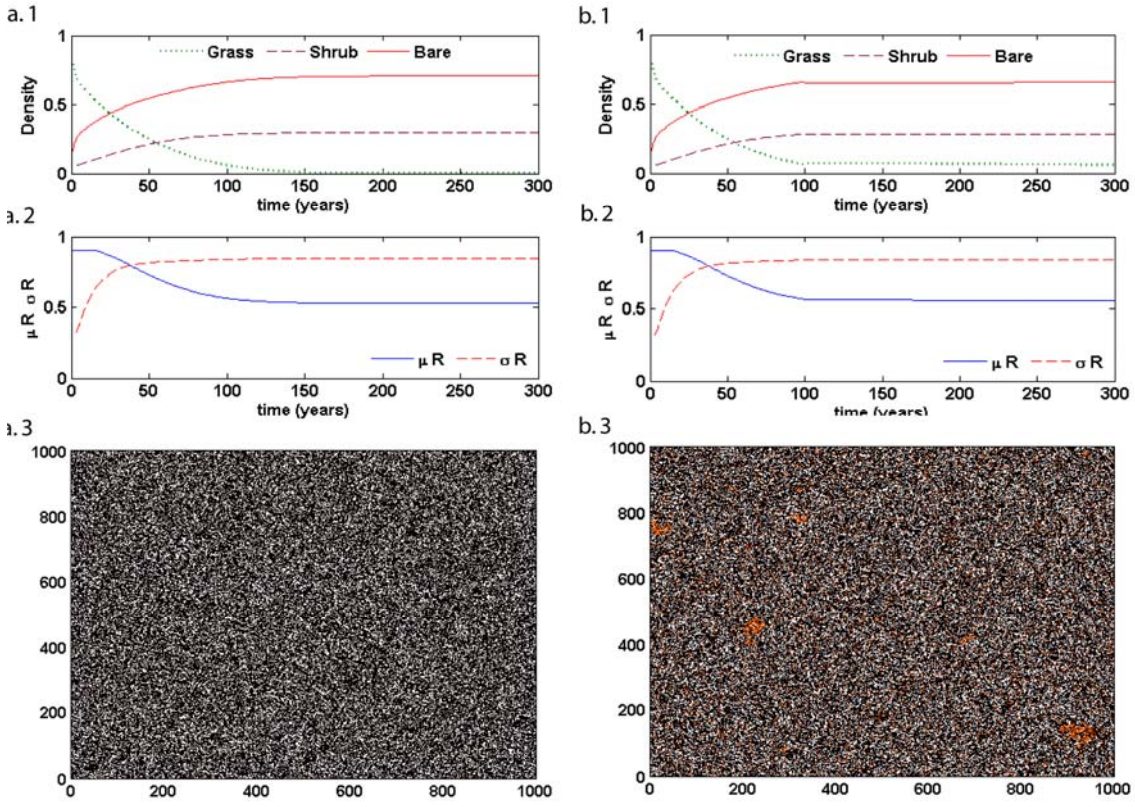


**Figure 8.2** (a) Over grazing and fire suppression (b) Overgrazing and fire suppression only for the first 100 years; for t>100 years an annual fire frequency (two ignitions per fire). (a. 1 & b. 1) vegetation density (a. 2 & b. 2) the spatial mean and standard deviation of resources and (a. 3 & b. 3) the modeled landscape in a 1000 pixel x 1000 pixel domain, colors – white (bare soil interspace), black (shrub) and orange (grass).

However if we manage (with fire and controlled grazing) the system at an earlier stage of shrub encroachment (75 years) the model indicates that the system can return to the initial state with around 70% grass cover (Figure 8.3 a). Fire occurrence in a shrub-grass system results in resource homogenization (decrease in heterogeneity) and may shift the dynamics towards a grassland state (Figure 8.3 a.2 & a.3), depending on the initial vegetation structure and resource levels.

To investigate how the post-fire enhancement of soil erosion (*Ravi et al*., 2007) affects the vegetation and resource dynamics of the system, the same model simulation was run with no post-fire enhancement of soil erosion rates (i.e., with $e_1=e$) from burned shrub patches (Figure 8.3 b). The result indicates that more grass recovery and subsequent decrease in resource heterogeneity occurred in the simulation with enhancement of post-fire soil erosion (Figure 8.3 a & b).

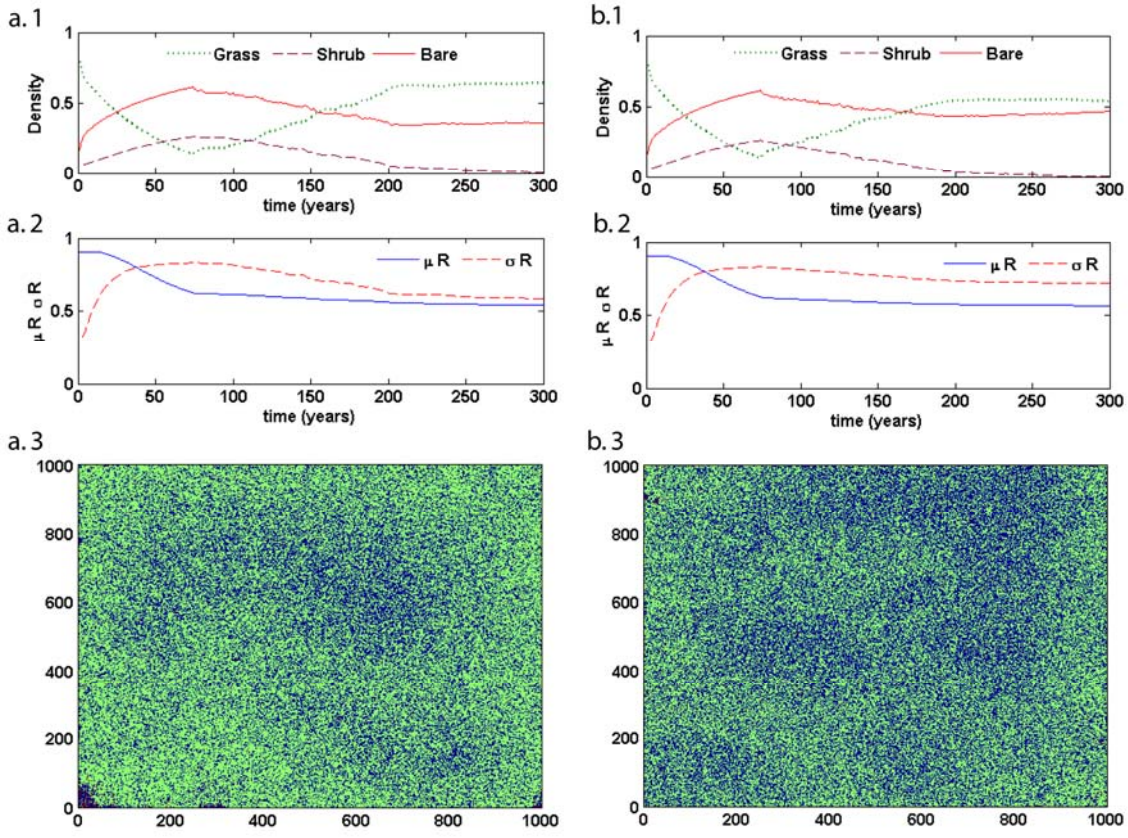


**Figure 8.3** Same as Figure 8.2 for the first 75 years. After 75 years (a) grazing pressure is decreased and fires are allowed to occur with a frequency of once every year (b) same as (a) but with no enhancement of erosion rates. (a. 1 & b. 1) vegetation density (a. 2 & b. 2) the spatial mean and standard deviation of resources and (a. 3 & b. 3) the modeled landscape in a 1000 pixel x 1000 pixel domain, colors – blue (bare soil interspace), red (shrub) and green (grass)

The simulation with fire and low grazing intensity, but with no post fire enhancement of soil erosion rates, shows that the system did not recover completely, and had around 50% grass cover and 50% bare interspaces compared to 65% grass cover and 35% bare interspaces in the simulation with fire-induced enhancement of soil erosion in the burned shrub patches. To show the relative importance of fire and grazing, the model was run using low grazing rates (managed grazing) after the first 25 and 75 years, and no fires throughout the simulation period (Figure 8.4 a & b). The results indicate that even if the grazing rate was reduced to 1% from the initial intensity of 10%, the system cannot recover. However if the low grazing intensity was combined with fires, the system recovered very well (Figure 8.5 a & b). The model simulations indicate that, had the management practices been introduced earlier (25 years), a fire frequency of once every two years would have been sufficient to maintain the grass cover (Figure 8.5 b).

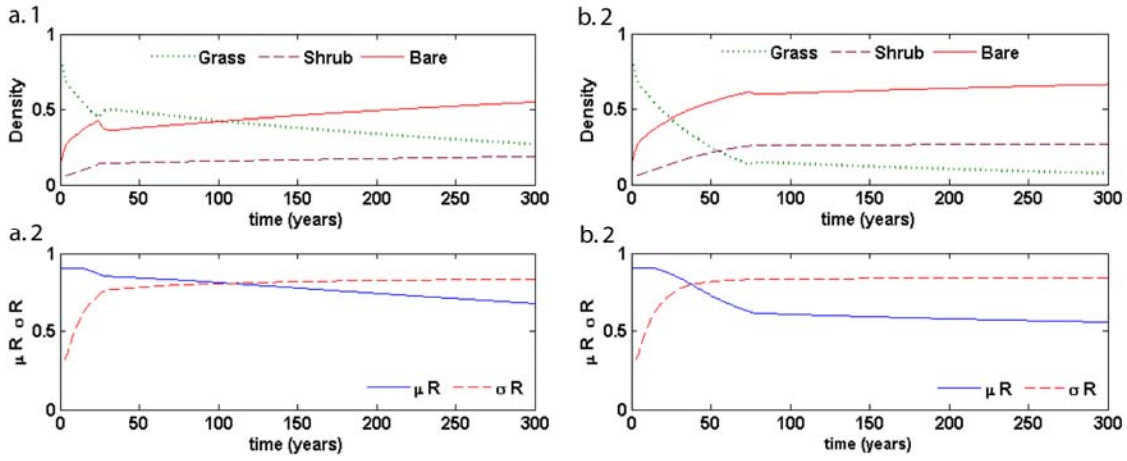


**Figure 8.4** Same as Figure 8.2 but with a decrease in grazing rates after (a) 25 years and (b) 75 years (still with no fires). (a.1 & b.1) vegetation density (a.2 & b.2) the mean and standard deviation of resources

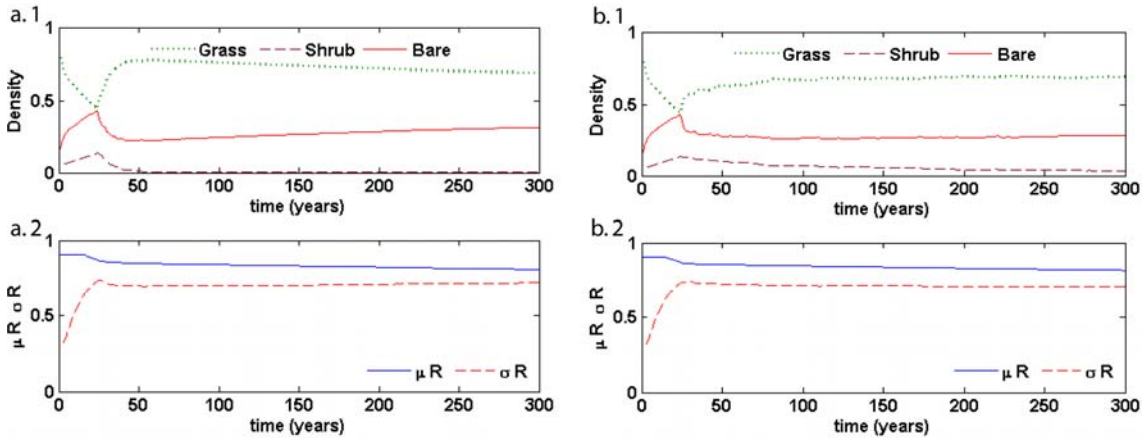


**Figure 8.5** Overgrazing and no fires - as in Figure 8.2 - for the first 25 years. After year 25 (a) fire applied annually, i.e., on average one fire (or 2 grass ignition events) occurs every year in the 1000 pixel x 1000 pixel domain, (b) fire applied on average once every 2 years in the same domain. (a.1 & b.1) vegetation density (a.2 & b.2) the mean and standard deviation of resources

## 4. Discussion

Fire suppression and grazing are often considered as two major contributing factors to the dominance of shrubs and an increase in the bare soil interspaces (Figure 8.2a). In the absence of management practices, the system reaches after 100-150 years an alternative stable shrubland state, with very limited resilience (Figure 8.2b). However if we limit the grazing intensity and establish an annual fire cycle 75 years after the beginning of the shrub encroachment process, the system recovers to the initial grassland state (Figure 8.3a). Thus, it is shown that in the shrub-grass transition zone fires have the ability to prevent the progression of the system towards a stable shrubland state. These results are consistent with our field experiments in shrub-grass transition zone in the Chihuahuan desert [*Ravi et al*., in review]. The model simulation without post-fire enhancement of erosion from burned shrub patches indicates that in the absence of this

process, the recovery of grass is lower compared to the former case. Thus the feedbacks between fires and soil-erosion contribute to the reversibility of vegetation dynamics in these landscapes, and to the dynamics of the islands of fertility. It is also shown that at a very early stage of shrub encroachment (25 years) even if the grazing intensity was reduced by $1/10^{th}$ of the initial intensity, the system cannot go back to the initial density of grasses in the absence of fire. A lower grazing intensity slows down the transition process of grassland to shrubland (Figure 8.4a). The results indicate that reducing the grazing intensity alone will not help in increasing the grass cover. Even though grazing management may slow down the grass decline rates, the shrub densities are not noticeably affected, as no mechanisms would be in place to contribute to shrub removal. Thus, fire is the major factor controlling the reversibility of grassland to shrubland conversions. Figure 8.5 clearly shows the importance of fire in the management of these shrub encroached landscape. If at an early stage (25 years) the system is managed with a lower grazing intensity and prescribed or natural fires, the grass cover can be maintained even with a lower fire frequency. However the season of fire application is also important. Fires applied in peak windy seasons and extended periods of drought can lead to loss of resources from the system, as fire exposes the soil to the erosive action of wind. Further the reversibility of shrub encroachment process depends on the shrub species and the growth stage, as the shrub mortality caused by fires depend on these factors. In a system with invasive annual grasses instead of native perennial grasses, the post fire resource redistribution could lead to the dominance of invasive grasses, which can have negative effect on ecosystem processes.

## 5. Conclusions

Our results indicate that the interactions between fires and soil erosion processes can provide some form of reversibility to the early stages of shrub encroachment by decreasing the spatial heterogeneity of soil resources in the system. This investigation shows the relative importance of fire and grazing in shrub-grass transition zones and highlights the role of fire as a management tool. By enhancing soil erodibility under burned shrubs, fires result in resource homogenization and favor grass regrowth. Thus fire-erosion feedbacks are major factors controlling the dynamics of desert grasslands. Global climate change, decline in vegetation cover, and droughts have resulted in drier conditions in arid and semi arid regions of the world. The increase in aridity results in the dominance of abiotic processes of land degradation such as the aeolian and hydrological transport processes. Further in shrub encroached landscapes, there is a dominance of wind erosion processes. Thus the modeling framework proposed here can be used to investigate qualitatively the possible changes in ecosystem structure and function under different management scenarios.

# CHAPTER: 9

## SUMMARY

Land degradation in drylands is one of the major global environmental issues of the 21st century because of its impact on the World's food security, environmental quality, regional climate change, and desertification. A common manifestation of land degradation in grasslands at the desert margins is associated with the rapid encroachment of shrubs and the increase in the extent of bare soil areas. This phenomenon has important ecological, hydrological and biogeochemical consequences. Despite the significance of this process of shrub encroachment, the factors controlling its reversibility remain poorly understood.

The novel research presented in this dissertation deals with fundamental processes controlling land degradation in grasslands at the desert margins. Particularly, I demonstrate that at the early stages of woody plant encroachment in desert grasslands, fires play a major role in the local scale redistribution of soil resources, thereby counteracting the heterogeneity forming dynamics of land degradation associated with woody plant encroachment. This redistribution is attributed to the enhancement of local scale soil erosion processes, mainly aeolian, which dominate in these dryland landscapes. Fires enhance local scale soil erodibility by altering the physical and chemical properties of the surface soil, leading to varying degrees of soil water repellency, depending on vegetation, soil type and fire characteristics. Despite the recognized relevance of both fires and wind erosion to the structure and function of these ecosystems, the interactions between these two processes remain poorly understood. Further, even though the effects

of fire induced water repellency on water erosion is well studied, its effects on aeolian erosion processes, which dominate in these shrub encroached desert grasslands have never been assessed before. The research presented in this dissertation shows that the levels of soil hydrophobicity developed by typical rangeland fires are able to enhance soil erodibility. The fire-induced soil hydrophobicity observed in the soils beneath burned vegetation (shrubs) enhances soil erodibility by weakening the interparticle wet-bonding forces. This ability of fire induced soil-water repellency in enhancing soil erodibility was tested in the laboratory and mechanistically explained. The wind tunnel tests were conducted using natural soils from arid grasslands, shrublands and shrub-grass transition zones to assess the role of vegetation type on fire induced water repellency and post-fire soil erosion processes. Wind tunnel tests using artificial soils, which were treated with water repellent organic compounds in the laboratory, indicated that fire induced water repellency enhances aeolian processes, even in the absence of confounding factors that might result from the fire treatment (e.g., effect of fires on microbial crusts). Further, replicated field manipulation experiments were conducted at a shrub-grass transition zone using a combination of erosion monitoring techniques, microtopography measurements, infiltration experiments and isotopic studies to show that fires interact with erosion processes to encourage a more homogeneous distribution of soil resources.

The research presented in this dissertation highlights the role of wind and water erosion processes in shrub encroached landscapes and how these processes are affected by disturbances like fires. The results of this study indicate that fires tend to counteract the heterogeneity-forming dynamics of land degradation associated with shrub encroachment, thereby enhancing the reversibility of the early stages of this process. It is

also demonstrated how the interaction between desert plants and soil erosion-deposition processes (aeolian and hydrological) may explain the relation between vegetation patterns and processes in dryland landscapes. These findings highlight the role of fire as a management tool in the early stages of the land degradation process associated with woody plant encroachment in arid grasslands.

This research has potential implications on the sustainability of agricultural and rangeland systems in arid and semi arid regions and the response of these systems to management practices and global climate change scenarios.

# APPENDIX: A

## DESCRIPTION OF STUDY SITES

The soil sampling for wind tunnel experiments was conducted in two different ecosystems from the southwestern United States which are prone to fires and wind erosion, namely, the Sevilleta National Wildlife Refuge (New Mexico, USA) and Cimarron National Grassland (Kansas, USA). The major part of the study was conducted at the Sevilleta Long Term Ecological Research site within the Sevilleta National Wildlife Refuge. The replicated field experiments and infiltration experiments were conducted at the Sevilleta LTER site (Chapter 4). The role of hydrologic and aeolian controls on vegetation patterns were investigated in a shrubland site at the Jornada Experimental Range (Chapter 2) and also in a grassland site at the Sevilleta Wildlife Refuge (Chapter 3).

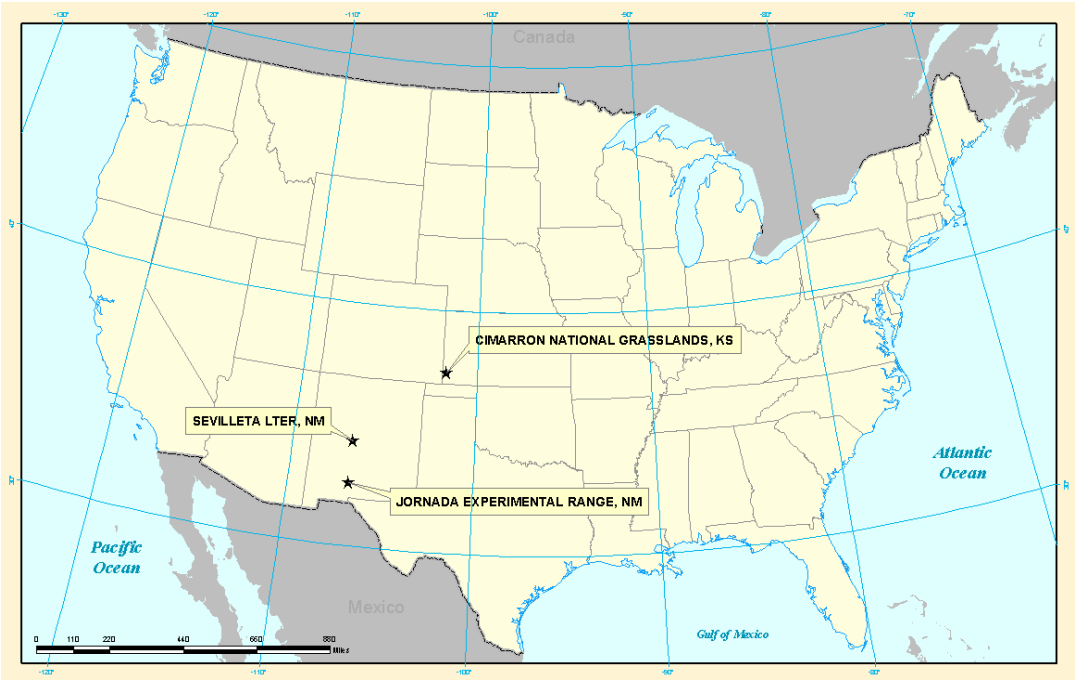


**Figure A.1** The map of United States showing location of the field sites

**SEVILLETA NWR, NEW MEXICO, USA**

Source: Sevilleta LTER, (http://sev.lternet.edu/ )

The Sevilleta LTER site is located in the northern Chihuahuan desert, 20 miles North of Socorro, NM, in and around the Sevilleta National Wildlife refuge. The mean annual temperature (from 1989-2002 at a grassland site) is 13.2$^{o}$ C with a low of 1.6$^{o}$ C in January and 25.1$^{o}$ C in July. However, large diurnal variations in temperature are common in this region. Average annual precipitation is less that 250 mm, and most of the precipitation comes during the summer monsoon season from June through September. The Sevilleta NWR consists of Chihuahuan desert grassland to the south and the Great plain grasslands to the north. The upper elevations of the neighboring mountains consist of Pinion-juniper woodlands and the middle of the Rio Grande Valley consists of riparian vegetation (Figure A.2).

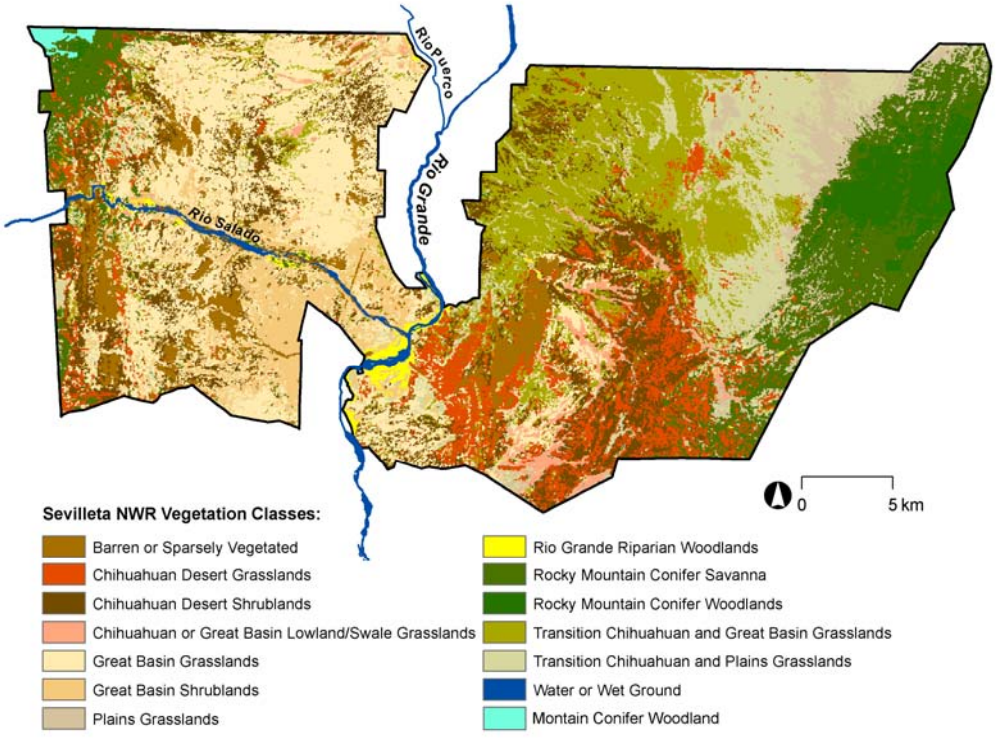


**Figure A.2** The vegetation types at Sevilleta NWR, USA (source: Sevilleta LTER).

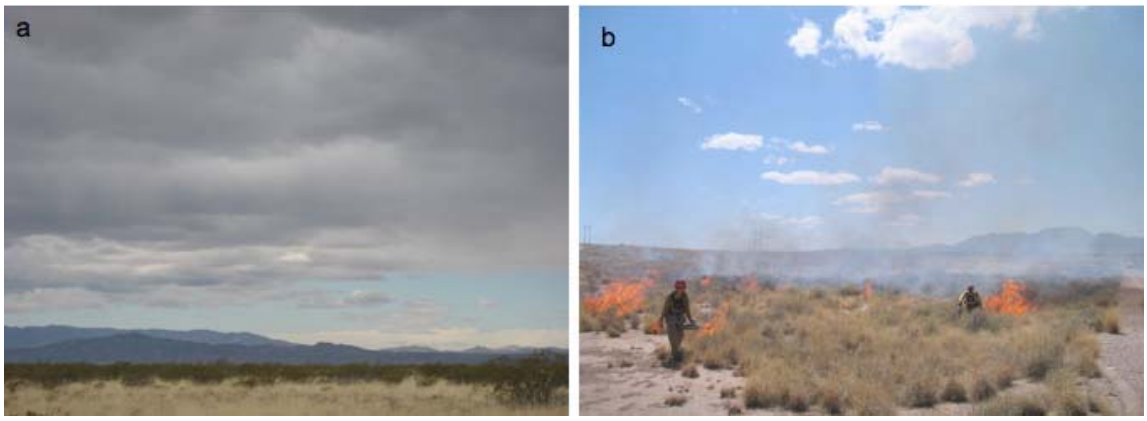


**Figure A.3** (a) Shrub-grass transition zone and (b) a prescribed burn at Sevilleta NWR, New Mexico, USA.

The field experiments were conducted in the proximity of a shrub encroachment front (34$^{o}$ 20$^{'}$ 17.0’ N, 106$^{o}$ 43’ 3.0’ W). The sites represented a transition between Chihuahuan desert grassland and desert scrub habitats (Figure A.3 a). The field sites were in a heterogeneous landscape with dense grass patches, scattered shrub patches and non vegetated (soil) interspaces. The grass cover was minimal at the shrub base but provided enough connectivity among shrubs to allow for the spread of fires in the presence of strong winds (Figure A.3 b). The soil is a sandy loam. The dominant grass species was black grama (*Bouteloua* eriopoda) and the dominant shrub species was creosote bush (*Larrea tridentata*) and snake weed (*Gutierrerzia spp*). Soil sampling (Chapter 7) was done on burned plots capitalizing on controlled burns that are routinely performed at these sites as part of fire management, to decrease the fuel load and to eliminate invasive species and shrubs. For the field experiments (Chapter 4) prescribed burns were conducted which were confined inside the replicated plots. The role of hydrological and aeolian controls on ring pattern formation in grasses was investigated in a blue grama (ring shaped) dominated grassland area.

**JORNADA LTER, NEW MEXICO, USA**

Source : Jornada LTER (http://jornada-www.nmsu.edu/index.php?withJS=true# )

Study site was Jornada Experimental Range (USDA-ARS), located in Northern Chihuahuan Desert, around 20 miles northeast of Las Cruces, New Mexico. The site was characterized by an average elevation of 1188 meters and average annual precipitation was 240 mm and most of the annual precipitation (around 50-80%) occurs in July to September. The average temperature varies from 13$^{o}$ C in January and 36$^{o}$ C in June. The infiltration experiments (Chapter 2) were conducted in a honey mesquite (*Prosopis glandulosa*) dominated shrubland.

**CIMARRON NATIONAL GRASSLANDS, KANSAS, USA**

Source: USDA- Forest Service (http://www.fs.fed.us/r2/psicc/cim/)

The Cimarron National Grasslands is located in Morton County, in the southwest corner of Kansas. This grassland covers 44,000 ha and the elevations range from 960 m to 1078 m. The climate is characterized by mild winters and hot dry summers. The average annual precipitation is around 400 mm per year and occurs mostly in April to September. In some areas of this grassland, there is large scale encroachment of yucca and sagebrush. The area is prone to severe wind erosion, severely affected by the dust bowl of 1930s. The vast rangelands are manipulated through livestock grazing and fire management. The wildlife at Cimarron includes pronghorn (antelope), mule and whitetail deer, and over 351 bird species and 31 species of amphibians and reptiles. The soil sampling for the wind tunnel experiments was conducted after a natural fire (termed the "Steeler Fire" and it burned an area of approximately 1700 ha). (Chapter 5 and 6)

# APPENDIX: B

## Global woody plant encroachment map (Figure 4.1)

The global map of woody plant encroachment (Figure 4.1) was prepared using MODIS land cover product (desert vegetation), Terra MODIS fire data (global annual burned area estimates) and a review of over 200 published studies on woody encroachment around the world. The woody plant encroachment locations were collected from around two hundred published studies on woody plant encroachment around the world including:

- **Africa** [*De Wolf*, 1998; *Hochberg et al.*, 1994; *Holmes*, 2001; *Hudak and Wessman*, 1998; *Jauffret and Lavorel*, 2003; *Jeltsch et al.*, 1997; *Menaut et al.*, 1990; *Palmer and van Rooyen*, 1998; *Prins and van der Jeugd*, 1993; *Roques et al.*, 2001; *Tews et al.*, 2004]
- **Asia** [*Carmel and Kadmon*, 1999; *Chen et al.*, 2005; *Dayal*, 2007; *Jadhav et al.*, 1993; *Li et al.*, 2004; *Li et al.*, 2006; *Sharma and Dakshini*, 1998]
- **Australia** [*Beringer et al.*, 2007; *Costello et al.*, 2000; *Friedel et al.*, 2003; *Sharp and Bowman*, 2004; *van Klinken et al.*, 2006; *van Klinken et al.*, 2007]
- Europe [*Badano and Pugnaire*, 2004; *Zarovali et al.*, 2007]
- **North America** [*Ansley et al.*, 2001; *Archer*, 1989; *Berlow et al.*, 2002; *Boutton et al.*, 1998; *Brown and Carter*, 1998; *Coppedge and Shaw*, 1997; *Gao and Reynolds*, 2003; *Goslee et al.*, 2003; *Hochstrasser and Peters*, 2004; *Jimenez-Lobato and Valverde*, 2006; *Jurena and Archer*, 2003; *Laliberte et al.*, 2004; *Lett and Knapp*, 2005; *Li and Wilson*, 1998; *McCarron and Knapp*, 2001; *McGlynn*

*and Okin*, 2006; *McPherson et al.*, 1988; *Ravi et al.*, 2008; *Ravi*, 2007; *Wheeler et al.*, 2007; *Yorks et al.*, 1994]

- **South America** [*Altesor et al.*, 2006; *Brener and Silva*, 1995; *Cabral et al.*, 2003; *Carretero et al.*, 2007; *de Camargo et al.*, 1999; *Jose and Farinas*, 1983; *Kitzberger et al.*, 2000].

The reference list has only selected publications from which the coordinates are taken to create the Figure 4.1 (Chapter 4).

**References**

Altesor, A., G. Pineiro, F. Lezama, R. B. Jackson, M. Sarasola, and J. M. Paruelo (2006), Ecosystem changes associated with grazing in subhumid South American grasslands, *Journal of Vegetation Science*, 17(3), 323-332.

Ansley, R. J., X. Ben Wu, and B. A. Kramp (2001), Observation: Long-term increases in mesquite canopy cover in a North Texas savanna, *Journal of Range Management*, 54(2), 171-176.

Archer, S. (1989), Have southern Texas savannas been converted to woodlands in recent history, *American Naturalist*, 134(4), 545-561.

Badano, E. I., and F. I. Pugnaire (2004), Invasion of *Agave species* (Agavaceae) in south-east Spain: Invader demographic parameters and impacts on native species, *Diversity and Distributions*, 10(5-6), 493-500.

Beringer, J., L. B. Hutley, N. J. Tapper, and L. A. Cernusak (2007), Savanna fires and their impact on net ecosystem productivity in North Australia, *Global Change Biology*, 13(5), 990-1004.

Berlow, E. L., C. M. D'Antonio, and S. A. Reynolds (2002), Shrub expansion in Montane meadows: The interaction of local-scale disturbance and site aridity, *Ecological Applications*, 12(4), 1103-1118.

Boutton, T. W., S. R. Archer, A. J. Midwood, S. F. Zitzer, and R. Bol (1998), delta C-13 values of soil organic carbon and their use in documenting vegetation change in a subtropical savanna ecosystem, *Geoderma*, 82(1-3), 5-41.

Brener, A. G. F., and J. F. Silva (1995), Leaf-cutting ants and forest groves in a tropical parkland savanna of Venezuela: Facilitated succession? *Journal of Tropical Ecology*, 11(4), 651.

Brown, J. R., and J. Carter (1998), Spatial and temporal patterns of exotic shrub invasion in an Australian tropical grassland, *Landscape Ecology*, 13(2), 93-102.

Cabral, A. C., J. M. De Miguel, A. J. Rescia, M. F. Schmitz, and F. D. Pineda (2003), Shrub encroachment in Argentinean savannas, *Journal of Vegetation Science*, 14(2), 145-152.

Carmel, Y., and R. Kadmon (1999), Effects of grazing and topography on long-term vegetation changes in a Mediterranean ecosystem in Israel, *Plant Ecology*, 145(2), 243-254.

Carretero, E. M., A. Dalmasso, and S. Trione (2007), Carbon storage in Larrea divaricata and L-cuneifolia (zygophyllaceae) in drylands of central-western Argentina, *Arid Land Research and Management*, 21(4), 273-285.

Chen, S. P., Y. F. Bai, G. H. Lin, and X. G. Han (2005), Variations in life-form composition and foliar carbon isotope discrimination among eight plant communities under different soil moisture conditions in the Xilin River Basin, Inner Mongolia, China, *Ecological Research*, 20(2), 167-176.

Coppedge, B. R., and J. H. Shaw (1997), Effects of horning and rubbing behavior by bison (Bison bison) on woody vegetation in a tall grass prairie landscape, *American Midland Naturalist*, 138(1), 189-196.

Costello, D. A., I. D. Lunt, and J. E. Williams (2000), Effects of invasion by the indigenous shrub *Acacia sophorae* on plant composition of coastal grasslands in south-eastern Australia, *Biological Conservation*, 96(1), 113-121.

Dayal, V. (2007), Social diversity and ecological complexity: how an invasive tree could affect diverse agents in the land of the tiger, *Environment and Development Economics*, 12, 553-571.

de Camargo, P. B., S. E. Trumbore, L. A. Martinelli, E. A. Davidson, D. C. Nepstad, and R. L. Victoria (1999), Soil carbon dynamics in regrowing forest of eastern Amazonia, *Global Change Biology*, 5(6), 693-702.

De Wolf, J. (1998), Species composition and structure of the woody vegetation of the Middle Casamance region (Senegal), *Forest Ecology and Management*, 111(2-3), 249-264.

Friedel, M. H., A. D. Sparrow, J. E. Kinloch, and D. J. Tongway (2003), Degradation and recovery processes in and grazing lands of central Australia. Part 2: vegetation, *Journal of Arid Environments*, 55(2), 327-348.

Gao, Q., and J. F. Reynolds (2003), Historical shrub-grass transitions in the northern Chihuahuan Desert: modeling the effects of shifting rainfall seasonality and event size over a landscape gradient, *Global Change Biology*, 9(10), 1475-1493.

Goslee, S. C., K. M. Havstad, D. P. C. Peters, A. Rango, and W. H. Schlesinger (2003), High-resolution images reveal rate and pattern of shrub encroachment over six decades in New Mexico, USA, *Journal of Arid Environments*, 54(4), 755-767.

Hochberg, M. E., J. C. Menaut, and J. Gignoux (1994), Influences of tree biology and fire in the spatial structure of the west-African savanna, *Journal of Ecology*, 82(2), 217-226.

Hochstrasser, T., and D. P. C. Peters (2004), Subdominant species distribution in microsites around two life forms at a desert grassland-shrubland transition zone, *Journal of Vegetation Science*, 15(5), 615-622.

Holmes, P. M. (2001), Shrubland restoration following woody alien invasion and mining: Effects of topsoil depth, seed source, and fertilizer addition, *Restoration Ecology*, 9(1), 71-84.

Hudak, A. T., and C. A. Wessman (1998), Textural analysis of historical aerial photography to characterize woody plant encroachment in South African savanna, *Remote Sensing Of Environment*, 66(3), 317-330.

Jadhav, R. N., M. M. Kimothi, and A. K. Kandya (1993), Grassland mapping monitoring of Banni, Kachchh (Gujarat) using remotely-sensed data, *International Journal Of Remote Sensing*, 14(17), 3093-3103.

Jauffret, S., and S. Lavorel (2003), Are plant functional types relevant to describe degradation in arid, southern Tunisian steppes? *Journal of Vegetation Science*, 14(3), 399-408.

Jeltsch, F., S. J. Milton, W. R. J. Dean, and N. Van Rooyen (1997), Analyzing shrub encroachment in the southern Kalahari: a grid-based modeling approach, *Journal of Applied Ecology*, 34(6), 1497-1508.

Jimenez-Lobato, V., and T. Valverde (2006), Population dynamics of the shrub Acacia bilimekii in a semi-desert region in central Mexico, *Journal of Arid Environments*, 65(1), 29-45.

Jose, J. J. S., and M. R. Farinas (1983), Changes In Tree Density And Species Composition In A Protected Trachypogon Savanna, Venezuela, *Ecology*, 64(3), 447-453.

Jurena, P. N., and S. Archer (2003), Woody plant establishment and spatial heterogeneity in grasslands, *Ecology*, 84(4), 907-919.

Kitzberger, T., D. F. Steinaker, and T. T. Veblen (2000), Effects of climatic variability on facilitation of tree establishment in northern Patagonia, *Ecology*, 81(7), 1914-1924.

Laliberte, A. S., A. Rango, K. M. Havstad, J. F. Paris, R. F. Beck, R. McNeely, and A. L. Gonzalez (2004), Object-oriented image analysis for mapping shrub encroachment from 1937 to 2003 in southern New Mexico, *Remote Sensing of Environment*, 93(1-2), 198-210.

Lett, M. S., and A. K. Knapp (2005), Woody plant encroachment and removal in mesic grassland: Production and composition responses of herbaceous vegetation, *American Midland Naturalist*, 153(2), 217-231.

Li, X., Z. Zhang, J. Zhang, X. Wang, and X. Jia (2004), Association between vegetation patterns and soil properties in the southeastern Tengger Desert, China, *Arid Land Research and Management*, 18, 369.

Li, X. D., and S. D. Wilson (1998), Facilitation among woody plants establishing in an old field, *Ecology*, 79(8), 2694-2705.

Li, X. R., X. H. Jia, and G. R. Dong (2006), Influence of desertification on vegetation pattern variations in the cold semi-arid grasslands of Qinghai-Tibet plateau, North-west China, *Journal of Arid Environments*, 64(3), 505-522.

McCarron, J. K., and A. K. Knapp (2001), C-3 woody plant expansion in a C-4 grassland: Are grasses and shrubs functionally distinct, *American Journal of Botany*, 88(10), 1818-1823.

McGlynn, I. O., and G. S. Okin (2006), Characterization of shrub distribution using high spatial resolution remote sensing: Ecosystem implications for a former Chihuahuan Desert grassland, *Remote Sensing of Environment*, 101(4), 554-566.

McPherson, G. R., H. A. Wright, and D. B. Wester (1988), Patterns of shrub invasion in semiarid Texas grasslands, *American Midland Naturalist*, 120(2), 391-397.

Menaut, J. C., J. Gignoux, C. Prado, and J. Clobert (1990), Tree community dynamics in a humid savanna of the Ivory-Coast - Modeling the effects of fire and competition with grass and neighbors, *Journal of Biogeography*, 17(4-5), 471-481.

Palmer, A. R., and A. F. van Rooyen (1998), Detecting vegetation change in the southern Kalahari using Landsat TM data, *Journal of Arid Environments*, 39(2), 143-153.

Prins, H. H. T., and H. P. van der Jeugd (1993), Herbivore population crashes and woodland structure in East Africa, *Journal of Ecology*, 81(2), 305-314.

Ravi, S., P. D'Odorico, T. M. Zobeck, and T. M. Over (2008), The effect of fire-induced soil hydrophobicity on wind erosion in a semiarid grassland: Experimental observations and theoretical framework, *Geomorphology*, *in press*.

Ravi, S., P. D'Odorico, T. M. Zobeck, T. M. Over, and S. L. Collins (2007), Feedbacks between fires and wind erosion in heterogeneous arid lands, *Journal of Geophysical Research*, 112*,* G04007.

Roques, K. G., T. G. O'Connor, and A. R. Watkinson (2001), Dynamics of shrub encroachment in an African savanna: relative influences of fire, herbivory, rainfall and density dependence, *Journal of Applied Ecology*, *38*(2), 268-280.

Sharma, R., and K. M. M. Dakshini (1998), Integration of plant and soil characteristics and the ecological success of two Prosopis species, *Plant Ecology*, 139(1), 63-69.

Sharp, B. R., and D. Bowman (2004), Patterns of long-term woody vegetation change in a sandstone-plateau savanna woodland, Northern Territory, Australia, *Journal of Tropical Ecology*, 20, 259-270.

Tews, J., F. Schurr, and F. Jeltsch (2004), Seed dispersal by cattle may cause shrub encroachment of Grewia lava on southern Kalahari rangelands, *Applied Vegetation Science*, *7*(1), 89-102.

van Klinken, R. D., J. Graham, and L. K. Flack (2006), Population ecology of hybrid mesquite (*Prosopis species*) in Western Australia: how does it differ from native

range invasions and what are the implications for impacts and management? *Biological Invasions*, *8*(4), 727-741.

van Klinken, R. D., D. Shepherd, R. Parr, T. P. Robinson, and L. Anderson (2007), Mapping mesquite (*Prosopis*) distribution and density using visual aerial surveys, *Rangeland Ecology and Management*, 60(4), 408-416.

Wheeler, C. W., S. R. Archer, G. P. Asner, and C. R. McMurtry (2007), Climatic/edaphic controls on soil carbon/nitrogen response to shrub encroachment in desert grassland, *Ecological Applications*, 17(7), 1911-1928.

Yorks, T. P., N. E. West, and K. M. Capels (1994), Changes In Pinyon-Juniper woodlands in western Utah pine-valley between 1933-1989, *Journal of Range Management*, 47(5), 359-364.

Zarovali, M. P., M. D. Yiakoulaki, and V. P. Papanastasis (2007), Effects of shrub encroachment on herbage production and nutritive value in semi-arid Mediterranean grasslands, *Grass and Forage Science*, 62(3), 355-363.

# APPENDIX: C

**The derivation of an expression for the interparticle wet bonding forces ($F_i$) to an express $F_i$ as a function of the contact angle. (Chapter 6)**

We generalize the theory of McKenna Neuman and Nickling (1989) to account for the dependence of interparticle bonding forces because of liquid-bridges on the contact angle. To this end, we use their schematic representation of soil grains as co-axial, dissymmetric cone surfaces touching each other at the vertices, as shown in Figure 6.6. The interparticle forces because of liquid-bridges can be expressed as the sum of two components, one associated with the pressure deficit inside the liquid-bridge acting through a circular surface of radius $r_1$ and the other the surface tension component in the $z$ direction acting along the line of contact between soil grains and the air-water interface. Thus, the force exerted by the liquid-bridge on soil grain 1 (Figure 6.6) can be expressed as

$$F_{i1} = \psi\pi r_1^{\,2} + 2\pi r_1 T_w \cos(\beta-\gamma), \tag{C.1}$$

which should be equal to the opposite force exerted by the liquid-bridge on grain 2

$$F_{i2} = \psi\pi r_2^{\,2} + 2\pi r_2 T_w \cos(\alpha-\gamma), \tag{C.2}$$

with $\psi$ being the water pressure (water potential), $T_w$ the surface tension of water, and $\gamma$ the contact angle. At the instant of particle motion (threshold), an equilibrium exists between these two forces, which can be represented as

$$\psi\pi r_1^{\,2} + 2\pi r_1 T_w \cos(\beta-\gamma) = \psi\pi r_2^{\,2} + 2\pi r_2 T_w \cos(\alpha-\gamma). \tag{C.3}$$

On the basis of the simple geometric considerations (see Fig. 6) we have

$$h_1 + h_2 = R_1 (\sin(\beta-\gamma) + \sin(\alpha-\gamma)), \tag{C.4}$$

$$h_1 = \frac{r_1}{\tan\beta} = \frac{R_1 + R_2 - R_1\cos(\beta-\gamma)}{\tan\beta}, \tag{C.5}$$

and

$$h_2 = \frac{r_2}{\tan\alpha} = \frac{R_1 + R_2 - R_1\cos(\alpha-\gamma)}{\tan\alpha}. \tag{C.6}$$

By inserting equations (C5) and (C6) in (C4) we obtain

$$R_1\left[\ \frac{1-\cos(\beta-\gamma)}{\tan\beta} + \frac{1-\cos(\alpha-\gamma)}{\tan\alpha} + R_1[\sin(\beta-\gamma)+\sin(\alpha-\gamma)]\ \right] = -R_2\left(\frac{1}{\tan\beta}+\frac{1}{\tan\alpha}\right). \tag{C.7}$$

Thus, we express $R_2$ as a function of $R_1$

$$R_1 C = R_2 \tag{C.8}$$

with $C$ depending on γ and on the angles α and β

$$C = f(\gamma) = \frac{\sin(\beta-\gamma)+\sin(\alpha-\gamma) - \dfrac{1-\cos(\beta-\gamma)}{\tan\beta} - \dfrac{1-\cos(\alpha-\gamma)}{\tan\alpha}}{\dfrac{1}{\tan\beta}+\dfrac{1}{\tan\alpha}} \tag{C.9}$$

The constant $C$ can be rewritten as

$$C = B\cos(\gamma) - 1 \tag{C.10}$$

with

$$B = \frac{\dfrac{1}{\sin\alpha}+\dfrac{1}{\sin\beta}}{\dfrac{1}{\tan\alpha}+\dfrac{1}{\tan\beta}}. \tag{C.11}$$

Equation (C.8) in (C.5) and (C.6) gives

$$r_1 = R_1(1-\cos(\beta-\gamma) + C) \text{ and } r_2 = R_1(1-\cos(\alpha-\gamma) + C) \tag{C.12}$$

Equations (C.12) can be inserted in (C.3) leading to the following equation

$$\psi R_1 = T_w \left( \frac{b_2 - b_1}{a_1 - a_2} \right) \tag{C.13}$$

with

$$a_1 = (1\text{-}\cos(\beta\text{-}\gamma) + C)^2 = (B\cos(\gamma) - \cos(\beta\text{-}\gamma))^2 \tag{C.14-a}$$

$$a_2 = (1\text{-}\cos(\alpha\text{-}\gamma) + C)^2 = (B\cos(\gamma) - \cos(\alpha\text{-}\gamma))^2 \tag{C.14-b}$$

and

$$b_1 = 2(1\text{-}\cos(\beta\text{-}\gamma)+C)\cos(\beta\text{-}\gamma) = 2(B\cos(\gamma)\text{-}\cos(\beta\text{-}\gamma))\cos(\beta\text{-}\gamma) \tag{C.15-a}$$

$$b_2 = 2(1\text{-}\cos(\alpha\text{-}\gamma)+C)\cos(\alpha\text{-}\gamma) = 2(B\cos(\gamma)\text{-}\cos(\alpha\text{-}\gamma))\cos(\alpha\text{-}\gamma). \tag{C.15-b}$$

Equations (C.12), (C.14-a), and (C.15-a) may be inserted into (C.1) to express the interparticle force as

$$F_i = F_{i1} = F_{i2} = \psi\pi R_1^2 (1\text{-}\cos(\beta\text{-}\gamma)+C)^2 + 2\pi R_1 (1\text{-}\cos(\beta\text{-}\gamma)+C) T_w \cos(\beta\text{-}\gamma)$$

$$= \psi\pi R_1^2 a_1 + \pi R_1 b_1 T_w \tag{C.16}$$

Using equation (C.13) we obtain

$$F_i = \pi R_1 T_w \left[ \left( \frac{b_2 - b_1}{a_1 - a_2} \right) a_1 + b_1 \right] = G \frac{\pi T_w^2}{\psi}, \tag{C.17}$$

with

$$G = a_1 D^2 + b_1 D \quad \text{and} \quad D = \frac{b_2 - b_1}{a_1 - a_2} = \frac{2B\cos(\gamma) - 2[\cos(\beta - \gamma) + \cos(\alpha - \gamma)]}{2B\cos(\gamma) - [\cos(\beta - \gamma) + \cos(\alpha - \gamma)]} . \tag{C.18}$$

$G$ modulates the dependence of $F_i$ on the contact angle, $\gamma$, and on the particle geometry.

To facilitate the comparison with the expression obtained by *Ravi et al.* [2006a] for the case of spherical soil grains, we use (C.12) and (C.14-a) and rewrite the first part of (C.17) in the form

$$G_1 = \frac{F_i}{\pi r_1 T_w} = \left[ D\sqrt{a_1} + \frac{b_1}{\sqrt{a_1}} \right] \tag{C.19}$$

In particular, in the case of symmetrical cones (i.e., α=β) equation (C.19) becomes

$$G_1 = \frac{F_i}{\pi r_1 T_w} = \frac{\cos(\gamma)}{\cos(\alpha)}. \tag{C.20}$$

## CITED REFERENCES

Adachi, N., I. Terashima, and M. Takahashi (1996), Mechanisms of central die-back of *Reynoutria japonica* in the volcanic desert on Mt Fuji: A stochastic model analysis of rhizome growth, *Annals of Botany*, 78(2), 169-179.

Adams, S., B. R. Strain, and M. S. Adams (1970), Water-repellent soils, fire, and annual plant cover in a desert scrub community of southeastern California, *Ecology*, 51, 696-700.

American Society for Testing and Materials (1981), *Annual Book of ASTM Standards*, American Society for Testing and Materials, Philadelphia, PA.

Anderies, J. M., M. A. Janssen, and B. H. Walker (2002), Grazing management, resilience, and the dynamics of a fire-driven rangeland system, *Ecosystems*, 5, 23-44.

Archer, S., D. S. Schimel, and E. A. Holland (1995), Mechanisms of shrubland expansion - Land-use, climate or $CO_2$, *Climatic Change*, 29(1), 91-99.

Archer, S. (1989), Have southern Texas savannas been converted to woodlands in recent history, *American Naturalist*, 134(4), 545-561.

Archer, S., C. Scifres, C.R. Bassham, and R. Maggio (1988), Autogenic succession in a subtropical savanna: conversion of grassland to thorn woodland, *Ecological Monographs*, 58(2), 111-127.

Asner, G. P., A. J. Elmore, L. P. Olander, R. E. Martin, and A.T. Harris (2004), Grazing systems, ecosystem responses, and global change, *Annual Reviews of Environment and Resources*, 29, 261-299.

Aubreville, A. (1949), *Climats, Forêts et Désertification de l'Afrique Tropicale*, Société d'Editions Géographiques, Maritimes et Coloniales, Paris, pp 255.

Bagnold, R. A. (1941), *The Physics of Blown Sand and Desert Dunes*, Methuen, London. pp 265.

Baez, S., S.L. Collins, D. Lightfoot and T. Koontz. (2006), Effects of rodent removal on community dynamics in desert grassland and shrubland vegetation, *Ecology*, 87: 2746-2754.

Barrett, G., Slaymaker, O. (1989), Identification, characterization and hydrological implications of water repellency in mountain soils, Southern British Columbia. *Catena*, 16, 477-489.

Batjargal, Z. (1992), The climatic and man-induced environmental factors of the degradation of ecosystem in Mongolia, International Workshop on Desertification, Ulaanbaatar, Mongolia, pp 19.

Bautista, S., Á. Mayor, J. Bourakhouadar, and J. Bellot (2007), Plant spatial pattern predicts hillslope runoff and erosion in a semiarid Mediterranean landscape, *Ecosystems*, 10, 987-998.

Belly, P. Y. (1964), *Sand Movement by Wind*, Technical Memorandum No. 1. U.S. Army Coastal Engineering Research Center, Washington, D.C.

Belnap, J., J. R. Welter, N. B. Grimm, N. Barger, and J. A. Ludwig (2005), Linkages between microbial and hydrologic processes in arid and semiarid watersheds, *Ecology*, 86(2), 298-307.

Ben-Hur, M., and J. Letey (1989), Effect of Polysaccharides, clay dispersion, and impact energy on rainfall infiltration, *Soil Science Society of America Journal*, 53, 233-238.

Bestelmeyer, B. T., J. P. Ward, and K. M. Havstad (2006), Soil-geomorphic heterogeneity governs patchy dynamics at an arid ecotone, *Ecology*, 87(4), 963-973.

Bhark, E. W., and E. E. Small (2003), Association between plant canopies and the spatial patterns of infiltration in shrubland and grassland of the Chihuahuan desert, New Mexico, *Ecosystems*, 6, 185-196.

Bonanomi, G., F. Giannino, and S. Mazzoleni (2005), Negative plant-soil feedback and species coexistence, *Oikos*, 111(2), 311-321.

Bond, R. D. (1964). The influence of the microflora on the physical properties of soils. II. Field studies on water repellent sands, *Australian Journal Soil Research, 2*,123-131.

Bowman, R. A., D. M. Mueller, and W. J. McGinnies (1985), Soil and vegetation relationships in a Central Plains saltgrass meadow, *Journal of Range Management*, 38(4), 325-328.

Breman, H., and J. J. Kessler (1995), *Woody Plants in Agro-Ecosystems of Semi-Arid Regions*, Springer, Berlin, pp 340.

Breshears, D. D., J. J. Whicker, M. P. Johansen, and J. E. Pinder III. (2003), Wind and water erosion and transport in semiarid shrubland, grassland, and forest ecosystems: Quantifying dominance of horizontal wind-driven transport, *Earth Surface Processes and Landforms,* 28, 1189–1209.

Briske, D. D., and A. M. Wilson (1977), Temperature effects on adventitious root development in blue grama seedlings, *Journal of Range Management*, 30(4), 276-280.

Buffington, L. C., and C. H. Herbel (1965), Vegetational changes on a semidesert grassland range from 1858 to 1963, *Ecological Monographs*, 35(2), 139-164.

Cabral, A. C., J. M. De Miguel, A. J. Rescia, M. F. Schmitz, and F. D. Pineda (2003), Shrub encroachment in Argentinean savannas, *Journal of Vegetation Science*, 14(2), 145 -152.

Campbell, G. S. and J. M. Norman (1998), *An Introduction to Environmental Biophysics*, Springer, Berlin, pp 286.

Castellanos, E. M., M. E. Figueroa, and A. J. Davy (1994), Nucleation and facilitation in salt-marsh succession - Interactions between *Spartina maritima* and *Arthrocnemum perenne*, *Journal of Ecology*, 82(2), 239-248.

Charley, J. L., and N. E. West (1975), Plant-induced soil chemical patterns in some shrub-dominated semi-desert ecosystems of Utah, *Journal of Ecology*, 63(3), 945-963.

Charney, J. C. (1975), Dynamics of deserts and droughts in the Sahel, *Quarterly Journal of the Royal Meteorological Society*, 101, 193-202.

Chauhan, S. S. (2003), Desertification control and management of land degradation in the Thar desert of India, *The Environmentalist*, 23, 219-227.

Colasanti, R. L., and J. P. Grime (1993), Resource dynamics and vegetation processes: a deterministic model using two-dimensional cellular automata, *Functional Ecology*, 7, 169-176.

Collins, S. L., R.L. Sinsabaugh, C. Crenshaw, L. Green, A. Porras-Alfaro, M. Stursova and L. Zeglin (2008), Pulse dynamics and microbial processes in aridland ecosystems, *Journal of Ecology*, doi:10.1111/j.1365-2745.2008.01362.x.

Cornelis, W. M., D. Gabriels., R. Hartmann (2004), A conceptual model to predict the deflation threshold shear velocity as affected by near-surface soil water: I. Theory, *Soil Science Society of America Journal*, 68(4), 1154-1161.

Cosby, H. E. (1960), Rings on the range, *Journal of Range Management*, 13(6), 283-288.

Couteron, P., and O. Lejeune (2001), Periodic spotted patterns in semi-arid vegetation explained by a propagation-inhibition model, *Journal of Ecology*, 89(4), 616-628.

Daily, G. C. (1995), Restoring value to the worlds degraded lands, *Science*, 269(5222), 350-354.

D'Antonio C. M., and P. M. Vitousek (1992), Biological invasion by exotic grasses, the grass-fire cycle, and global change, *Annual Reviews of Ecology and Systematics*, 23, 63-87.

Dalgleish, H. J., and D. C. Hartnett (2006), Below-ground bud banks increase along a precipitation gradient of the North American Great Plains: a test of the meristem limitation hypothesis, *New Phytologist*, 171(1), 81-89.

Danin, A., and G. Orshan (1995), Circular arrangement of *Stipagrostis ciliata* clumps in the Negev, Israel and near Gokaeb, Namibia, *Journal of Arid Environments*, 30(3), 307-313.

Danin, A., Y. Bar-or, I. Dor, and T. Yisraeli (1989), The role of cyanobacteria in stabilization of sand dunes in Southern Israel, *Ecologia Mediterranea XV*, 55-64.

Darkoh, M. B. K. (1998), The nature, causes and consequences of desertification in the drylands of Africa, *Land Degradation and Development*, 9, 1-20.

DeBano, L. F. (2000), The role of fire and soil heating on water repellence in wildland environments: A review, *Journal of Hydrology*, 231, 195-206.

DeBano, L. F. 1966. Formation of non-wettable soils involves heat transfer mechanism. USDA Forest Service, Pacific Southwest Forest and Range Experiment Station, Research Note PSW-132, pp 8.

DeBano, L. F., and J. S. Krammes (1966), Water repellent soils and their relation to wildfire temperatures, *International Bulletin of the Association of Hydrological Scientists*, 2, 14–19.

D'Odorico, P., K. Caylor, G. S. Okin, and T. M. Scanlon (2007), On soil moisture-vegetation feedbacks and their possible effects on the dynamics of dryland ecosystems, *Journal of Geophysical Research - Biogeosciences*, 112, G04010.

D'Odorico, P., F. Laio, and L. Ridolfi (2006), Patterns as indicators of productivity enhancement by facilitation and competition in dryland vegetation, *Journal of Geophysical Research*, 111, G03010.

D'Odorico P., and I. Rodriguez-Iturbe (2000), Space-time self-organization of mesoscale rainfall and soil moisture, *Advances in Water Resources*, 23(4), 349-357.

Doerr, S. H., R. A. Shakesby, and R.P.D. Walsh (2000), Soil water repellency**:** its causes, characteristics and hydro-geomorphological significance, *Earth-Science Review*s, 51, 33-65.

Doerr, S. H. (1998), On standardizing the 'water drop penetration time' and the 'molarity of an ethanol droplet' techniques to classify soil hydrophobicity: A case study using medium textured soils, *Earth Surface Processes and Landforms,* 23(7), 663-668.

Dregne, H. E. (2002), Land degradation in the drylands, *Arid Land Research and Management*, 16(2), 99-132.

Dregne, H. E., and N. T. Chou (1992), Global desertification dimensions and costs, in *Degradation and restoration of arid lands*, Texas Tech University, Lubbock.

Dregne, H. E. (1983), *Desertification of Arid Lands*, Harwood Academic Publishers, New York, pp 242.

Dregne, H. E. (1976), Desertification: Symptoms of a crisis, in *Desertification, Process, problems, Perspectives,* Paylore, P and R. A. Haney (editors), University of Arizona Press, Tucson.

Duce, R. A., and N. W. Tindale (1991), Atmospheric transport of iron and its deposition in the ocean, *Limnology and Oceanography*, 36, 1715-1726.

El-Morsy, E. A., M. Malik, and J. Letey (1991), Polymer effects on the hydraulic conductivity of saline and sodic soil conditions, *Soil Science,* 151(6), 430-435.

Fearnehough, W., M. A. Fullen, D. J. Mitchell, I. C. Trueman and J. Zhang (1998) Aeolian deposition and its effect on soil and vegetation changes on stabilized desert dunes in northern China, *Geomorphology*, 23,171-182.

Fecan, F., B. Marticorena, and G. Bergametti (1999), Parametrization of the increase of the aeolian erosion threshold wind friction velocity due to soil moisture for arid and semiarid areas, *Annales Geophysicae,* 17, 149-157.

Fensham, R. J., R. J. Fairfax, and S. R. Archer (2005), Rainfall, land use and woody vegetation cover change in semi-arid Australian savanna, *Journal of Ecology*, 93(3), 596-606.

Fisher, R. A. (1926), On the capillary forces in an ideal soil. Correction to formulae given by W. B. Haines, *Journal of Agricultural Sciences*, 16, 492-505.

Fryrear, D. W. (1985), Soil cover and wind erosion, *Transactions of the American Society of Agricultural Engineers*, 28(3), 781-784.

Gavlak, R. G., D. A. Horneck, and R. O. Miller (1994), *Plant, Soil, and Water Reference Methods for the Western Region*, WREP 125 (Method S 10.20).

Gatsuk, L. E., O. V. Smirnova, L. I. Vorontzova, L. B. Zaugolnova, and L. A. Zhukova (1980), Age states of plants of various growth forms - A review, *Journal of Ecology*, 68(2), 675-696.

Gee, G. W., M. D. Campbell., G. S. Campbell., and J. H. Campbell (1992), Rapid measurement of low soil water potentials using a water activity meter, *Soil Science Society of America Journal*, 56, 1068-1070.

Geist H. J., and E. F. Lambin (2004), Dynamic causal patterns of desertification, *Bioscience*, 54(9), 817-829.

Giglio, L., I. Csiszar, and C. O. Justice (2006), Global distribution and seasonality of active fires as observed with the Terra and Aqua Moderate Resolution Imaging Spectroradiometer (MODIS) sensors, *Journal of Geophysical Research-Biogeosciences*, 111, G02016.

Glantz, M. H (1987), *Drought and Hunger in Africa: Denying Famine a Future*, Cambridge University Press, pp 457.

Glantz, M. H. (editor) (1977), *Desertification: Environmental Degradation in and around Arid lands*, Westview Press, Boulder.

Gregory, J. M. and M. M. Darwish (1990), Threshold friction velocity prediction considering water content, *Proceedings of American Society of Agricultural Eng*ineers, Paper No. 90-2562, New Orleans, pp16.

Greigsmith, P. (1979), Pattern in vegetation, *Journal of Ecology*, 67(3), 755-779.

Hare, K. (1977), Connections between climate and desertification, *Environmental Conservation*, 4(2), 81-90.

Harnby, N. (1992), The mixing of cohesive powders, in *Mixing in the Process Industries*, edited by N. Harnby *et al*., Butterworth-Heinemann Ltd., Oxford, pp. 79-98.

Harper, K. T., and J. Belnap (2001), The influence of biological soil crusts on mineral uptake by associated vascular plants, *Journal of Arid Environments*, 47, 347-357.

Helm, P. J., and C. S. Breed (1999), Instrumented field studies of sediment transport by wind. In: Breed, C. S. and M. C. Reheis (editors.), *Desert Winds: Monitoring Wind-Related Surface Processes in Arizona, New Mexico and California*, US Geological Survey Professional Paper 1598. G.P.O., Washington, USA, pp 31-51.

Herrmann S. M., and C. F. Hutchinson (2005), The changing contexts of the desertification debate, *Journal of Arid Environments*, 63, 538-555.

Hibbard, K. A., S. Archer, D. S. Schimel, and D. W. Valentine (2001), Biogeochemical changes accompanying woody plant encroachment in a subtropical savanna, *Ecology*, 82(7), 1999-2011.

Higgins, S.I., W. J. Bond, and W.S.W. Trollope (2000), Fire, resprouting and variability: a recipe for tree-grass coexistence in savanna. *Journal of Ecology,* 88, 213-229.

Hillel, D. (1980), *Fundamentals of Soil Physics*, Academic Press, NY.

HilleRisLambers, R., M. Rietkerk, F. van den Bosch, H. H. T. Prins, and H. de Kroon (2001), Vegetation pattern formation in semi-arid grazing systems, *Ecology*, 82(1), 50-61.

Hook, P. B., and I. C. Burke (2000), Biogeochemistry in a shortgrass landscape: Control by topography, soil texture, and microclimate, *Ecology*, 81(10), 2686-2703.

Hutchinson C. F. (1996), The Sahelian desertification debate: a view from the American South West, *Journal of Arid Environments*, 33(4), 519-524.

Huxman T. E, B. P. Wilcox, R. L. Scott, K. Snyder, K. Hultine, E. Small, D. D. Breshears, W. Pockman, R. B. Jackson (2005), Ecohydrological implications of woody plant encroachment, *Ecology*, 86, 308-319.

Hyder, D. N., A. C. Everson, and R. E. Bement (1971), Seedling morphology and seeding failures with blue grama, *Journal of Range Management*, 24(4), 287-292.

Imeson, A. C., and H. A. M. Prinsen (2004), Vegetation patterns as biological indicators for identifying runoff and sediment source and sink areas for semi-arid landscapes in Spain, *Agriculture, Ecosystems and Environment*, 104(2), 333-342.

Jackson, R. B., and M. M. Caldwell (1993), The scale of nutrient heterogeneity around individual plants and its quantification with geostatistics, *Ecology*, 74(2), 612-614.

Janeau, J. L., A. Mauchamp, and G. Tarin (1999), The soil surface characteristics of vegetation stripes in Northern Mexico and their influences on the system hydrodynamics: An experimental approach, *Catena*, 37(1-2), 165-173.

Jeltsch, F., S. J. Milton, W. R. J. Dean, and N. Van Rooyen (1997), Analyzing shrub encroachment in the southern Kalahari: a grid-based modeling approach, *Journal of Applied Ecology*, 34(6), 1497-1508.

Kassas, M. (1977), Arid and semi-arid lands: Problems and prospects, *Agro-Ecosystems*, 3, 185-204.

Krammes, J. S. and L. F. DeBano (1965), Soil wettability: a neglected factor in watershed management, *Water Resources Res*earch, 1, 283-286.

Kurc, S. A., and E. E. Small (2004), Dynamics of evapotranspiration in semiarid grassland and shrubland ecosystems during the summer monsoon season, central New Mexico, *Water Resources Re*search, 40, W09305.

Lal, R. (2001), Soil degradation by erosion, *Land degradation and Development*, 12, 519-539.

Lauenroth, W. K., O. E. Sala, D. P. Coffin, and T. B. Kirchner (1994), The importance of soil-water in the recruitment of *Bouteloua gracilis* in the shortgrass steppe, *Ecological Applications*, 4(4), 741-749.

Lee, D. H. (1999), Experimental investigation of the removal of hydrophobic organic compounds from two Iowa soils using food grade surfactants and recovery of used surfactants. Ph.D. Dissertation, Iowa State University, Ames, USA, pp 200.

Lefever, R., and O. Lejeune (1997), On the origin of tiger bush. *Bulletin of Mathematical Biology*, 59, 263–294.

Lepers, E. , E. F Lambin, A. C. Janetos, R. De Fries, F. Achard (2005), A synthesis of rapid land-cover change information for the 1981-2000 period, *Bioscience*, 55(2), 19-26.

Leprun, J. C. (1999), The influences of ecological factors on tiger bush and dotted bush patterns along a gradient from Mali to northern Burkina Faso, *Catena*, 37(1-2), 25-44.

Letey, J., J.F. Osborn., and N. Valoras (1975), Soil water repellency and the use of nonionic surfactants. *Technical Completion Report. 154,* University of California, Water Resources Center, Riverside, pp 11–18.

Letey, J. (2001), Causes and consequences of fire-induced soil water repellency, *Hydrological Processes*, 15, 2867-2875.

Lewis, J. P., S. L. Stofella, and S. R. Feldman (2001), Monk's tonsure-like gaps in the tussock grass *Spartina argentinensis* (Gramineae), *Revista De Biologia Tropical*, 49(1), 313-316.

Li, J., G. S. Okin, L. Alvarez, and H. Epstein (2007), Quantitative effects of vegetation cover on wind erosion and soil nutrient loss in a desert grassland of southern New Mexico, USA, *Biogeochemistry*, 85(3), 317-332.

Li, H., and J.F. Reynolds (1997), Modeling effects of spatial pattern, drought, and grazing on rates of rangeland degradation: a combined Markov and cellular automata approach, in Quattrochi D.A., and M.F. Goodchild (editors), *Scales in Remote Sensing and GIS*, Lewis Publishers, Boca Raton, F. L, pp 211–230.

Li, X. R., X. P. Wang, T. Li, and J. G. Zhang (2002), Microbiotic soil crust and its effect on vegetation and habitat on artificially stabilized desert dunes in Tengger Desert, North China, *Biology and Fertility of Soils*, 35(3), 147-154.

Liu, C. and J. B. Evett (1984), *Soil Properties: Testing, Measurement, and Evaluation*, Prentice Hall, Englewood Cliffs, NJ.

Ludwig, J., R. Bartley, A. Hawdon, B. Abbott, and D. McJannet (2007), Patch configuration non-linearly affects sediment loss across scales in a grazed catchment in North-east Australia, *Ecosystems*, 10(5), 839-845.

Ludwig, J. A., D. J. Tongway, and S. G. Marsden (1999), Stripes, strands or stipples: modelling the influence of three landscape banding patterns on resource capture and productivity in semi-arid woodlands, Australia, *Catena*, 37(1-2), 257-273.

Ludwig, J. A., D. J. Tongway, D. O. Freudenberger, J. C. Noble., and K. C. Hodgkinson, editors (1997), *Landscape Ecology, Function and Management: Principles from Australia's Rangelands,* CSIRO Publishing, Melbourne, Australia.

Lyles, L., and J. Tatarko (1986), Wind erosion effects on soil texture and organic matter, *Journal of Soil and Water Conservation,* 46, 191-193.

Mabbutt, J. A., and A. E. Wilson (editors) (1980), *Social and Environmental Aspects of Desertification,* The United Nations University, Tokyo.

Ma'shum, M., M. E. Tate., G. P. Jones, and J.M. Oades (1988), Extraction and characterization of water-repellent materials from Australian soils, *Journal of Soil Science,* 39, 99-110.

McHale, G., M. I. Newton., N. J. Shirtcliffe (2005), Water-repellent soil and its relationship to granularity, surface roughness and hydrophobicity: A materials science view, European *Journal of Soil Science*, 56(4), 445-452.

McKenna Neuman, C. (2003), Effects of temperature and humidity upon the entrainment of sedimentary particles by wind, *Boundary-Layer Meteorology*, 108, 61-89.

McKenna Neuman, C., and W. G. Nickling (1989), A theoretical and wind tunnel investigation of the effect of capillary water on the entrainment of sediment by wind, *Canadian Journal of Soil Sci*ence, 69, 79-96.

Middleton, N., and D. Thomas (1997), *World Atlas of Desertification*, Arnold, London.

Millennium Ecosystem Assessment (2005), *Ecosystems and Human Well-Being: Desertification Synthesis*, World Resources Institute, Washington D.C.

Moreno, J. M., and Oechel, W. C (1991), Fire Intensity Effects On Germination Of Shrubs And Herbs In Southern California Chaparral, *Ecology*, 72 (6), 1993-2004.

Morley, C.P., K.A. Mainwaring, S. H. Doerr, P. Douglas, C. T. Llewellyn, and L.W. Dekker (2005), Organic compounds at different depths in a sandy soil and their role in water repellency, *Australian Journal of Soil Research*, 43, 239-249.

Mueller, I. M. (1941), An experimental study of rhizomes of certain prairie plants, *Ecological Monographs*, 11(2), 165-188.

National Climatic Data Center (2006), Climate of 2006: Wildfire Season Summary, http://www.ncdc.noaa.gov/oa/climate/research/2006/fire06.html.

Neave, M., and A. D. Abrahams (2002), Vegetation influences on water yields from grassland and shrubland ecosystems in the Chihuahuan desert, *Earth Surface Processes and Landforms*, 27, 1011-1020.

Neff *et al*. (2008), Increasing eolian dust deposition in the western United States linked to human activity, *Nature Geoscience*, 1, 189-195.

Nicholson, S. (2000), Land surface processes and Sahel climate, *Reviews of Geophysics*, 38,117-139.

Nicholson, S. E., C. J. Tucker, and M. B. Ba (1998), Desertification, drought, and surface vegetation: An example from the West African Sahel, *Bulletin of the American Meteorological Society*, 79(5), 815-829.

Nnoli, O. (1990), Desertification, refugees and regional conflict in West Africa, *Disasters*, 14, 132-139.

Offer, Z. Y., E. Zaady, and M. Shachak (1998), Aeolian particle input to the soil surface at the Northern limit of the Negev desert, *Arid Soil Research and Rehabilitation*,12 (1), 55-62.

Okin, G. S. (2002), Toward a unified view of biophysical land degradation processes in arid and semi-arid lands, *in Global Desertification: Do Humans Cause Deserts?*, Reynolds J. F. and D. M. Stafford Smith (editors), pp 95-109.

Okin, G. S., D. A. Gillette, and J. E. Herrick (2006), Multi-scale controls on and consequences of aeolian processes in landscape change in arid and semi-arid environments, *Journal of Arid Environments*, 65(2), 253-275.

Okin, G. S., N. Mahowald, O. A. Chadwick, and P. Artaxo (2004), Impact of desert dust on the biogeochemistry of phosphorus in terrestrial ecosystems, *Global Biogeochemical Cycles*, 18, GB2005.

Okin, G. S., and Gillette, D.A. (2001), Distribution of vegetation in wind-dominated landscapes: Implications for wind erosion modeling and landscape processes, *Journal of Geophysical Research*, 106(9), 9673-9683.

Oldeman L. R., R. T. A. Hakkeling, and W.G. Sombroek (1991), World map of the status of human-induced soil degradation: an explanatory note, second revised edition, International Soil Reference and Information Center/ United Nations Environment Program, Wageningen/Nairobi.

Orozco, A. A. (2000), Fine particulate matter generation under controlled laboratory and wind tunnel conditions, Ph.D. Dissertation, Texas Tech University, Lubbock, TX.

Osmet, B. D. J. (1963), The drop wise condensation of steam, in Moillet, J.L. (editors), *Water Proofing and Water-Repellency*, pp 384-413.

Packer, A., and K. Clay (2000), Soil pathogens and spatial patterns of seedling mortality in a temperate tree, *Nature*, 404(6775), 278-281.

Pickup, G. (1998), Desertification and climate change- the Australian perspective, *Climate Research*, 11, 51-63.

Pierson, F. B., K. E. Spaeth, M. A. Weltz, and D. H. Carlson (2002), Hydrologic response of diverse western rangelands, *Journal of Range Management*, 55(6), 558-570.

Pierson, F. B., P. R. Robichaud, and K. E. Spaeth, (2001), Spatial and temporal effects of wildfire on the hydrology of a steep rangeland watershed, *Hydrological Processes*, 15(15), 2905-2916.

Pope, C. A. III., D. V. Bates, and M. E. Raizenne (1996), Health effects of particulate air pollution: Time for reassessment? *Environmental Health Perspectives*, 103, 472-480.

Puigdefabregas, J. (2005), The role of vegetation patterns in structuring runoff and sediment fluxes in drylands, *Earth Surface Processes and Landforms,* 30(2), 133-147.

Ramanathan, V., P. J. Crutzen, J. T. Kiehl, and D. Rosenfeld (2001), Aerosols, climate, and the hydrological cycle, *Science*, 294, 2119-2124.

Rango, A., S. L. Tartowski, A, Laliberte, J. A, Wainwright, and A. J. Parsons (2006), Islands of hydrologically enhanced biotic productivity in natural and managed arid ecosystems. *Journal of Arid Environments,* 65, 235-252.

Raupach, M. R., N. Woods, G. Dorr, J. F. Leys, and H. A. Cleugh (2001), The entrapment of particles by windbreaks, *Atmospheric Environment*, 35(20), 3373 - 3383.

Rauzi, F., and F. M. Smith (1973), Infiltration rates: Three soils with three grazing levels in northeastern-Colorado, *Journal of Range Management*, 26(2), 126-129.

Ravi, S., P. D'Odorico, and G. S. Okin (2007), Hydrologic and aeolian controls on vegetation patterns in arid landscapes, *Geophysical Research Letters*, 34, L24S23.

Ravi, S., P. D'Odorico, T. M. Zobeck, T. M. Over, and S. L. Collins (2007), Feedbacks between fires and wind erosion in heterogeneous arid lands, *Journal of Geophysical Research*, 112, G04007.

Ravi, S., P. D'Odorico, B. Herbert, T. M. Zobeck, and T. M. Over (2006a), Enhancement of wind erosion by fire-induced water repellency, *Water Resources Research*, 42, W11422.

Ravi, S., T. M. Zobeck., T. M. Over, G. S. Okin, and P. D'Odorico (2006b), On the effect of wet bonding forces in air-dry soils on threshold friction velocity of wind erosion, *Sedimentology*, 53 (3), 597-609.

Ravi, S., and P. D'Odorico (2005), A field-scale analysis of the dependence of wind erosion threshold velocity on air humidity, *Geophysical Research Letters*, 32, L21404.

Ravi, S., D'Odorico, P., Over, T. M., Zobeck, T. M. (2004), On the Effect of Air Humidity on Soil Susceptibility to Wind Erosion: The Case of Air-Dry Soils, *Geophysical Research Letters*, 31 (9), L09501.

Reich, P., H. Eswaran, S. Kapur and E. Akca (2000), Land Degradation and Desertification in Desert Margins, *International Symposium on Desertification*, (Available online http://www.toprak.org.tr/isd/isd).

Reid, K. D., B. P. Wilcox, D. D. Breshears and L. MacDonald (1999), Runoff and erosion in a Pinon-Juniper woodland: Influence of vegetation patches, *Soil Science Society of America Journal*, 63, 1869-1879.

Reynolds J. F., and D. M. Stafford Smith (2002), Do humans cause deserts?, *in Global Desertification: Do Humans Cause Deserts?* Reynolds, J. F., and D. M. Stafford Smith (editors), pp1-21.

Reynolds, J. F., R. A. Virginia, and W. H. Schlesinger (1996), Defining functional types for models of desertification, in *Plant Functional Types*, Smith, T. M., H. H. Shugart, and F. I. Woddward (editors), Cambridge University Press, London.

Rietkerk, M., M. C. Boerlijst, F. van Langevelde, R. HilleRisLambers, J. van de Koppel, L. Kumar, H. H. T. Prins, and A. M. de Roos (2002), Self-organization of vegetation in arid ecosystems, *American Naturalist*, 160(4), 524-530.

Rietkerk, M., and J. van de Koppel (1997), Alternate stable states and threshold effects in semiarid grazing systems, *Oikos*, 79, 69-76.

Robertson, J. H. (1939), A quantitative study of true-prairie vegetation after three years of extreme drought, *Ecological Monographs*, 9(4), 431-492.

Roques, K. G., T. G. O'Connor, and A. R. Watkinson (2001), Dynamics of shrub encroachment in an African savanna: relative influences of fire, herbivory, rainfall and density dependence, *Journal of Applied Ecology*, 38(2), 268-280.

Rosenfield, D., Y, Rudich, and R. Lahav (2001), Desert dust suppressing precipitation: A possible desertification feedback loop, *Proceedings of the National Academy of Sciences of the United States of America*, 98(11), 5975-5980.

Roy, J. L. and W. B. McGill (2002), Assessing soil water repellency using the molarity of ethanol droplet (MED) test, *Soil Science*, 167(2), 83-97.

Saleh, M. A., and J. Letey (1989), The effect of two polymers and water qualities on dry cohesive strength of three soils, *Soil Science Society of America Journal*, 53, 255-259.

Sankaran, M., J. Ratnam, and N. P. Hanan (2004), Tree-grass coexistence in savannas revisited – insights from an examination of assumptions and mechanisms invoked in existing models, *Ecology Letters*, 7, 480-490.

Savage, S. M., J. P. Martin, and J. Letey (1969), Contribution of some soil fungi to natural and heat-induced water repellency in sand, *Soil Science Society of America Proceedings*, 33,405-409.

Scanlon, T. M., K. K. Caylor, S. A. Levin, and I. Rodriguez-Iturbe (2007), Positive feedbacks promote power-law clustering of Kalahari vegetation, *Nature*, 449(7159), 209-212.

Schlesinger, W. H., and A. M. Pilmanis (1998), Plant-soil interactions in deserts, *Biogeochemistry*, 42(1-2), 169-187.

Schlesinger, W. H. and N. Gramenopoulos (1996), Archival photographs show no climate-induced changes in woody vegetation in the Sudan, 1943-1994, *Global Change Biology*, 2, 137-141.

Schlesinger, W. H., J. F. Reynolds, G. L. Cunningham, L. F. Huenneke, W. M. Jarrell, R. A. Virginia, and W. G. Whitford (1990), Biological feedbacks in global desertification, *Science*, 147, 1043-1048.

Scholes, R.J., and S.R. Archer (1997), Tree-grass interactions in savannas, *Annual Reviews of Ecology and Systematics*, 28, 517-544.

Sheffer, E., H. Yizhaq, E. Gilad, M. Shachak, and E. Meron (2007), Why do plants in resource-derived environments form rings? *Ecological Complexity*, 4(4), 192-200.

Shen, W. (1988), Community features of the artificial vegetation on the sand land in the Shapotou area, *Journal of Desert Research*, 8 (3), 1-8.

Silvertown, J., S. Holtier, J. Johnson and P. Dale (1992), Cellular automata models of interspecific competition from space- the effect of pattern on processes, *Journal of Ecology*, 80, 527-534.

Singer, M. J., and I. Shainberg (2004), Mineral soil surface crusts and wind and water erosion, *Earth Surface Processes and Landforms*, 29(9), 1065-1075.

Sinha, R. K., S. Bhatia, and R. Vishnoi (1999), Desertification control and rangeland management in the Thar desert of India, *RALA Report* No. 200.

Stout, J. E. and T. M. Zobeck (1997), Intermittent saltation, *Sedimentology*, 44, 959-970.

Stursova, M., C. L. Crenshaw, and R.L. Sinsabaugh (2006), Microbial response to long-term N deposition in a semiarid grassland, *Microbial Ecology*, 51(1), 90-98.

Swap, R., M. Garstang, S.A. Macko, P. D. Tyson, W. Maenhaut, P. Artaxo, P. Kallberg, and R. Talbot (1996), The long-range transport of southern African aerosols to the tropical South Atlantic, *Journal of Geophysical Research*, 101(19), 23,777-23,791.

Taylor, C. .M., E. F. Lambin. N. Stephenne, R.J. Harding, and R .L. H. Essery (2002), The influence of land use change on climate in the Sahel, *Journal of Climate*, 15(24), 3615-3629.

Thomas, D. S. G. (1997), The science and the desertification debate, *Journal of Arid Environments*, 37, 599-608.

Thurow, T. L., W. H. Blackburn, and C. A. Taylor, Jr (1986), Hydrologic characteristics of vegetation types as affected by livestock grazing systems, Edwards Plateau, Texas, *Journal of Range Management*, 39, 505-509.

Turner, M. G. (1989), Landscape Ecology: The effect of pattern on process, *Annual Review of Ecology and Systematics*, 20(1), 171-197.

Tyler, C. M. (1995), Factors contributing to postfire seedling establishment in chaparral: Direct and indirect effects of fire, *Journal of Ecology*, 83(6), 1009-1020.

United Nations (2003), Press release: SG/SM/8750-OBV/355, available online at: http://www.un.org/News/Press/docs/2003/sgsm8750.doc.htm.

United Nations Convention to Combat Desertification (1994), Elaboration of an International Convention to Combat Desertification in Countries Experiencing Serious Drought and/or Desertification, Particularly in Africa" (*U.N. Doc. A/AC.241/27, 33 I.L.M. 1328*).

US Forest Service (2006), Investigation continues into wildfire on Cimarron Grassland, http://www.fs.fed.us/r2/psicc/news/2006/index.shtml.

Valentin, C., and J. M. d'Herbes (1999), Niger tiger bush as a natural water harvesting system, *Catena*, *37*(1-2), 231-256.

Van Auken, O.W. (2000), Shrub invasions of North American semiarid grasslands, *Annual Review of Ecology and Systemtics*, 31, 197-215.

van de Koppel, J., M., Rietkerk, F. van Langevelde, L. Kumar,C.A. Klausmeier, J. M. Fryxell, J. W. Hearne, J. van Andel, N. de Ridder, A. Skidmore, L. Stroosnijder, and H. H. T. Prins (2002), Spatial heterogeneity and irreversible vegetation change in semi-arid grazing systems, *American Naturalist*, 159(2), 209-218.

Van Langevelde, F., C. A. D. M. van de Vijver, L. Kumar, J. van de Koppel, N. de Ridder, J. van Andel, A. K. Skidmore, J. W. Hearne, L. Stroosnijder, W. J. Bond, H. H. T. Prins, and M. Rietkerk (2003), Effects of fire and herbivory on the stability of savanna ecosystems, *Ecology*, 84(2), 337-350.

van Wijk, M. T., and I. Rodriguez-Iturbe, Tree-grass competition in space and time: Insights from a simple cellular automata model based on ecohydrological dynamics, *Water Resources Research*, 38(9), 1179.

Van Wilgen, B.W., W.S.W. Trollope, H. C. Biggs, A. L. F. Potgieter, and B. H. Brockett (2003), Fire as a Driver of Ecosystem Variability, in, *The Kruger Experience: Ecology and Management of Savanna Heterogeneity,* Du Toit, J.T., K.H. Rogers, and H.C. Biggs (editors), Island Press, Washington D.C., pp 149-170.

Vermeire, L. T., D. B. Wester, R. B. Mitchell, and S. D. Fuhlendorf (2005), Fire and Grazing Effects on Wind Erosion, Soil Water Content, and Soil Temperature, *Journal of Environmental Quality*, 34(5), 1559-1565.

Veron S.R., J. M. Paruelo, and M. Oesterheld (2006), Assessing desertification, *Journal of Arid Environments*, 66(4), 751-763.

Vinton, M. A., and I. C. Burke (1995), Interactions between individual plant-species and soil nutrient status in shortgrass steppe, *Ecology*, 76(4), 1116-1133.

Virginia, R. A., and W. M. Jarrell (1983), Soil properties in a mesquite-dominated Sonoran Desert ecosystem, *Soil Science Society of America Journal*, 47, 138-144.

von Hardenberg, J., E. Meron, M. Shachak, and Y. Zarmi (2001), Diversity of vegetation patterns and desertification, *Physical Review Letters*, 87, 198101-1-4.

Wan, C. G., and R. E. Sosebee (2000), Central dieback of the dryland bunchgrass Eragrostis curvula (weeping lovegrass) re-examined: The experimental clearance of tussock centres, *Journal of Arid Environments*, 46(1), 69-78.

Wang, G. and E. A. B. Eltahir (1999). Biosphere-atmosphere interactions over West Africa. 2. Multiple climate equilibria, *Quarterly Journal of the Royal Meteorological Society*, 126, 1261-1280.

Wang, L., P. D'Odorico, S. Ringrose, S. Coetzee, and S. A. Macko (2007), Biogeochemistry of Kalahari sands, *Journal of Arid Environments*, 71(3), 259-279.

Wang, L., P. P. Mou, and R. H. Jones (2006), Nutrient foraging via physiological and morphological plasticity in three plant species, *Canadian Journal Of Forest Research-Revue Canadienne De Recherche Forestiere*, 36(1), 164-173.

Wang, X., X. Li, H. Xiao, R. Berndtsson, J. Zhang, and Z. Zhang (2007), Effects of surface characteristics on infiltration patterns in an arid shrub desert, *Hydrological Processes*, 21, 72-79.

Walker, B. H., D. Ludwig, C. S. Holling, and R. M. Peterman (1981), Stability of semiarid savanna grazing systems, *Journal of Ecology*, 69, 473-498.

Watt, A. S. (1947), Pattern and Process in the Plant Community, *The Journal of Ecology*, 35(1/2), 1-22.

Weaver, J. E., and F. W. Albertson (1936), Effects on the Great Drought on the prairies of Iowa, Nebraska, and Kansas, *Ecology*, 17(4), 567-639.

West, N. E. (1990). Structure and function of microphytic soil crusts in wildlife ecosystems of arid to semi-arid regions, *Advances in Ecological Research*, 20, 179-223.

Whicker, J. J., J. E. Pinder, D. D. Breshears, and C. F. Eberhart (2006), From dust to dose: Effects of forest disturbances on increased inhalation exposure, *Science of the Total Environment*, 368(2-3), 519-530.

Whicker, J. J., D. D. Breshears, P. T. Wasiolek, T.B. Kirchner, R. A. Tavani, D. A. Schoep, and J. C. Rodgers (2002), Temporal and spatial variation of episodic wind erosion in unburned and burned semiarid shrubland, *Journal of Environmental Quality*, 31, 599-612.

White, C. S., and S. R. Loftin (2000), Response of 2 semiarid grasslands to cool-season prescribed fire, *Journal of Range Management*, *53*(1), 52-61.

White, C. S., R. L. Pendleton, and B. K. Pendleton (2006), Response of two semiarid grasslands to a second fire application, *Rangeland Ecology and Management*., 53, 52-61.

White, L. P. (1971), Vegetation stripes on sheet wash surfaces, *The Journal of Ecology*, 59(2), 615-622.

Wikberg, S., and L. Mucina (2002), Spatial variation in vegetation and abiotic factors related to the occurrence of a ring-forming sedge, *Journal of Vegetation Science*, 13(5), 677-684.

Wikberg, S., and B. M. Svensson (2003), Ramet demography in a ring-forming clonal sedge, *Journal of Ecology*, 91(5), 847-854.

Worster, D. (1979), *Dust Bowl: The Southern Plains of 1930s*, Oxford University press, New York, pp 277.

Wood, J. C., M. K. Wood, and J. M. Tromble (1987), Important factors influencing water infiltration and sediment production on arid lands in New Mexico, *Journal of Arid Environments*, 12, 111-118.

Wood, M. K., G. B. Donart, and M. Weltz (1986), Comparative infiltration rates and sediment production on fertilized and grazed blue grama rangeland, *Journal of Range Management*, 39(4), 371-374.

Xue, Y., and J. Shukla (1993), The influence of land surface properties on Sahel climate. Part I: desertification. *Journal of Climate*, 6, 2232-2245.

Yizhaq, H., E. Gilad, and E. Meron (2005), Banded vegetation: biological productivity and resilience, *Physica A-Statistical Mechanics and its Applications*, 356(1), 139-144.

Yoneyama, T., T. Matsumaru, K. Usui, and W. Engelaar (2001), Discrimination of nitrogen isotopes during absorption of ammonium and nitrate at different nitrogen concentrations by rice (*Oryza sativa* L.) plants, *Plant Cell and Environment*, 24(1), 133-139.

Zeng, G. P., I. Chlamtac, and Y. Su (2004), Nonlinear observers for two classes of perturbed systems. *Computers and Mathematics with Applications*, 48 (3-4), 387-398.

Zeng, N., J. D. Neelin, K. M. Lau, C. J. Tucker (1999), Enhancement of interdecadal climate variability in the Sahel by vegetation interaction, *Science*, 286, 1537-1540.

Zhang, R. D. (1997), Determination of soil sorptivity and hydraulic conductivity from the disk infiltrometer, *Soil Science Society of America Journal*, 61(4), 1024-1030.

Zhao, H. L., X. Y. Zhao, R. L. Zhou, T. H. Zhang, and S. Drake (2005), Desertification processes due to heavy grazing in sandy rangeland, Inner Mongolia, *Journal of Arid Environments*, 62(2), 309-319.

Zobeck, T. M., D. W. Fryrear, and R. D. Pettit (1989), Management effects on wind-eroded sediment and plant nutrients, *Journal of Soil and Water Cons*ervation, 44, 160-163.

Zobeck, T. M. and D. W. Fryrear (1986), Chemical and physical characteristics of wind blown sediment. II. Chemical characteristics and total soil and nutrient discharge, *Transactions of the American Society of Agricultural Engineers*, 29, 1037-1041.